Chaperones and Quality Control of the hERG and CFTR Ion Channels

Christine Hantouche

Department of Physiology
McGill University
Montreal, Quebec, Canada

January, 2015

A thesis submitted to McGill University in partial fulfillment of the requirements for the degree Doctor of Philosophy

"The journey of a thousand miles begins with a single step"

Lao Tzu

The completion of this thesis is a step in my journey towards greater achievements and successes.

These accomplishments are made possible by the support of distinguished individuals in my life.

To you my wonderful family I dedicate this work, Uncle Ibrahim Itani, Dad Michel,

Mom Mona, siblings Naji, Elie, Mireille and Charbel.

You have been my support system.

Abstract

Protein misfolding diseases represent a major medical challenge. Although the genetic mutations that cause many misfolding diseases have been identified, there are no cures yet available for most of these diseases. Among the examples in which the underlying cellular and molecular mechanisms are well understood are diseases due to misfolding of integral membrane proteins that normally function as ion channels at the plasma membrane. Synthesis of integral membrane proteins begins at the endoplasmic reticulum (ER). In the case of wild type (WT) forms that are properly folded, they exit the ER and traffic along the secretory pathway to the cell surface. If the ion channel is misfolded, due to mutations in the protein, it is retained by the endoplasmic reticulum quality control (ERQC) system and sent for endoplasmic reticulum-associated proteasomal degradation (ERAD). Molecular chaperones play a role in both protein folding and degradation. The chaperones assist in the proper folding of the cytosolic domains of the ion channels and participate in targeting the misfolded forms for ERAD. Because of the dual function of chaperones, diseases due to misfolding and impaired trafficking of ion channels can be considered to be the result of inefficient chaperone folding activity and/or over activity of the ERAD. An interesting possibility is that manipulation of these chaperones could help alleviate the symptoms of ion channel misfolding diseases through promoting mutant channel folding and thereby rescuing trafficking leading to restored function. The heat shock protein 70 (Hsp70) chaperone has a key role in the quality control of many proteins, and its activity is regulated by a variety of co-chaperones. The aim of this thesis is to understand the role of the Hsp70 chaperone system in the quality control of two ion channel misfolding diseases: long QT syndrome type 2 (LQT2), which is a cardiac disorder due to mutations in the potassium channel, human ether-a-

go-go related gene (hERG) protein, and cystic fibrosis (CF), which is due to mutations in the chloride channel, cystic fibrosis transmembrane conductance regulator (CFTR) protein. The initial aspect involved the characterization of the role of the Hsp70 co-chaperones, DNAJA1 and DNAJA2, in hERG biogenesis. Both DNAJA1 and DNAJA2 induce hERG proteasomal degradation through the E3 ligase, C-terminus of Hsp70 interacting protein (CHIP), whereas only DNAJA1 promotes hERG folding. A second aspect assessed the importance of another Hsp70 co-chaperone, Bcl2-associated athanogene 1 (Bag1), in hERG biosynthesis. In brief, it was found that Bag1 induces hERG misfolding and thereby proteasomal degradation by increasing its ubiquitination through the ER-membrane anchored E3 ligase, translocation in renal carcinoma, chromosome 8 gene (TRC8), which cooperates with its cytosolic E2 enzyme, Ube2g2. We also identify a novel role for Bag1 in shifting hERG degradation pathway away from CHIP towards other E3 ligases that act independently of Hsp70. After assessing the role of the Hsp70 system in hERG synthesis, the focus of the thesis was shifted to an examination of the importance of this chaperone system for CFTR. We found that both DNAJA1 and DNAJA2 are required for CFTR maturation while only DNAJA2 promotes its proteasomal degradation through CHIP. Hsp70 also induces CFTR degradation, however, through the lysosomes. We propose a model in which specific DNAJ activities, or the lack of it, regulate the degradation of hERG and CFTR in cells.

Resumé

Les maladies associées aux anomalies de repliement des protéines représentent un défi médical majeur. Bien que les mutations génétiques qui causent de nombreuses maladies de repliement aient été identifiées, il n'existe présentement aucun remède disponible pour la plupart de ces maladies. En particulier, les maladies dues au mauvais repliement des protéines membranaires intégrales, qui fonctionnent en tant que canaux ioniques dans la membrane plasmique, représentent un exemple de maladies dans lesquels les mécanismes cellulaires et moléculaires responsables sont bien compris. La synthèse des protéines membranaires intégrales commence au niveau du reticulum endoplasmique (RE). Dans le cas des formes de type sauvage qui sont bien pliées, les protéines sortent du RE et trafiquent le long de la voie de sécrétion vers la surface cellulaire. Si le canal ionique est mal replié, en raison de mutations dans la protéine, il est retenu par le système de contrôle de qualité du RE et envoyé pour la dégradation par le protéasome associée au réticulum (ERAD). Les chaperons moléculaires jouent un rôle à la fois dans le repliement des protéines et dans leur dégradation. Les chaperons aident au repliement correct des domaines cytosoliques des canaux ioniques et participent à cibler les formes mal repliées pour ERAD. En raison de la double fonction des chaperons, les maladies dues à un mauvais repliement et à l'altération du trafic des canaux d'ions peuvent être considérées comme le résultat de l'inefficacité de l'activité de pliage des chaperons et/ou de la suractivité de l'ERAD. Par conséquent, une possibilité intéressante serait la manipulation de ces chaperons pour aider à soulager les symptômes des maladies dues aux anomalies de repliement des canaux ioniques par la promotion de pliage des canaux mutés, sauvant ainsi leur trafic et restaurant leur fonction. La protéine de choc thermique 70 (Hsp70) est un chaperon qui a un rôle clé dans le contrôle de

qualité de nombreuses protéines, et son activité est régie par une variété de co-chaperons. L'objectif de cette thèse est de comprendre le rôle du système de chaperon Hsp70 dans le contrôle de qualité de deux maladies reliées à l'anomalie de repliement de canaux ioniques: le syndrome du QT long de type 2 (LQT2), qui est un trouble cardiaque due à des mutations dans le canal de potassium éther-a-go-go humain (hERG); et la fibrose kystique (FK), qui est due à des mutations dans le canal de chlorure, la protéine dénommée régulateur de conductance transmembranaire de la fibrose kystique (CFTR). L'aspect initial a impliqué la caractérisation du rôle des co-chaperons de la protéine Hsp70, DNAJA1 et DNAJA2, dans la biogenèse de la protéine hERG. Tandis que chacune de DNAJA1 et DNAJA2 induit la dégradation de hERG par le protéasome à travers la ligase E3, CHIP (C-terminus of Hsp70 interacting protein), seul DNAJA1 favorise le pliage de hERG. Un deuxième aspect a été d'évaluer l'importance d'un autre co-chaperon de Hsp70, la protéine Bcl2-associé athanogène 1 (Bag1), dans la biosynthèse de hERG. En bref, on a constaté que Bag1 induit le mauvais repliement de hERG et de ce fait, sa dégradation par le protéasome, en augmentant son ubiquitination par la ligase E3 ancrée dans la membrane du RE, la protéine TRC8, qui coopère avec l'enzyme cytosolique E2, Ube2g2. En plus, nous avons également identifié un nouveau rôle pour Bag1 dans le déplacement de la voie de dégradation de hERG loin de CHIP vers d'autres ligases E3 qui agissent indépendamment de Hsp70. Après l'évaluation du rôle du système Hsp70 dans la synthèse de hERG, l'objet de la thèse a été déplacé vers l'examen de l'importance de ce système de chaperon pour la protéine CFTR. Nous avons constaté que les protéines DNAJA1 et DNAJA2 toute les deux, sont nécessaires pour la maturation de CFTR alors que seul DNAJA2 favorise sa dégradation par le protéasome à travers CHIP. Hsp70 induit également la dégradation de la protéine CFTR, cependant, à travers les lysosomes. Nous proposons donc un modèle dans lequel l'activité de

certaines DNAJ spécifiques, ou l'absence de celle-ci, régule la dégradation de hERG et de CFTR dans les cellules.

Original Contributions to Knowledge

Chapter 2:

In chapter 2, I showed the importance of Hsc/p70 chaperones in hERG folding. Next, I identified the role of the cytosolic Hsp70 co-chaperone, DNAJA1 in hERG folding. This role is unique among the type I Hsp40 proteins. I also characterized the mechanistic requirements of another cytosolic Hsp70 co-chaperone, DNAJA2, to promote hERG degradation, which led to the conclusion that the internal protein mechanisms of the DNAJs required for folding are also required for degradation.

Chapter 3:

In chapter 3, I characterized the role of the nucleotide exchange factor (NEF), Bag1, in hERG biogenesis. In my experiments, I showed that Bag1 reduces hERG interaction with Hsc/p70 resulting in its misfolding and inducing its proteasomal degradation. This is a novel mechanism by which Bag1 promotes substrate degradation. It was previously suggested that Bag1 promotes degradation of Hsc/p70 substrates by providing a link to the proteasome through its ubiquitin-like (UBL) domain, but we find no evidence for that. On the contrary, our data suggests that the UBL domain is dispensable for the Bag1 effect on hERG. Furthermore, I identified a novel ERAD pathway for hERG, the Ube2ge/TRC8 pathway, that was not implicated before in quality control but rather in regulated ERAD.

Chapter 4:

In chapter 4, I characterized the role of the Hsp70 chaperone system in CFTR biogenesis. First, I demonstrated the role of Hsc/p70 and its associated type I Hsp40 co-chaperones in CFTR folding and quality control. Through knockdown experiments, I showed that contrary to its effect on hERG, Hsc/p70 seems to be involved primarily in CFTR degradation. Next, I demonstrated that the Hsp70 co-chaperones, DNAJA1 and DNAJA2, are both required for CFTR folding. However only DNAJA2 promotes its proteasomal degradation through CHIP. These findings are novel in that the role of these DNAJ co-chaperones was not previously addressed in CFTR biosynthesis.

Contribution of Authors

As permitted under the "Guidelines for Thesis Preparation" provided by the Graduate and Postdoctoral Studies Office, Chapters 2, 3, and 4 of this thesis include manuscripts either published or to be submitted for publication. They have been reformatted to give a uniform layout of the thesis. The contributions of authors are listed below:

Chapter 2:

The contents of this chapter have been published:

Walker VE, Wong MJ, Atanasiu R, Hantouche C, Young JC, Shrier A. Hsp40 chaperones promote degradation of the HERG potassium channel. *J Biol Chem*. 285(5): 3319-29, 2010.

Baaklini I, Wong MJ, Hantouche C, Patel Y, Shrier A, Young JC. The DNAJA2 substrate release mechanism is essential for chaperone-mediated folding. *J Biol Chem*. 287(50): 41939-54, 2012.

The contributions made by collaborators for this chapter:

This chapter is the result of different collaborations with a previous PhD student in our lab, Valerie Walker, and a member of the Young lab, Imad Baaklini. First, Valerie Walker showed the DNAJs, DNAJA1, DNAJA2, and DNAJA4, promote hERG proteasomal degradation through CHIP (Figures 2.3 and 2.6). Then, I showed that Hsc/p70 is important for hERG folding (Figure 2.1) and DNAJA1 but not DNAJA2 is the co-chaperone that assists Hsc/p70 in its pro-folding activity (Figure 2.2). This showed the functional differences between the DNAJs. Next, as part of Imad Baaklini's project, where he wanted to understand the mechanism of function of the DNAJs, I performed experiments on hERG with DNAJA2 mutant constructs that he provided. Therefore, to understand the mechanism by which DNAJA2 promotes hERG degradation, I

performed pulse chase experiments in an overexpression system of both hERG and the different DNAJA2 constructs. Overall, these experiments showed the importance of DNAJA2 internal structures in inducing hERG degradation (Figure 2.5). I analyzed all experiments that I performed. Michael Wong and Roxana Atanasiu performed other experiments for the paper, which are not included in this thesis.

Chapter 3:

The contents of this chapter will be submitted for publication:

Christine Hantouche, William C. Valinsky, Jason C. Young and Alvin Shrier. Bag1 shifts hERG degradation towards the Ube2g2/TRC8 pathway at the endoplasmic reticulum. *Manuscript.*

The contributions made by collaborators for this chapter:

I designed, performed and analyzed all experiments in this study except for the patch clamp experiments (Figure 3.1D), which were conducted by William Valinsky. I wrote the initial draft of the manuscript, which was edited by Drs. Young and Shrier. Together they supervised this project and provided critical review and revision of the manuscript.

Chapter 4:

The contents of this chapter will be submitted for publication:

Patrick Kim Chiaw, Christine Hantouche, Yogita Patel, Alvin Shrier and Jason C. Young. Dual roles of Hsp70 and DNAJA2 in the degradation of CFTR. *Manuscript.*

The contributions made by collaborators for this chapter:

This chapter is in collaboration with a member of the Young lab, Patrick Kim Chiaw, who performed the experiments related to Hsp70 under various conditions (Figures 4.4, 4.5, 4.6),

and Yogita Patel, who characterized the Hsp70-T636D mutant (Figure 4.5B). I addressed the DNAJ aspects of the project and the pulse-chase experiments on CFTR with manipulation of Hsc/p70 (Figures 4.1, 4.2, 4.3). I helped in establishing the new assay, using inducible CFTR in HEK293 Tet-On cells, that we used in this study. I analyzed all experiments that I performed.

Acknowledgements

During my years in research, I have had assistance from several eminent professors to whom I am greatly indebted.

Dr Jason Young and Dr Alvin Shrier, thank you for your supervision. Your passion for science is a representation of what true love is. Thank you for being an inspiration. Thank you for your patience and faith. Thank you for your continuous support and encouragement. I wouldn't be here were it not for you.

Dr Ursula Stochaj and Dr Gergely Lukacs, thank you for being on my supervisory committee offering me guidance for my project along the way.

Dr Michael Hallett, everything shines so bright through your eyes. Thank you for your positivity. I see beauty when I look at things from your perspective.

On my journey, I have also encountered messengers of peace, who gave hope in times of despair and light in complete darkness. Many thanks to each and everyone, who eased my way in one way or another.

The best is always yet to come. Life is good…

List of Abbreviations

AAA+	ATPase associated with various cellular activities
ABC	ATP-binding cassette
Aha1	activator of Hsp90 ATPase
ASL	airway surface liquid
Bag	Bcl2-associated athanogene
β2m	β2-microglobulin
CC	coiled-coil
CF	cystic fibrosis
CFTR	cystic fibrosis transmembrane conductance regulator
CG	core-glycosylated
CHIP	C-terminus of HSP70-interacting protein
CHX	cycloheximide
cNBD	cyclic nucleotide binding domain
CNX	calnexin
COPII	coat protein II
CQ	chloroquine
CRT	calreticulin
EAG	ether-a-go-go
ECG	electrocardiogram
ENaC	epithelial Na^+ channel
ER	endoplasmic reticulum
ERAD	endoplasmic reticulum-associated degradation
ERAF	ER-associated folding pathways
ERQC	ER quality control
FG	fully glycosylated
G/F	glycine and phenylalanine
HC	heavy chains
HRD1	HMG-CoA reductase degradation 1
HCMV	human cytomegalovirus
hERG	human ether-a-go-go-related gene
HIV	human immunodeficiency virus
HMG-CoAR	3-hydroxy-3-methyl-glutaryl-CoA reductase
HOP	HSP-Organizing Protein
HSP	heat shock protein
HSPBP1	HSP70 binding protein 1
IP	immunoprecipitation
IP_3R	inositol 1,4,5-triphosphate receptors
LQT	long QT
LQT2	long QT syndrome type 2
MC	middle/C-terminal
MHC	major histocompatibility complex

MRH	mannose-6-phosphate receptor homology
MSD	membrane-spanning domains
NBD	nucleotide-binding domain
NEF	nucleotide exchange factor
NLS	nuclear localization signal
PAS	Per-Arnt-Sim
PCL	periciliary liquid
PLCγ	phospholipase C-γ
PM	plasma membrane
PN	proteostasis network
PPIase	peptidyl-prolyl isomerase
PQC	protein quality control
PUB	PNGase/UBA or UBX
QC	quality control
RING	really interesting new gene
R	regulatory
RMA1	ring finger protein with a membrane anchor
SBD	substrate-binding domain
SCAP	SREBP cleavage-activating protein
SCF	Skp1-Cullin-Fbox
sHSP	small HSP
SPFH	stomatin, prohibitin, flotilin, and HflC/HflK
SQLE	squalene monooxygenase
TdP	torsades de pointes
TM	transmembrane
TMUB1	transmembrane and Ub-like domain-containing 1
Tom70	translocases of outer membrane 70
TPR	tetratricopeptide-repeat
TRC8	translocation in renal carcinoma, chromosome 8 gene
UBL	ubiquitin-like
UPS	ubiquitin-proteasome system
UCH-L1	ubiquitin C-terminal hydrolyse-L1
UGGT	UDP-glucose/glycoprotein glucosyl transferase
Usp19	ubiquitin specific protease 19
WT	wild type

Table of Contents

List of Figures

Chapter 1

General Introduction

Proteins are the most abundant and structurally versatile macromolecules in living systems. They serve crucial functions in essentially all biological processes. Protein synthesis occurs on ribosomes as linear chains of up to several thousand amino acid building blocks linked together by peptide bonds. The linear amino acid sequence, encoded by the DNA, determines the final three-dimensional conformation and specific function unique to the protein. Given the fundamental role proteins play in all cellular functions, it is not surprising that the cells have evolved an elaborate machinery of molecular chaperones to preserve the functionality of their proteome. [1]

Molecular chaperones ensure protein folding efficiently and on a biologically relevant timescale. Both the chaperone system and the degradation machinery constitute the main elements of protein quality control (PQC) for the maintenance of protein homeostasis, or proteostasis. [2] These components function as a coordinated proteostasis network (PN) to achieve proteome maintenance and prevent accumulation of aberrantly folded species. Proteins are in a constant kinetic competition between protein folding, which leads to function, and misfolding, which leads to loss-of-function or aggregation. Therefore, a major role of the PN is to optimize the efficiency of folding and to minimize misfolding, which would compromise function thereby leading to a variety of diseases that are classified as protein misfolding diseases.

Protein misfolding diseases arise due to increased protein degradation, which leads to loss-of-function, where mutated proteins unable to fold are removed by degradation as is the case in cystic fibrosis (CF) and long QT (LQT) syndrome, or inefficiency in degradation, where aberrantly folded proteins aggregate and form intra- and extra-cellular toxic deposits that are increasingly recognized as the root cause of cytotoxicity in a range of neurodegenerative disorders such as Alzheimer's and Parkinson's. [3]

In light of the growing number of protein misfolding diseases, understanding the precisely balanced nature of the PN in order to pharmacologically correct imbalances in the system is of great medical interest. [1]

1.1. Components of the Proteostasis Network

Proteostasis is maintained by a range of factors that form complex networks including:

- Molecular Chaperone System
- Degradation Machinery

1.1.1. Molecular Chaperone System

Molecular chaperones are proteins that interact with and assist the folding of other proteins through binding and release cycles without being part of the final native structure. Chaperones cooperate in the folding of a wide range of newly synthesized proteins, as well as refolding aberrantly folded states. [4] In addition to protein folding and refolding, chaperones are involved in several other cellular processes, including protein targeting, oligomeric complex assembly, protein trafficking, assistance of proteolytic degradation, and signal transduction. [1]

There are several conserved families of chaperones structurally unrelated to each other that form cooperative pathways and networks in cells. These are known as heat shock proteins since many (though not all) chaperones are upregulated under conditions of conformational stress where there is an increased propensity for misfolding. The heat shock protein (HSP) families were originally classified according to their molecular weight (HSP40, HSP60, HSP70, HSP90, HSP100 and the small HSP (sHSP)). [4] The HSP70s, HSP90s and the chaperonins (HSP60s) are multicomponent molecular machines that participate broadly in protein biogenesis. They promiscuously recognize hydrophobic stretches of amino acids exposed in non-native proteins and promote folding through ATP- and cofactor-regulated cycles of binding and release. These HSPs are involved in protein folding processes as well as degradation pathways. The HSP100s are hexameric chaperones classified as AAA+ (ATPase associated with various cellular activities) ATPases in that they couple ATP binding and hydrolysis to various protein-remodeling activities including (un)folding of proteins and disassembly of protein complexes on one hand and protein degradation and quality control on the other. [5] Members of the sHSP family exhibit chaperone-like activity through preventing protein aggregation. sHSPs are important for stress tolerance. These are also involved in protein folding as well as degradation. [6] Overall, the cellular chaperone machinery forms complex networks that are indispensible for proteostasis.

In the following sections, we will illustrate the basic mechanisms of the main cytosolic protein folding machineries:

- The HSP70 System
- The HSP90 System

1.1.1.1. The HSP70 System

The HSP70 family comprises a set of abundant molecular chaperones that are engaged in a plethora of protein folding processes in almost all cellular compartments. Historically, HSP70 chaperones were identified by induction under heat shock during which they provide an essential protection against stress conditions by preventing the aggregation of misfolded proteins and assisting the refolding of partially unfolded proteins. HSP70 proteins also have essential house-keeping functions under normal non-stress conditions. [7] They assist the folding of newly synthesized proteins as they emerge from ribosomes, transport proteins across organellar membranes, disassemble oligomeric protein structures, facilitate proteolytic degradation of unstable proteins, and in some cases control the activity of regulatory proteins. [8] All of these cellular functions of HSP70 proteins rely on their basic mechanism, which is to bind and release short hydrophobic segments of an unfolded substrate in an ATP-hydrolytic reaction cycle. [9-12] While binding stabilizes the unfolded state, controlled release may result in the progression along the folding pathway. [8]

Although much of our knowledge of the biochemical functions of HSP70 is derived from studies of the *Escherichia coli* HSP70 homolog, DnaK, the outlines of the mechanism appear to be conserved across species. The orthologous cytosolic HSP70 forms in eukaryotes – the constitutively expressed Hsc70 (*HSPA8*) and heat shock inducible Hsp70 (*HSPA1*) in humans, the HSP70 homolog in *Saccharomyces cerevisiae* Ssa1, and DnaK – all share a common mechanism. [7,13,14] The HSP70 proteins function primarily as monomers, although they can transiently contact regulatory co-chaperone proteins. As a common structural feature, all HSP70 members consist of two major domains: an N-terminal highly conserved nucleotide-binding domain (NBD) with ATPase activity and a more variable C-terminal substrate-binding domain

(SBD) joined by a conserved linker. The fundamental HSP70 ATP hydrolysis reaction cycle has been well established. In the ATP-bound state, an Hsp70 has low affinity for polypeptide substrate with accelerated on and off rates for the peptide. Meanwhile, when in the ADP-bound state, Hsp70 binds substrate with high affinity. [11,15-17]

Crystallographic studies of Hsp70 domains provided an initial molecular basis for the elucidation of this cycle. [18,19] The NBD consists of two lobes separated by a deep central cleft, and nucleotide binding occurs at the base of the cleft. Each lobe can be further subdivided into two subdomains 1a and 1b in the first lobe and 2a and 2b in the other with 1a and 2a linked to form the base of the nucleotide-binding pocket. A cleft surface between 1a and 2a on the opposite side from the nucleotide pocket may be a regulatory interaction site. Flexibility among the subdomains allows their conformational changes from ATP to ADP or nucleotide-free states, with conserved amino acids forming the active site where nucleotide binding and catalysis occurs. [18] The SBD also contains two subdomains, a β-sandwich base with a hydrophobic groove where polypeptide binding takes place and an α-helical structure forming a lid over the polypeptide binding site (Figure 1.1A). The SBD therefore binds short hydrophobic stretches in an extended conformation exposed within an accessible polypeptide backbone in non-native substrates. [19] To fulfill the ATPase reaction cycle, chemical energy from ATP hydrolysis in the NBD must be coupled to mechanical work that results in the opening and closing of the SBD. Whereas ATP binding seems to promote flexibility between the base and lid of SBD inducing conformational changes that open up the polypeptide-binding site, peptide binding in the SBD can also transmit changes to the NBD increasing the rate of ATP hydrolysis. [7] The conserved interdomain linker has an essential role in the allosteric regulation between the two domains. [20,21] Recent structural studies on the ATP-bound state revealed that the SBD subdomains, the β sheet

Figure 1.1. The Hsp70 and Hsp40 type I machinery. A, Schematic of Hsp70 domains with original structures shown below [18,19] B, Schematic of type I Hsp40 domains with original structures shown below [22,23] C-E, Structures of Hsp70 two-domain constructs: C, ATP-bound open conformation of Hsp70 [24]; D, domains separated in the ADP-bound state [25] Colours of the domains are as in A. (Figure 1.1 modified from [26])

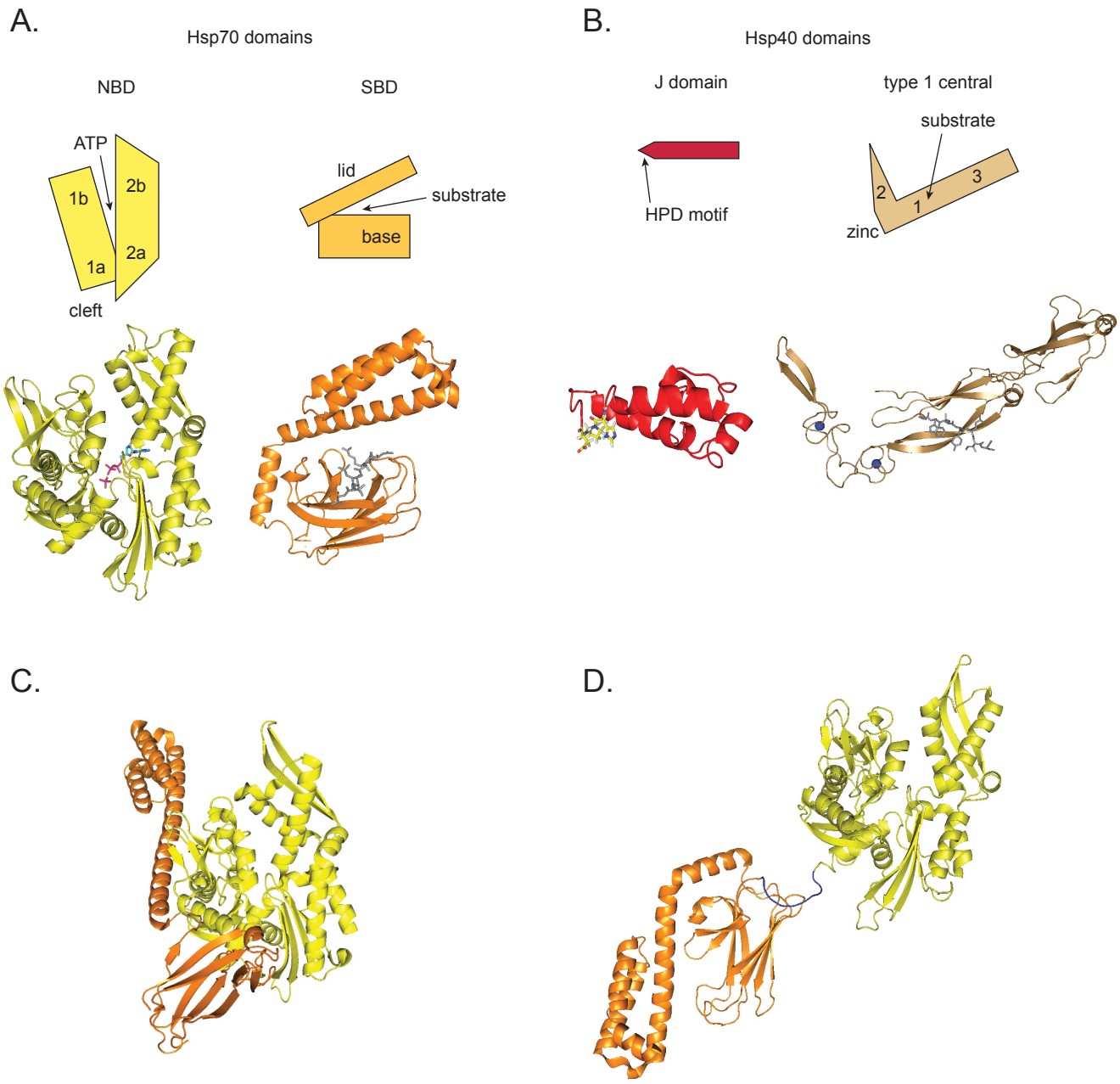
A.
Hsp70 domains
NBD
SBD
ATP
1b
2b
1a
2a
cleft
lid
substrate
base
B.
Hsp40 domains
J domain
type 1 central
HPD motif
substrate
2
3
1
zinc
C.
D.

and α-helical lid, are detached from one another and contact different subdomains of the NBD (Figure 1.1A). This interaction reveals the mechanism of allosteric regulation between the two domains. It occurs sequentially and is influenced by protein substrate binding. [24]

In the cytosol of human cells, both Hsc70 and Hsp70 are normally expressed, but only Hsp70 is greatly upregulated in the heat shock response. Other cytosolic HSP70 proteins are only expressed under stress, or in specific tissues. [14] There is some evidence that Hsc70 and Hsp70 may have certain biological differences (see below regarding hERG and CFTR). However, they cannot be distinguished from each other in other studies and biochemical differences between them have not been established. They will be referred to generally as Hsc/p70. The Hsp70 knockout mice were viable, presumably because Hsc70 could substitute, but they displayed genomic instability and increased radiosensitivity, which implies that Hsp70 plays an essential function in maintaining the stability of the genome under stress conditions. [27]

Initial studies on *E. coli* DnaK identified two key Hsp70 co-chaperones as regulators of chaperone action. Both characterized co-chaperones, DnaJ and GrpE, act at different steps of the DnaK ATPase cycle and regulate its affinity for substrate by regulating its ATPase activity. DnaJ, the first member of the HSP40 family discovered, accelerates the rate of hydrolysis of ATP by DnaK thereby inducing substrate binding by Hsp70. In opposition, GrpE binds DnaK and acts as a nucleotide exchange factor (NEF) resulting in the exchange of ADP for ATP, thereby weakening the DnaK-polypeptide interaction, which results in complex dissociation (Figure 1.2A). [28,29] Furthermore, DnaJ has chaperone activity of its own although it is not an ATPase and does not have an intrinsically regulated cycle of binding and release. DnaJ has the ability to bind unfolded polypeptide, recruit DnaK, and activate its ATPase activity resulting in substrate transfer onto the Hsp70 chaperone and DnaJ dissociation from DnaK-substrate complex. [11,13,29]

Figure 1.2. Hsc70 ATPase cycle and the NEF, Bag1. A, Hsc70 in the ATP-bound state does not bind substrate polypeptide, while in the ADP-bound state substrate is tightly bound. Hsp40-family chaperones including DJA1 and DJA2 bind substrate, activate ATP hydrolysis and substrate binding by Hsc70, and dissociate from the complex. Nucleotide exchange factors (NEFs) including Bag1 promote the release of ADP, re-binding of ATP, and the release of substrate from Hsc70. B, Domain organization of Bag1L, Bag1M and Bag1S isoforms. All contain a ubiquitin-like (UBL) domain and a BAG domain with NEF activity. Both Bag1L and Bag1M contain a TRSEEX motif. Bag1L contains a nuclear localization signal (NLS). (Figure 1.2A modified from [30])

A.

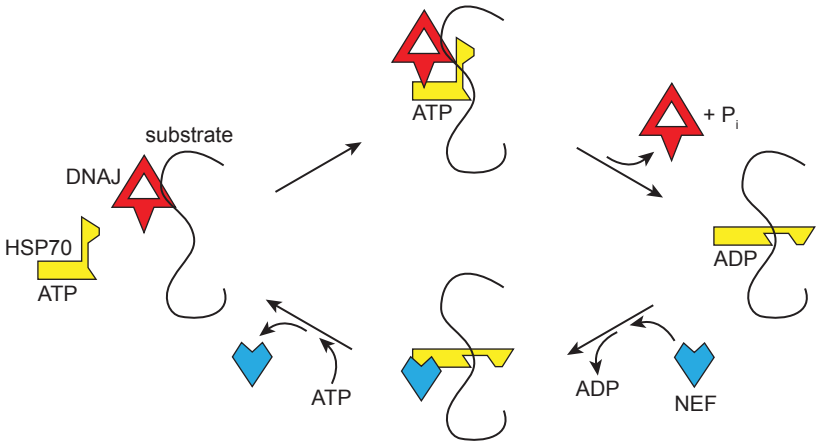
substrate
DNAJ
HSP70
ATP
ATP
+ P_i
ADP
ADP
NEF
ATP

B.

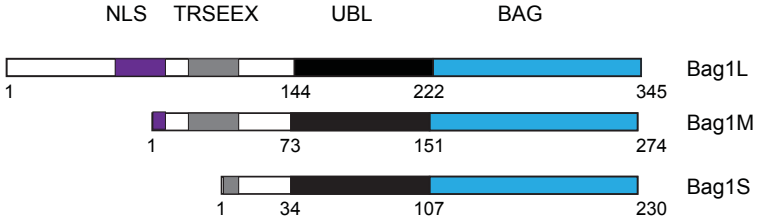
NLS
TRSEEX
UBL
BAG
Bag1L
1
144
222
345
Bag1M
1
73
151
274
Bag1S
1
34
107
230

In the following sections, we will discuss the two key HSP70 co-chaperones:

- HSP40 Family
- NEF Family

We will also briefly discuss another class of HSP70 co-chaperones that possess tetratricopeptide-repeat (TPR) clamp domains, the TPR-containing proteins.

1.1.1.1.1. HSP40 Family

All members of the HSP40 family of molecular chaperones have a highly conserved J-domain that regulates the activity of Hsp70s. It is the contact site with the Hsp70 chaperones and stimulates their ATPase activity. The J-domain, a ~70 amino acid sequence, is comprised of four helices (I-IV) with a loop region between helices II and III that contains the functionally significant and highly conserved histidine, proline, and aspartic acid tripeptide (the HPD motif) (Figure 1.1B). [31,32] There are at least 41 J-domain containing proteins in the human genome and they are classified into three classes depending on their different domains: type I, type II and type III. [33]

In DnaJ, the N-terminal J-domain is followed by a glycine and phenylalanine (G/F) rich linker, a central domain that possesses two zinc-finger motifs and known to bind client proteins, and a C-terminal homodimerization domain (Figure 1.1B). HSP40 proteins preserving this domain architecture are classified as type I family members. [34] In humans, there are three cytosolic type I co-chaperones: DJA1 (DNAJA1/Hdj2/dj2/HSDJ), DJA2 (DNAJA2/dj3/HIRIP4) and DJA4 (DNAJA4/Hdj4). DJA1 and DJA2 are constitutively expressed, while DJA4 is less abundant and may be specialized. [35-37] These type I HSP40s often have a conserved cysteine farnesylation site at their C-termini. Type I HSP40s generally promote folding with DJA1 and

DJA2 being the predominant co-chaperones dedicated for this role. The biological functions of type I J-domain co-chaperones are discussed in further details below. Ydj1 is the type I Hsp40 in *S.cerevisiae*, and is the most studied eukaryotic form.

Type II proteins contain an N-terminal J-domain with an adjacent G/F linker, but diverge in the rest of the protein, lacking the zinc-finger motifs and possessing a distinct homodimerization domain. Some type II Hsp40s support folding while others promote degradation. The major human cytosolic type II protein is DJB1 (DnaJB1/Hdj1/dj1/Hsp40), which is normally expressed at low levels but strongly induced upon heat shock. DJB1 was discovered early on and was considered as a main element in protein folding; [38,39] however, data suggests that it has moderate activity compared to DJA1, which was discovered later. Other type II HSP40s, such as DNAJB2, DNAJB6 and DNAJB8, target client proteins to degradation. These chaperones were shown to prevent toxicity associated with polyglutamine-containing proteins and/or poly-Q peptides. [40-44] Sis1 is the equivalent protein in *S. cerevisiae*, but has functions under normal growth conditions. [33,34]

Type III proteins lack all the conserved regions except for the J-domain and contain various unrelated domains, which are thought to direct HSP70 proteins for specialized functions. For example, CSPα is a type III HSP40 chaperone involved in various neurodegenerative diseases. It is present on synaptic vesicles, [45] exocrine vesicles [46] and endocrine vesicles in neurons. [47] CSPα has various presynaptic targets such as BK channels, [48,49] dynamin1, [50] and SNAP25. [51] Other possibly interesting CSPα client proteins include voltage-dependent Ca^{2+} channels, heterotrimeric G proteins, syntaxin and synaptotagmin. [52] Another example of a specialized type III J-domain protein is auxilin, which is involved in uncoating of clathrin-coated vesicles. [53]

Despite the differences in their conserved regions, both type I and type II proteins function similarly and bind non-native substrates. In contrast, type III proteins cannot bind substrate and therefore should not function as molecular chaperones on their own. [34,54]

Next, we will focus on the main type I Hsp40 co-chaperones, DJA1 and DJA2.

1.1.1.1.1a. *Type I HSP40 Family*

DJA1 was the first type I HSP40 family member to be identified in the human cytosol. DJA1 immuno-depletion from rabbit reticulocyte lysate indicated that DJA1 is required for efficient mitochondrial import of a precursor protein, pre-ornithine transcarbamylase, from the cytosol. Purified DJA1 was also thought to promote the folding of denatured luciferase by activating Hsc70. [35] DJA1, in association with Hsc70, prevented aggregation of a cytosolic fragment of the cystic fibrosis transmembrane conductance regulator (CFTR) chloride channel, and was proposed to assist channel folding. [55] Later study showed that DJA1 interaction with Hsp70 is required to promote client substrate progesterone receptor conformational maturation through the Hsp90 pathway. [56]

A second member of the type I HSP40 family in the mammalian cytosol is DJA2, which is expressed at similar levels as DJA1. DJA2 was also reported to function with Hsc70 in promoting mitochondrial import as well as luciferase refolding. [36] A third type I HSP40 protein is DJA4, which seems to have more specialized functions, as its expression is tissue-specific where it is found mostly in the heart and testes of mice. [37] In vivo experiments were done on DJA1 knockout mice, which were viable but had greatly reduced fertility. This sterility was attributed to defects in spermatogenesis due to overactivity in signaling by the androgen receptor,

which is a known substrate of the cytosolic HSP40-HSP70 system. These results showed a unique role for DJA1 in male spermatogenesis, as DJA2 and DJA4 could not substitute for this function. Thus, the different type I HSP40 chaperones are not functionally equivalent in vivo and have distinct biological and biochemical properties. [57] This functional diversity was also shown in a more recent study discussed below, where DJA1 but not DJA2 was involved in the folding of the cardiac potassium channel, human ether-a-go-go-related gene (hERG) protein. Nevertheless, all three HSP40s induced its degradation. Another recent paper found that DJA1 and not DJA2 was required for the function of activation-induced deaminase during B-cell development. [58]

Furthermore, all three human cytosolic type I HSP40 co-chaperones were found to be complexed with a mitochondrial precursor protein that is imported through translocases of outer membrane 70 (Tom70) in an Hsc70-dependent manner. [59] Co-precipitation experiments showed that the binding of the DJAs to substrate was through the central region of the C-terminal domain and the truncation of the J-domain inhibits mitochondrial pre-protein import in organelle. All three HSP40s were able to stimulate Hsp70 ATPase activity to the same extent. While DJA1 had little activity in luciferase refolding in vitro, DJA2 was able to promote refolding by Hsc70 to the greatest extent, and DJA4 had an intermediate effect. Nevertheless, DJA1 was more active than DJA2 in promoting luciferase expression in cell culture [60], although those effects were complicated by transcriptional effects. Then, to further study the substrate binding patterns and Hsc70 ATPase stimulation of DJA1 and DJA2, different chimeras of the proteins were used. A chimera with the J-domain and G/F linker of DJA1 attached to the central and C-terminal region of DJA2 was able to bind substrate and induce Hsc70 ATPase activity, but could not assist Hsc70-mediated folding. [61] This suggests that the J domain, G/F linker, and substrate-binding

domain within DJA1 and DJA2 may have to function together for proper protein activity indicating that there are interactions between the different structural units. Next, using a cell culture assay that reported directly on Hsc/p70-mediated folding, knockdown and overexpression experiments confirmed that DJA2 but not DJA1 was effective in promoting luciferase refolding. Then to address the functional mechanisms of DJA1 and DJA2, a recent study from our lab showed that the subdomain attached to the zinc finger motif, which is conserved in these type I HSP40s, is essential for folding activity and release of substrate triggered by the Hsc70 ATPase. Differences in the transfer kinetics are thought to contribute to the functional differences between DJA1 and DJA2. Interestingly, another chimera with the J domain of DJA1 fused to the G/F linker and central/C-terminal region of DJA2 now had some activity in assisting folding, suggesting that the linker may interact more closely with the substrate-binding region. [62]

1.1.1.1.2. NEF Family

The human and *S. cerevisiae* co-chaperone NEFs are structurally unrelated to the *E. Coli* NEF GrpE. This is surprising given the conservation in HSP70 and HSP40 proteins. In the human cytosol, NEF co-chaperones belong to three structurally unrelated families: the Bag (Bcl2-associated athanogene) family, the HSP110 family and HSPBP1 (HSP70 binding protein 1) (Figure 1.1E and Figure 1.1F). [63]

The Bag family consists of a multifunctional group of proteins that are involved in diverse functions ranging from apoptosis to tumorigenesis. While *S. cerevisiae* have one Bag-type NEF (Snl1), humans have five Bag family members (Bag1 to Bag5) that are in the cytosol and/or nucleus. Bag1 is the founding member of this family and the best studied. Its biological functions will be discussed in greater detail below. The Bag proteins are all distinguished by a

common conserved region near the C-terminus, termed the BAG domain, that mediates direct interaction with the NBD of Hsc/p70 and regulate its ATPase activity. In addition to the conserved BAG domain, the Bag proteins have several other divergent domains that are likely to modulate target specificity and Bag protein localization within the cells. [15,64] For example Bag1 is thought to play a role in substrate degradation because it possesses a ubiquitin-like (UBL) domain that is suggested to mediate interaction with the proteasome. [65] Contrary, Bag2 was shown to have an opposing effect by inhibiting the degradation of a client protein CFTR. [66] Bag3 has a WW domain and a proline-rich region, which mediates its interaction with inactive phospholipase C-γ (PLCγ) and modulates its activity.[67] Bag4 signals transduction pathways implicated in apoptosis by binding to the receptors that signal cell death, TNFR1 and DR3. [68] Bag5 associates with the E3 ubiquitin ligase Parkin and promotes associated substrate ubiquitination and thus degradation. [69]

Three cytosolic mammalian members belong to the HSP110 NEF family: Hsp110/Hsp105 (*HSPH1*), Apg1 (*HSPA4L*), and Apg2 (*HSPA4*). The main family member in the cytosol of human cells is Hsp110, and the counterpart Sse1 in *S. cerevisiae*. Homologous to Hsp70, the HSP110 proteins consist of a NBD connected by a flexible linker region to a SBD that is thought to bind substrate. Contrary to Hsp70 though, the HSP110 NBD lacks ATPase activity. [70] Therefore HSP110 proteins may function as "holdases" which prevent aggregation. [71-73]

Human HspBP1 was initially identified as an inhibitor of Hsc70 but it was later found to have NEF activity despite being different than the Bag domain; its *S. cerevisiae* ortholog is Fes1. [74-77]

In the following section, we will focus on the NEF that belongs to the Bag family, Bag1.

1.1.1.1.2a. *Bag Family NEFs*

The Bag1 protein was originally identified as a Bcl-2 binding partner that potentiates its anti-apoptotic function. [78] It was later found to stimulate nucleotide exchange on and modulate chaperone activity of both mammalian cytosolic Hsc70 and Hsp70 by binding their ATPase domains. [79-81] Bag1 exists in the mammalian cytosol as multiple isoforms produced from a single mRNA by alternative translation start sites. Three major Bag1 isoforms are expressed in human cells: Bag1L (~ 50 kDa), Bag1M (~ 46 kDa) and Bag1 S (~ 36 kDa) (Figure 1.2B). [82,83] A fourth Bag1 isoform of 29 kDa has also been identified but is often present in very low abundance or undetected. [84] The different isoforms are distinguished by the lengths of their amino termini. Various domains have been identified in this region and their presence or absence in distinct isoforms determines functional diversity as well as subcellular localization. A nuclear localization signal (NLS) is present in the unique N-terminus of Bag1L but is absent in Bag1M or Bag1S. Consequently, Bag1L localizes predominantly to the nucleus, whereas Bag1M and Bag1S are mainly found in the cytosol. [83] In addition, Bag1L and Bag1M possess a DNA-binding motif that is characterized by a cluster of lysine and arginine residues and is not sequence-specific, but Bag1S lacks this sequence. [59,85] Bag1S also lacks the functionally uncharacterized hexapeptide motif TRSEEX, whereas different numbers of this motif are present at the N-termini of Bag1L and Bag1M. Despite this heterogeneity at the N-terminus, the various Bag1 isoforms share a common C-terminus. All isoforms contain a UBL domain structurally related to the degradation marker ubiquitin, and a conserved region of about 110 aa termed the BAG domain. [86] Although the precise function of the UBL domain is unknown, it has been

suggested to interact with the proteasome thereby providing a link between the chaperone system and degradation machinery. [65] Meanwhile, the BAG domain plays a key role in mediating Bag1 functions since it contacts Hsc70 ATPase domain and regulates its chaperone activity. [79-81] Bag1 increases Hsc70 ATPase activity by stimulating the release of bound ADP from Hsc70 after an initial Hsp40-induced conversion of the chaperone into the ADP-bound form. [79] The crystal structure of the Bag domain in complex with the Hsc70 NBD reveals that Bag1, which forms a three-helix bundle, interacts with Hsc70 ATP-binding pocket through the second and third helices. This binding is electrostatic mainly mediated by residues Glu^{212}, Asp^{222}, Arg^{237}, and Gln^{245} in Bag1M. [87] These residues are highly conserved in all Bag proteins, and their individual substitution with alanine results in Bag mutants that are deficient in stimulating Hsc70 ATPase activity and therefore substrate release, consistent with a reduced affinity for the Hsc70 ATPase domain. [88]

The identification of Bag1 as an NEF for Hsc/p70 and a proteasome-binding protein provides a framework for understanding the various functions of Bag1. Many cellular functions were assigned for Bag1 ranging from protection from cell death, [89,90] to neuronal differentiation, [91] cell motility, [92] transcription regulation, [59,85,93] and stress signaling [94]. Bag1 interaction with a wide range of substrates enables it to impact all of these biological processes. For example its interaction with protein kinase Raf1 is of particular relevance for its stress signaling effects. [94] Steroid hormone receptors are another group of important Bag1 binding partners. [59,95-97] Furthermore, Bag1 induces opposing effects on different substrates for example it protects Tau protein from degradation [98] while it promotes BCR-ABL proteasomal [99] and CFTR lysosomal degradation. [100] Bag1 has also been reported to affect the ubiquitin-proteasome system as a whole, as its knockdown reduced the degradation of a GFP reporter fused to various degradation

signals. Knockdown of the related NEF Bag3 had the opposite effect but impaired autophagic degradation. Because the only similarity between Bag1 and Bag3 is in their BAG domains, and Bag3 contains several other domains with different functions, functional differences between the NEFs might be due to the domains and interactions specific to each. [101]

1.1.1.1.3. TPR-Domain Co-chaperones

Another class of co-chaperones interacts with Hsc/p70 through their TPR clamp domains, which recognize the C-terminal IEEVD motif of Hsc/p70. These, however, do not directly affect Hsc/p70 ATPase cycle. [102] One TPR clamp co-chaperone, C-terminus of HSP70-interacting protein (CHIP), has an E3 ubiquitin ligase activity and mediates Hsc/p70 substrate degradation through the proteasome. [103,104] Another TPR domain protein, HSP-organizing protein (Hop), links Hsc/p70 to Hsp90, which is essential to complete the folding of a subset of substrates. [105,106]

1.1.1.2. The HSP90 System

1.1.1.2.1. Hsp90 Structure and ATPase Cycle

The Hsp90 system functions downstream of the Hsp70 chaperone system in many cases, and plays an important role in the final maturation and conformational regulation of numerous signaling molecules and transcription factors. [107] In humans, the highly conserved Hsp90 chaperone family includes two cytosolic Hsp90 isoforms, Hsp90α and Hsp90β, both of which are constitutively expressed and stress inducible. [108,109] Hsp90 forms a homodimer, with each subunit consisting of three domains, an N-terminal domain that binds ATP, an extended central region with binding sites for client proteins and certain co-chaperones, and a C-terminal dimerization domain with an MEEVD motif that anchors TPR-domain co-chaperones. [1,105,108,110-112] Hsp90

appears to recognize its substrates in a near native state and thus at a late stage of folding. Similar to Hsp70, Hsp90 homodimer undergoes an ATP-driven reaction cycle that is accompanied by extensive conformational rearrangements. In the ATP-bound state, the N-terminal domains dimerize forming the Hsp90 molecular clamp. This results in a compaction of the Hsp90 homodimer in which the individual subunits twist around each other. In this closed state, Hsp90 is thought to support a substrate polypeptide along its side. After ATP hydrolysis, the N-termini dissociate resulting in the release of bound substrate and Hsp90 returns to its open V-shaped conformation. [113-117] Inhibition of ATP binding and hydrolysis either by mutagenesis of the NBD or by specific inhibitors such as geldanamycin and radicicol, demonstrated the functional requirement of the Hsp90 ATPase. [105]

1.1.1.2.2. Hsp90 Co-chaperones

Hsp90 operates as part of a highly evolved multi-chaperone machinery in the cytosol. It interacts with a variety of co-chaperone proteins that modulate different steps of the ATP-regulated reaction cycle. [102] The largest class of these co-chaperones possess a TPR domain and compete for binding to the MEEVD sequence motif at the extreme C-terminus of Hsp90. [118,119] The TPR domains have been identified fused to a range of other domains containing additional enzymatic activities such as peptidyl-prolyl isomerase (PPIase) domains (immunophilins and cyclophilins) and serine/threonine phosphatase 5.[120] Hsp90-binding TPR domains are also found attached to other TPR domains, which recognize Hsp70, and thus form a link between Hsp90 and Hsp70 (Hop and TPR2/DnaJC7). Hsc70 and Hsp70 contain a related motif at their C-termini, IEEVD, which is recognized by their specific TPR domains. [119,121] Another TPR-containing cofactor is CHIP, which was shown to link Hsp90 to the degradation machinery through

controlling substrate ubiquitination and proteasomal degradation, in parallel to its function with Hsc/p70. [103]

Other co-chaperones unrelated to the TPR-domain containing proteins bind the mature Hsp90 complexes. The Hsp90 cofactor, p23, facilitates substrate protein maturation by stabilizing the closed ATP-bound conformation of Hsp90. As a result, p23 partially inhibits ATP hydrolysis, which is indispensible for the release of bound polypeptide. The activator of Hsp90 ATPase (Aha1) stimulates ATP hydrolysis by Hsp90, although effects on substrate binding or release have not yet been directly addressed. [4,105,122-126]

1.1.2. Degradation Machinery

The ER, which is the site of entry for proteins destined to the secretory pathway, provides an oxidizing environment that facilitates nascent protein folding and assembly into their native structures with the help of a distinct set of molecular chaperones, folding factors, and covalent modifications. [127] Approximately one third of newly synthesized proteins in eukaryotes are targeted to the secretory pathway. Therefore, the folding environment in the ER must be able to accommodate a range of substrates that vary in their structural features, oligomerization state and rate of folding. This diversity underlies the requirement for a stringent protein quality control machinery that ensures proper folding and prevents the accumulation of misfolded and potentially toxic proteins. The importance of proper quality control (QC) is evidenced by the numerous human diseases that can arise from protein misfolding in the secretory pathway. [128] Endoplasmic reticulum-associated degradation (ERAD) consists of a collection of QC mechanisms charged with clearance of aberrantly folded proteins in the ER. ERAD substrates that have been integrated in the ER membrane or translocated into the lumen are

polyubiquitinated and eventually degraded by the ubiquitin-proteasome system (UPS). Substrate ubiquitination requires the cooperation of three enzymes, a Ub-activating enzyme (E1), a Ub-conjugating enzyme (E2), and a Ub-ligase (E3). However, translocating substrates from the ER lumen or membrane to the cytosol for degradation poses a topological problem of access since substrates are in a different compartment than the degradative proteolytic system. Therefore, the ERAD machinery spans the ER membrane and degradation is mechanistically coupled to translocation of substrates across the ER bilayer to the cytosol.

ERAD encompasses a sequence of events that can be divided into four distinct coupled steps: In the first step, substrate is recognized in the crowded ER environment (Substrate Recognition). This is followed by substrate dislocation across the ER lipid bilayer into the cytosol (Substrate Dislocation). On the cytosolic side of the ER membrane, the substrate is polyubiquitinated by membrane integrated E3 ligases (Substrate Polyubiquitination) and finally degraded by the 26S proteasome (Substrate Degradation) (Figure 1.3). [129]

1.1.2.1. Substrate Recognition

1.1.2.1.1. ERAD Substrates

ERAD substrates include misfolded proteins that have failed to reach their native structure due to mutations, translational misincorporation, or substoichiometric amounts of a binding partner. Certain folded, perfectly functional proteins are also targeted for degradation. This is part of regulatory ERAD through which the abundance of certain proteins is controlled in response to metabolic signals. Some viruses can also exploit the ERAD machinery to target host proteins towards destruction and thus evade detection by the immune system. Moreover, some

Figure 1.3. Steps involved in ERAD. ERAD can be divided into four distinct steps. Step 1: Substrate Recognition: Molecular chaperones and lectins residing in the ER lumen interact with misfolded substrates and bind adaptor proteins that link aberrantly folded proteins to the dislocation machinery. Step 2: Substrate Dislocation: Substrates are thought to be transferred across the ER lipid bilayer through dislocons that form proteinaceous pores. This process is coupled to the energy derived from ATP hydrolysis by p97/VCP. Step 3: Substrate polyubiquitination: Once in the cytosol substrates are ubiquitinated by E3 ubiquitin-ligases. Step 4: Degradation: In the final step substrates are degraded by the 26S proteasome. (Figure 1.3 modified from [127])

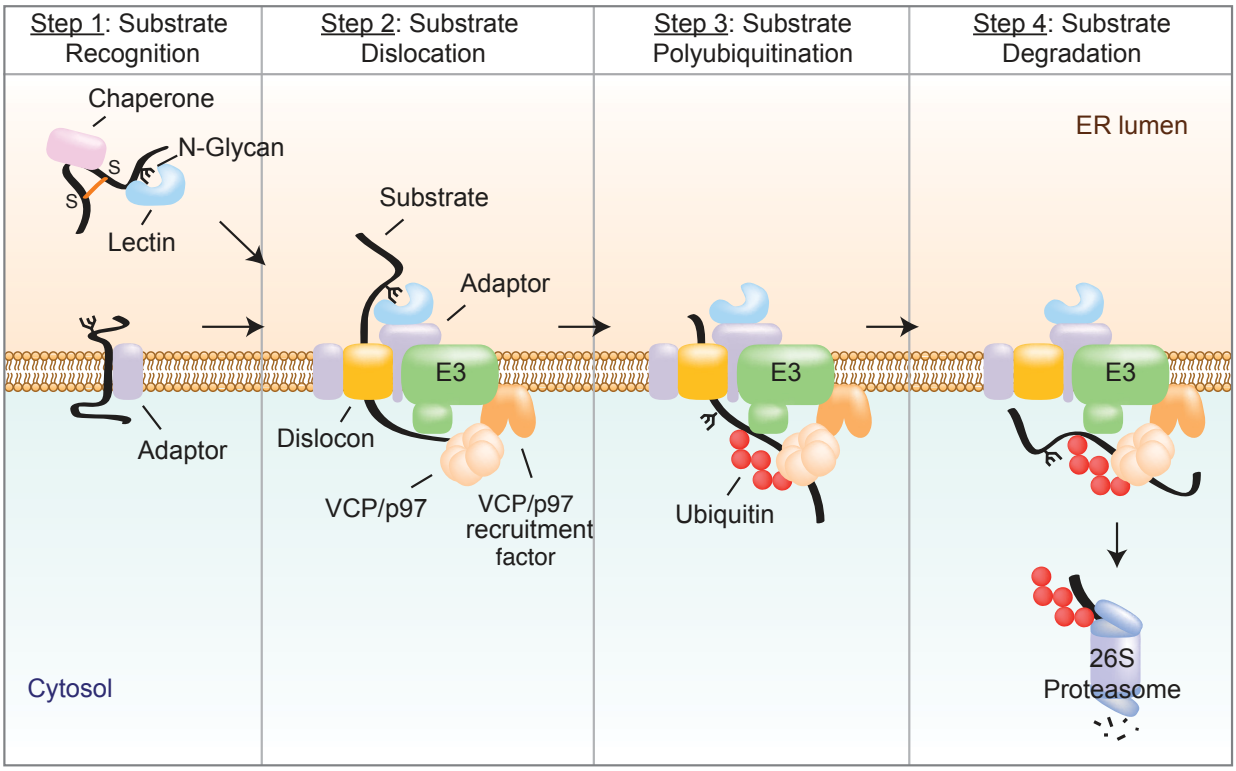
Step 1: Substrate Recognition
Step 2: Substrate Dislocation
Step 3: Substrate Polyubiquitination
Step 4: Substrate Degradation
Chaperone
N-Glycan
S
S
Lectin
Adaptor
Substrate
Adaptor
E3
Dislocon
VCP/p97
VCP/p97 recruitment factor
E3
Ubiquitin
E3
ER lumen
26S Proteasome
Cytosol

bacterial toxins use the ERAD components to escape the ER lumen and reach the cytosol where they ultimately act.

1.1.2.1.2. N-Glycans as Sensors of Glycoprotein Folding

The vast majority of proteins that traverse the eukaryotic secretory pathway are glycoproteins. As they enter the ER lumen, these proteins are modified at asparagine (Asn) residues found in the Asn-X-Ser/Thr sequence by the addition of branched core oligosaccharides composed of three glucose, nine mannose, and two N-acetylglucosamine residues, Glc_3–Man_9–$GlcNAc_2$. The glycan moieties play a central role in the QC system, which surveys the conformational maturation of the proteins where those that are properly folded are sent to the ER exit sites from which they are deployed to other compartments in the secretory pathway, while those that are misfolded are directed for destruction through ERAD. [130] Early glycan processing enzymes such as glucosidases I and II, deglucosylate the glycan moieties to Glc_1–Man_9–$GlcNAc_2$. The lectin chaperones calnexin (CNX) or calreticulin (CRT) specifically bind the single glucose moiety, and facilitate the oxidative folding of newly synthesized proteins through recruitment of the thioredoxin (protein disulfide isomerase) ERp57. Further deglucosylation removes the remaining glucose residue from the N-glycan, thereby allowing the release of the glycoprotein from CNX/CRT, enabling the protein to progress to the ER exit sites. Proteins that have failed to acquire their native structure are substrates of an enzyme UDP-glucose/glycoprotein glucosyl transferase (UGGT) that reglucosylates incompletely folded glycoproteins on the Man_9–$GlcNAc_2$ glycan, and therefore returns them to CNX/CRT for further rounds of oxidative folding. This cycle retains improperly folded glycoproteins in association with the folding machinery in the ER and underlies the mechanism of oxidative folding of

proteins with very different folding rates. [131] If a glycoprotein fails to fold, as a result of a mutation for example, it escapes the CNX/CRT cycle and is directed towards ERAD. This escape is due to the action of ER-resident mannosidases, which progressively trim terminal mannose residues from core glycans, triggering the binding of a second set of mannose specific lectins that engage the protein in ERAD. [132] Sequential removal of terminal mannose residues by ERManI, [133,134] EDEM1, [135,136] EDEM3, [137,138] or Golgi-resident Man1C1 [139] results in glycoproteins with deglucosylated, demannosylated glycans which therefore cannot be reglucosylated by UGGT. This glycan signature differentiates terminally misfolded proteins from their folding competent counterparts.

1.1.2.1.3. Mannose-Specific Lectins Couple Glycoprotein Structure to ERAD

The soluble ER-resident proteins OS-9 and XTP3-B use their glycan-binding domains, the mannose-6-phosphate receptor homology (MRH) domains, to interact with trimmed oligosaccharides produced by ERManI/EDEM1-3 in misfolded glycoproteins. [140,141] OS-9 and XTP3-B share little sequence homology beyond the MRH domain, which suggests that they may not serve as functional paralogs. Individual downregulation of these lectins has generally no or mild effects on stabilization of ERAD substrates. [138,142,143] Knockdown of both lectins, however, slowed the degradation of model lumenal ERAD substrates, which suggests that OS-9 and XTP3-B are interchangeable and functionally redundant. [143]

Although the vast majority of secretory pathway proteins are N-linked glycoproteins and glycans represent a common feature for recognition, naturally occurring non-glycosylated misfolded proteins are also directed towards ERAD. Therefore, features in addition to oligosaccharide removal may target misfolded proteins to ERAD. Indeed, both ERAD factors

OS-9 and XTP3-B bind non-glycosylated proteins and contribute to their diversion to degradation. A recent study revealed that an amyloidogenic mutant of the naturally nonglycosylated protein transthyretin (TTR-D18G) induces exposure of a cryptic N-glycosylation site that triggers posttranslational STT3B-dependent N-glycosylation and EDEM3-mediated N-glycan-dependent ERAD. [144] Therefore, it is plausible that posttranslational glycosylation may shift the degradation of non-glycosylated proteins from an N-glycan-independent to an N-glycan-dependent ERAD pathway. Alternatively, ERAD of glycoproteins may depend on a dual recognition signal provided by both trimmed glycans and unfolded segments within a substrate. [145] XTP3-B and OS-9 associate with BiP, the ER lumenal Hsp70 form, an interaction that may allow these lectins to identify misfolded regions independent of N-glycan recognition. [141] In addition to their glycan recognition capacity, XTP3-B and OS-9 may also bind polypeptide. [138] In mammals, Grp94, the Hsp90 homolog in the ER, interacts with OS-9 [142] although with very few identified substrates requiring this chaperone interaction so far. [146,147] It is therefore plausible that Grp94 together with OS-9 and XTP3-B may play a role in ERAD substrate recognition.

1.1.2.2. Substrate Dislocation

Despite being structurally different, all ERAD substrates whether lumenal or membrane embedded must be dislocated to the cytosol to be degraded by the UPS. Since many ERAD substrates are extremely hydrophobic proteins, it is crucial to tightly couple these two processes of dislocation and degradation. This coupling is reflected by the fact that membrane-integrated ubiquitin ligases are at the center of the ERAD machinery, where they link substrate dislocation to degradation, and are thought to form part of the channels or dislocons through which

substrates are translocated. ERAD substrates are recruited to the dislocons through adaptor proteins that recognize a variety of features that characterize substrates committed to degradation.

1.1.2.2.1. SEL1L Is an Adaptor that Links Glycan Recognition to the Dislocon

Most substrates committed to ERAD through the lectins OS-9 or XTP3-B are soluble lumenal glycoproteins although some are membrane integrated with lumen-exposed domains. SEL1L is an ER-resident glycoprotein that links ERAD-substrate recognition factors within the lumen to HRD1, a transmembrane protein proposed to form part of the dislocon and possesses a RING finger domain at the cytosolic side with E3 ubiquitin ligase activity. [148] SEL1L associates with OS-9 and XTP3-B, [14-16] EDEM1, [149] and EDEM3. [148,149] SEL1L is therefore part of the HRD1 ubiquitin ligase complex that provides a scaffold through which many ERAD components associate including Derlin-1, Derlin-2, AUP1, UBXD8, VIMP, and Herp, [141,142,150-154] which consequently recruits the p97/VCP complexes required for dislocation. Reduction of the levels of SEL1L inhibits the degradation of both lumen-resident and membrane-integrated ERAD substrates irrespective of their glycosylation state. [142,143,150,154,155] Similar to its yeast ortholog Hrd3p, SEL1L is absolutely required to transfer substrates from ER lectins to the E3 ubiquitin ligase HRD1. [142,156-158] SEL1L, therefore, serves as a critical component of the ERAD machinery that links substrate recognition with its dislocation.

1.1.2.2.2. Erlins May Be Intramembrane Substrate Adaptors

Erlin1 and Erlin2 are stomatin, prohibitin, flotilin, and HflC/HflK (SPFH) domain-containing proteins that form a heteromeric ER membrane complex of ~2MDa. The Erlin1/2 complex binds to inositol 1,4,5-triphosphate receptors (IP_3R) after their stimulation and recruits

the E3 ubiquitin ligase RNF170, which mediates IP_3R ubiquitination and degradation in response to Ca^{2+}-dependent signals that promote receptor downregulation. [159-161] Erlin1/2 role as adaptors is not only limited to linking RNF170 and IP_3Rs. They also associate with other E3 ligases such as gp78, HRD1, and TRC8. [154,162] Another ER membrane protein TMUB1 (transmembrane and Ub-like domain-containing 1) bridges gp78 to Erlin2 and mediates sterol-induced ERAD of the cholesterol biosynthetic enzyme 3-hydroxy-3-methyl-glutaryl-CoA reductase (HMG-CoAR). Knockdown of either gp78 or TMUB1 impairs sterol-induced ubiquitination and degradation of endogenous reductase. [162] Therefore, Erlin1/2 are key ERAD pathway components in mammalian cells that act as a substrate recognition factors.

1.1.2.2.3. Insigs Are Client-Specific Adaptors

HMG-CoAR sterol-accelerated degradation is also achieved through the sterol-induced interaction of the reductase with an ER membrane protein Insig-1. When sterol levels are high, formation of the HMG-CoAR:Insig-1 complex results in the recruitment of gp78, which ubiquitinates the reductase leading to its dislocation to the cytosol through the VCP/p97-Ufd1-Npl4 complex and ultimately its proteasomal degradation. [163-165] Both Insig-1 and related Insig-2 also bind another E3 ubiquitin ligase TRC8, which leads to sterol-induced ubiquitination and proteasomal degradation of the reductase, HMG-CoAR. [166,167] Insig-1, but not Insig-2, degradation is in turn sterol-regulated. When sterol levels are high, Insig-1 binds to another ER membrane protein SREBP cleavage-activating protein (SCAP), which protects Insig-1 and prevents it from ubiquitination through gp78. Consequently, this results in an increase in HMG-CoAR ERAD through the E3 gp78 ubiquitin ligase complex. Conversely, when sterol levels are

low, Insig-1 remains unprotected by SCAP and is degraded, preventing HMG-CoAR degradation and permitting cholesterol biosynthesis. [168]

Similar to mammals, the yeast HMG-CoAR homologue, Hmg2, is subjected to sterol-regulated degradation controlled by the Insig-like proteins, Nsg1 and Nsg2, and requires the E3 ligase Hrd1. [169,170] Nevertheless, contrary to the case in mammalian cells, Hmg2 binding to Nsg1 promotes Hmg2 stabilization, which implies that substrate recognition is mechanistically different in the two systems. [171]

Another enzyme of the sterol biosynthetic pathway that is subject to regulated ERAD in both yeast and mammals is squalene monooxygenase (SQLE). The sterol dependent degradation of this monooxygenase is mediated by the yeast E3 ligase Doa10 or its mammalian homologue Teb4 and Insigs seem to be dispensible. [172,173] Therefore, sterol biosynthesis is tightly controlled through two different branches of the ERAD pathway.

The ubiquitin ligases, whether together with the Insigs or on their own, play an important role in the regulation of the sterol biosynthetic pathway and reestablishment of membrane lipid homeostasis through tightly regulating the ERAD of different sterol biosynthetic enzymes.

1.1.2.2.4. F-Box Proteins Capture Dislocated Glycoproteins in the Cytosol

Fbx2/Fbs1 and Fbx6/Fbs2 are members of the F-box protein family that act as adaptors that recognize high mannose N-glycans in ERAD substrates and link then to SCF (Skp1-Cullin-Fbox) E3 ubiquitin protein ligases. [174,175] Glycoproteins are usually deglycosylated upon cytosolic exposure through the action of an amidase NGly1/PNGase. [176] Some N-glycans, however, evade the NGly1 and are therefore recognized by F-box proteins as a backup recognition mechanism for cytosolically exposed glycoproteins.

1.1.2.2.5. Viral-Encoded Adaptors

Some viruses use their host ERAD machinery to target specific folded proteins to degradation by substrate-specific adaptors. For example, the human immunodeficiency virus (HIV-1) encodes the adaptor glycoprotein Vpu, which targets CD4 to ubiquitination and degradation through the SCF ubiquitin ligase complex. [177,178] Another example is the human cytomegalovirus (HCMV), which encodes two adaptor proteins US2 and US11, both of which are classified as immunoevasins since they bind to newly synthesized major histocompatibility complex (MHC) class I heavy chains (HC) and induce their degradation, thereby enabling virus-infected cells to evade the immune system. [179] MHC class I molecules are composed of two subunits: MHC class I HC and β2-microglobulin (β2m), which if properly assembled together are trafficked to the cell surface. In case MHC class I HCs fail to assemble with β2ms, they are targeted for degradation through the E3 ligase HRD1 and E2 Ub-conjugating enzyme UBE2J1. [180] However, the presence of HCMV-encoded US2 adaptor protein reroutes MHC class I HC degradation to another ERAD pathway that involves the TRC8 (translocation in renal carcinoma, chromosome 8 gene) E3 Ub-ligase complex. [181,182] When the immunoevasin US11 is involved, MHC class I degradation depends on a complex that contains SEL1L, [150] Derlin-1, [183] and other HRD1 cluster components such as UBE2J1, AUP1, and UBXD8. [151]

1.1.2.2.6. The Enigmatic Dislocon

Different proteins are required for substrate dislocation and therefore were suggested to form the dislocon based on their multitransmembrane domains and their immediate interaction with ERAD substrates. These include the Derlins 1-3, [183,184] signal peptide peptidase, [185] Sec61, [186,187] and the E3 ligase HRD1. [148] Current focus is on either the Derlins or HRD1, all of which

have multiple transmembrane helices. Recently, crosslinking in live yeast was used to show that a misfolded lumenal protein interacted with the transmembrane interior of Der1, the yeast homolog of Derlin-1, as a necessary first step in its dislocation. Der1 binding occurred after interactions with Hrd3 (yeast SEL1L) and before ubiquitination by Hrd1, overall suggesting that Der1 is the disolocon in the complete Hrd1 complex. [188] In contrast, another recent study reconstituted the same model protein into artificial liposomes containing only purified yeast Hrd1, and dislocation was observed upon addition of an E1 ubiquitin activating and an E2 conjugating enzyme, Cdc48 (yeast VCP/p97), Ufd1 and Npl4. Hrd1 was the only transmembrane protein in the liposomes, and therefore it was proposed to be the minimum dislocation machinery. [189] Further studies will be needed to reconcile these ideas. In addition, it is possible that different substrates require specific dislocons, for example, signal peptide peptidase is involved in MHC class I HC dislocation degradation is induced by US2, but not by loss of β2m. [180,185]

1.1.2.2.7. What drives dislocation?

VCP/p97 is a homohexameric AAA+ ATPase protein that is essential for ERAD. p97 couples the energy from ATP hydrolysis to substrate unfolding and extraction from the ER membrane and is thought to be crucial for dislocation of most ERAD substrates. [190] This is illustrated by the stabilization of nearly all ERAD substrates tested upon removal or inhibition of p97. [191-194] p97 is cytosolic, however, so it does not have the opportunity to bind lumenal proteins before they are partially translocated across the membrane. It is possible that long polyUb chains provide the first interactions with p97, through its cofactors Ufd1 and Npl4. [195] The energy required to initiate protein translocation prior to this remains enigmatic although it is

possible that p97 produces this effect through inducing conformational changes in transmembrane components of the dislocation complex.

1.1.2.3. Substrate Polyubiquitination and Degradation

1.1.2.3.1. Ub E3 Ligases Implicated in ERAD

Two main ER resident transmembrane really interesting new gene (RING) domain E3 ligases, HRD1 [196,197] and gp78, [198] primarily define mammalian ERAD. Other E3 ligases are involved in the degradation of more specific substrates. These E3 ligases include TEB4/MARCH6, [199] RNF5/RMA1, [200,201] TRC8, [181,182] RFP2/TRIM13, [202,203] Kf-1/RNF103, [204] Nixin, [205] and RNF170. [161] Other cytosolic E3 ligases are also implicated in ERAD. These include Parkin, [206] CHIP, [104] SCF complexes with the F-box proteins Fbx2, Fbx6 [174,175] and β-TrCP1/2, [207] Smurf1, [208] and Nrdp1 [209] have also been implicated in ERAD. Furthermore, another 15 ER localized membrane-spanning E3s with a RING-finger domain await confirmation for a role in ERAD. [205]

1.1.2.3.2. Cooperativity among E3 Ub-Ligases

Several ligases are required for complete processing of an ERAD substrate. There are different possibilities for this cooperativity. Multiple E3s might act in parallel when they have the same specificity for the substrate, either simultaneously to ubiquitinate the substrate at different sites, cooperatively where one is required first for an initial monoubiquitination followed by an elongation through what has been termed an E4 activity, or through sequential rounds of substrate ubiquitination and de-ubiquitination. [210] For example, TRC8 and gp78 cooperate to degrade HMG-CoAR through sterol-induced binding to Insig-1/2. [166] Alternatively,

RMA1 and CHIP act sequentially on different regions of misfolded CFTRΔF508. [200] RMA1 might also act as an E3 important for primary ubiquitination of CFTRΔF508 that is followed by ubiquitin chain extension by gp78, in an E4-like activity. [201] There is also evidence that two discrete rounds of ubiquitination are required between dislocation and degradation. The deubiquitinating enzyme YOD1 removes polyUb from several model substrates, allowing VCP/p97 to act by threading the polypeptides through its central pore. The substrates then must be re-ubiquitinated by E3 or E4 activities to be targeted to the proteasome. [211]

In addition to substrate ubiquitination, E3s could also ubiquitinate each other as a negative feedback mechanism where monoubiquitination represents a form of ERAD tuning that regulates the activity of an existing E3 pool and polyubiquitination regulates the size of an available pool of E3s through degradation. [166,201,212,213]

1.1.2.3.3. Multiple Adaptors Recruit VCP/p97 to Components of the ERAD Machinery

VCP/p97 is involved in a variety of cellular processes through its different associations with a large number of interaction partners and is tightly coupled to proteasomal degradation of misfolded ER proteins. The p97 cofactors required for most ERAD substrates are Ufd1 and Npl4, which recognize polyUb. [190,191] However, there are cases in which p97 acts without Ufd1 and Npl4, for example in US2-induced degradation of MHC class I HC. [214] Multiple membrane-embedded ERAD components have p97-binding motifs. These include UBX domains (UBXD2 [215] and UBXD8 [216]), VIM motifs (gp78 [217] and VIMP [184]), SHP boxes (Derlin-1 and Derlin-2 [218]), and unknown cytosolic domains of HRD1 and VIMP. [219]

In addition to its role in substrate dislocation, p97 acts as a scaffold that links the extracted substrates to cofactors in the cytosol that further modify and process them. For example, the deglycosylating enzyme PGNase interacts with p97 through its PUB (PNGase/UBA or UBX) domain and is therefore recruited to the dislocation complex to remove N-glycans from ERAD substrates thereby facilitating proteasomal clearance. [220] VCP/p97 also associates with de-ubiquitinating enzymes (YOD1, VCIP135, Usp19, and Ataxin-3), and a dedicated E4 ubiquitin extension enzyme (Ube4a) that have been implicated in ERAD.

1.2. Protein Misfolding Diseases

After having explained the components of the PN in details in the previous sections, we will discuss the involvement of this machinery in two protein misfolding diseases that we study in our lab:

- Cystic Fibrosis
- Long QT Syndrome.

1.2.1. Cystic Fibrosis

1.2.1.1. CFTR Structure and Function

CF, the most common autosomal recessive lethal genetic disease in the Caucasian population with an incidence of approximately 1 in 2000 Caucasians, is due to loss of function mutations of the CFTR protein. [221,222] CFTR is a polytopic transmembrane glycoprotein that belongs to the superfamily of ATP-binding cassette (ABC) transporters. It functions as a Cl^- channel regulated by cAMP-activated phosphorylation at the plasma membrane of secretory

epithelia in the airways, intestine, pancreas, testis and exocrine glands, as well in some non-epithelial cell types. The 1480 aa CFTR polypeptide chain is composed of two membrane-spanning domains (MSD1 and MSD2) with six transmembrane domains each, two nucleotide-binding domains (NBD1 and NBD2) that bind to and hydrolyze ATP, and a regulatory R domain with phosphorylation sites that regulate channel gating (Figure 1.4A). [223] The loop between TM7 and TM8 contains two N-linked glycosylation sites. Although approximately 2000 different CF-causing CFTR mutations have been identified (http://www.genet.sickkids.on.ca/cftr) deletion of the phenylalanine residue at position 508 (ΔF508), is by far the most common and is present in one or both alleles in nearly 90% of CF patients in some populations. [224] CFTR mutations result in a loss-of-function phenotype by inhibiting the translation of the full-length protein or disrupting CFTR folding and stability as well as Cl^- channel function. As discussed below, the ΔF508 mutation interferes with CFTR folding and trafficking. [221]

1.2.1.2. Classes of CFTR Mutations

CFTR mutations are divided into five distinct classes based on the specific defect they cause in CFTR biogenesis or trafficking. This division is critical when considering multiple CF therapies. Class I mutations affect biosynthesis leading to elimination of CFTR production and thus prevents proper synthesis of full-length, normal CFTR protein. Class II mutations affect protein maturation/post-translational processing resulting in lack of functional CFTR at the cell surface due to defects in folding or trafficking. Class III mutations affect Cl^- channel regulation/gating producing a channel that traffics to the cell surface but does not respond to cAMP. Class IV mutations affect Cl^- conduction leading to complete or partial inhibition of Cl^- conduction. Class V mutations result in a reduction in synthesis of a normal CFTR transcript

Figure 1.4. hERG and CFTR Structure. A, Schematic of CFTR chloride channel that has 2 membrane-spanning domains (MSD1 and MSD2), 2 nucleotide-binding domains (NBD1 and NBD2) and a regulatory R domain. B, Schematic of a hERG subunit that consists of a Per-Arnt-Sim (PAS) domain, 6 transmembrane domains and a cyclic nucleotide binding domain (cNBD); hERG functional channels form tetramers. C, Schematic of the secretory pathway adapted from Alberts, B. et al., Molecular Biology of the Cell, 5th edn., 751. (Garland Science,2008).

A.

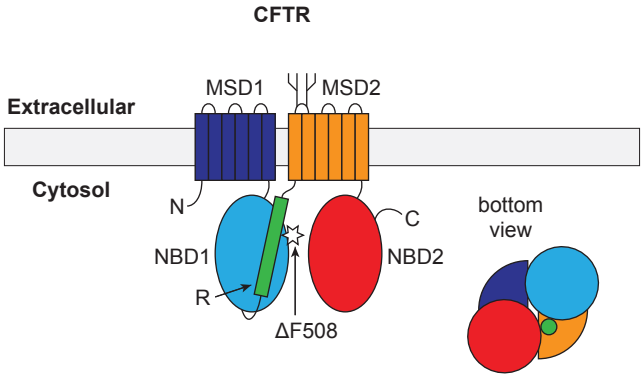
CFTR
Extracellular
Cytosol
MSD1
MSD2
N
C
NBD1
NBD2
R
ΔF508
bottom
view

B.

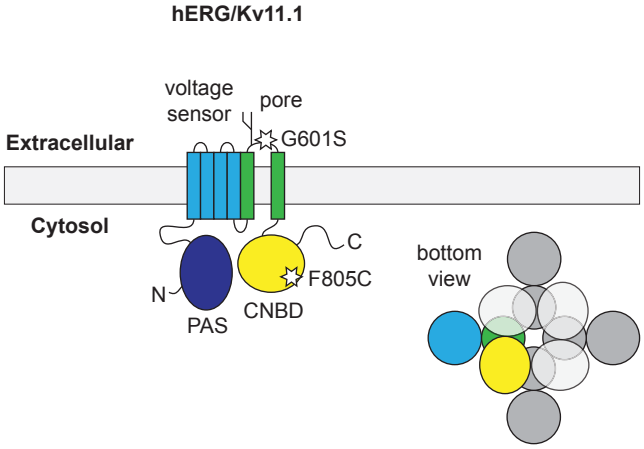
hERG/Kv11.1
voltage
sensor
pore
G601S
Extracellular
Cytosol
C
F805C
N
PAS
CNBD
bottom
view

C.

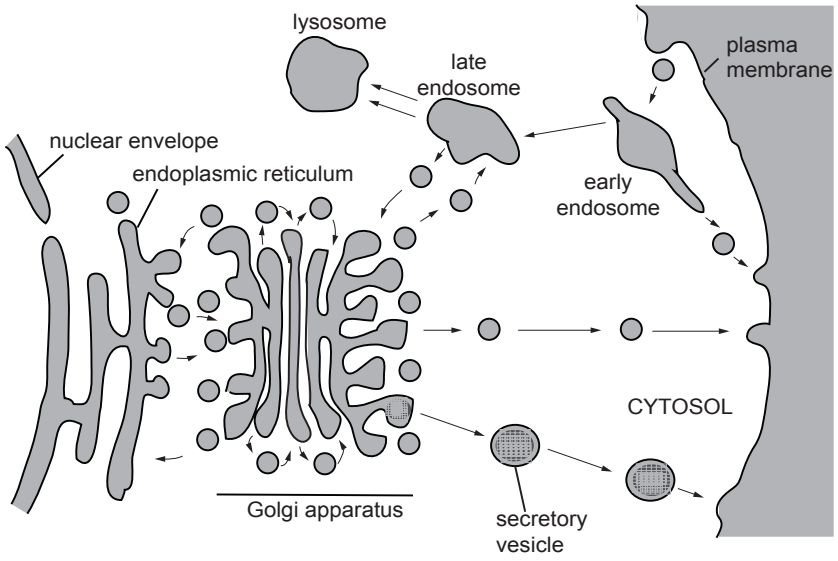
lysosome
late
endosome
plasma
membrane
nuclear envelope
endoplasmic reticulum
early
endosome
CYTOSOL
Golgi apparatus
secretory
vesicle

therefore producing less normal CFTR. [225,226] Another class was also suggested which affects protein stability at the cell surface leading to increased CFTR protein turnover at the cell surface, but this may overlap mechanistically with Class II.

1.2.1.3. CF Physiology

CF is a complex multisystem disease that affects epithelia in several organs and results in various pathologies such as chronic lung infection with progressive deterioration of lung function, pancreatic insufficiency, hepatobiliary disease, male infertility, and meconium ileus in infancy. [222] The life expectancy of individuals with CF has enhanced considerably over the past few decades. Currently, the median predicted age of survival for patients with CF is around 40 years in the US, with pulmonary disease as the main reason of morbidity and mortality (Cystic Fibrosis Foundation 2012 Patient Registry Report at http://www.cff.org/). Various therapies aimed at treating CF symptoms have emerged including antibiotics, anti-inflammatories mucolytic drugs, inhaled hypertonic saline, pancreatic enzyme replacement, and lung transplantation. [227] New mechanism-based therapies that treat the key mechanisms in CF disease pathogenesis or target the underlying defects involved in CFTR loss-of-function are currently in development. This however requires a thorough understanding of how loss of CFTR function leads to CF disease, in particular CF airway disease.

The origin of lung pathology is not well understood, which has generated multiple theories supporting diverse pathogenic mechanisms including reduced airway surface liquid (ASL) volume. Over the past decade mounting evidence from research data on cultured human bronchial cells and mouse models as well as human clinical trials suggests that CF lung disease is initiated as a result of airway surface dehydration. [228] The airways are lined with a thin film of

fluid, the ASL, that possesses two components, the periciliary liquid (PCL) or the sol layer, which surrounds the cilia and lines the surface epithelial cells, and the mucous component above it, which traps inhaled particles. The role of the PCL is to provide a low-viscosity watery microenvironment to permit proper cilia function in clearing inhaled particulate matter trapped by the mucous. This is a vital process that plays a major role in defending the lung against infection. [229] In normal airways, the length of the PCL is approximately that of the outstretched cilia (~7 μm), whereas the height of the mucous layer varies considerably (7 to 70 μm in vivo). [230,231] In contrast, in CF lungs, the PCL almost disappears and the mucous sits on the cilia and prevents them from beating properly thereby rendering them ineffective at clearing the airways, resulting in the arrest of mucociliary clearance. This provides an environment for infection particularly by *Pseudomonas aeruginosa*. These organisms are difficult to eliminate in CF patients, but are harmless in normal individuals. [228] In CF lungs, the reduction in ASL volume leading to pulmonary disease pathogenesis is due to a deficiency in CFTR function, which results in ion transport imbalance in the airways. This imbalance is a result of reduced Cl^- secretion into the airway lumen by epithelial cells and unregulated Na^+ absorption through the epithelial Na^+ channel (ENaC). The result is an increase in Na^+ absorption from the apical surface leading to a concomitant decrease in water in the airway and thus ASL dehydration (Figure 1.5A). [227]

Despite our incomplete knowledge of the mechanisms of CF pathogenesis, it is widely accepted that restoring ΔF508-CFTR surface expression by correcting its folding alleviates CF organ pathology. ΔF508 mutation belongs to the Class II group of mutations. F508 is located in NBD1 of CFTR and its deletion results in protein misfolding, which limits its escape from the ER and reduces its stability at the cell surface thereby resulting in its degradation. Given the

Figure 1.5. Underlying mechanisms for CF and LQT2. A, Schematic showing the mechanism by which loss of CFTR function leads to pulmonary disease in CF patients. B, Schematic showing the temporal relation between cardiac action potential (phases 0-4) and the QT interval on the surface electrocardiogram (ECG). The QT interval is prolonged in LQT patients.

A.

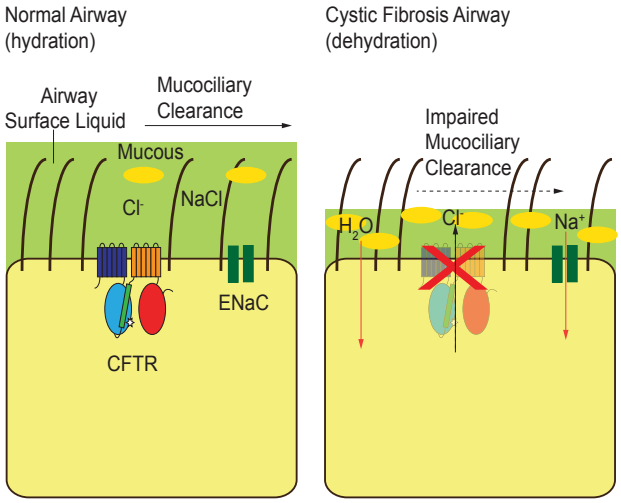
Normal Airway
(hydration)
Cystic Fibrosis Airway
(dehydration)
Airway
Surface Liquid
Mucociliary
Clearance
Mucous
Cl-
NaCl
ENaC
CFTR
Impaired
Mucociliary
Clearance
H2O
Cl-
Na+

B.

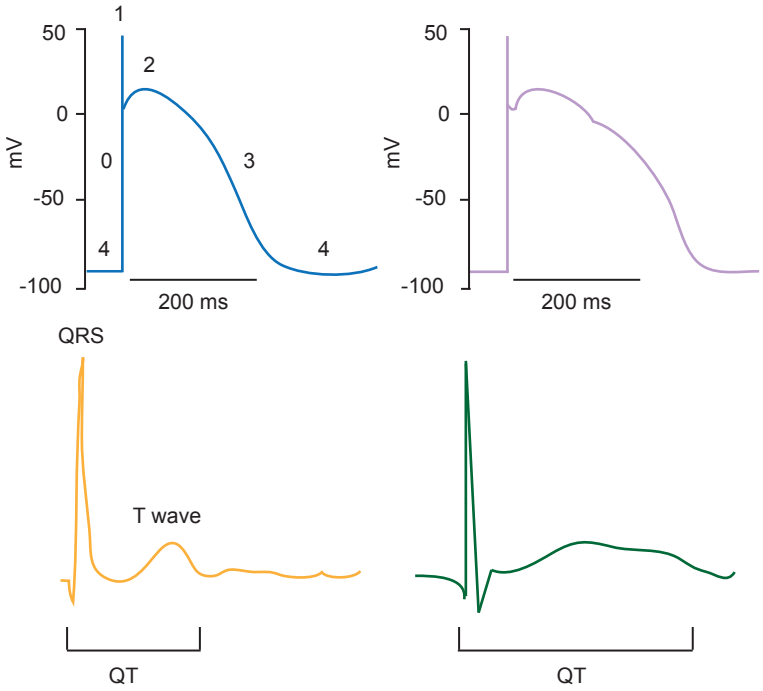
50
0
-50
-100
mV
1
2
0
3
4
4
200 ms
50
0
-50
-100
mV
200 ms
QRS
T wave
QT
QT

cooperative folding mechanism of CFTR, ΔF508 mutation not only leads to local misfolding in NBD1 but also induces global misfolding by interfering with intramolecular domain-domain interactions. [221,232-234]

1.2.1.4. CFTR Biosynthesis

CFTR biogenesis starts with its co-translational insertion into the ER membrane where N-linked glycosyl groups are added at two asparagine residues 894 and 900 on a consensus Asn-X-Ser/Thr sequence located in the 4th extracellular loop thus constituting the core-glycosylated form also known as band B of 140–150 kDa. If it is properly folded, this immature form of CFTR is transported to the Golgi apparatus by COPII (coat protein II)-coated vesicles. Once in the Golgi, CFTR acquires different modifications at its glycan moiety to produce the fully glycosylated mature form, also known as band C, of about 170–180 kDa. [235] Mature CFTR is then trafficked to the apical membranes of epithelial cells where it forms functional interactions, such as with PDZ (PSD-95, Dlg, ZO-1) domain proteins, and becomes activated. [223] However, if newly synthesized CFTR is improperly folded, it is recognized by the ERQC machinery, retained at the ER and sent for ERAD through the UPS (Figure 1.4C). [236,237]

1.2.1.4.1. CFTR Chaperone System

1.2.1.4.1a. *ERQC Machinery*

A significant fraction of newly synthesized WT CFTR (up to 70% in many cell models) as well as inefficiently folded ΔF508 CFTR (~99%) is degraded by the UPS after being dislocated from the ER to the cytoplasm. Molecular chaperone and co-chaperone complexes can sense the folded state of CFTR and either assist folding or promote ubiquitination-dependent

degradation. How the result is determined is still unclear, but the biophysical details and dwell-time of the chaperone-CFTR interaction are most likely the key factors. Cytosolic chaperone complexes composed of Hsc/p70 and Hsp90 in concert with a subset of their co-chaperones, such as DJA1 [55], HspBP1 [238], Hop [239], and p23 [240], comprise the two main cytosolic folding machineries that monitor the folding state of the cytosolic domains of CFTR. [241-243] Hsp90 has been directly shown to be required for the folding and trafficking of CFTR, and its co-chaperones Aha1 and p23 act to inhibit and promote CFTR trafficking, respectively. [240,241] The functional evidence for Hsc/p70 is less direct: DJA1 assists Hsc70 in stabilizing the NBD1 domain, and is important for CFTR trafficking in cells. [55,244] The lumenal chaperones CNX and CRT retain CFTR folding intermediates at the ER until their folding cycle or degradation is completed, but do not appear to actively promote CFTR folding. [245,246] Furthermore, N-linked core glycans physically stabilize the native CFTR conformation. [247]

Ubiquitination, a necessity for CFTR ERAD, depends on the rate of ubiquitin conjugation and de-ubiquitination. Different E3 ubiquitin ligases are involved in the co- and post-translational ubiquitination of misfolded CFTR. These recognize misfolding in different ways, with chaperone involvement through different mechanisms. The transmembrane E3 ubiquitin ligase Rma1 recognizes misfolded CFTR co-translationally and targets it for ERAD. [200] gp78, another transmembrane E3 ligase, assists possibly by extending polubiquitin chains on CFTR initiated by RMA1. [201] The ER-associated Hsp40 protein DnaJB12 cooperates with cytosolic Hsc70 to promote RMA1 activity. [244] Alternatively, the cytosolic E3 ligase CHIP targets misfolded CFTR post-translationally for degradation, and requires Hsc70 binding to CFTR. [104,200] UCH-L1 (ubiquitin C-terminal hydrolyse-L1) and Usp19 (ubiquitin specific protease 19) catalyze polyUb cleavage, thereby stabilizing misfolded CFTR. [248,249] The cytosolic E3 ligases

Nedd4-2 and Fbs1 are also involved in misfolded CFTR ERAD, and appear to be chaperone-independent. [175,250]

1.2.1.4.1b. *Peripheral QC Machinery*

In addition to being detected by the ERQC, which promotes its ERAD, misfolded CFTR is also recognized by a peripheral quality control (PQC) system that promotes its endocytosis and lysosomal degradation. CHIP was also shown to be a key factor in misfolded CFTR PQC, in concert with a distinct set of chaperones and co-chaperones such as Hsc70, DJA1, and Bag1. [100] In addition the E3 ligase c-Cbl was also implicated in WT CFTR endocytosis. [251] Conversely, activation of Usp10, a deubiqitination enzyme, stabilizes WT CFTR by assisting its recycling. [252]

1.2.2. Long QT Syndrome

1.2.2.1. Long QT and Cardiac Action Potential

LQT syndrome is an autosomal dominant congenital cardiac disorder characterized by an abnormal lengthening of the QT interval on the surface electrocardiogram (ECG) (≥450 ms in men and ≥460 ms in women) (Figure 1.5B). [253] The incidence of congenital LQTS is estimated at about 1:3000 in the general population. Affected individuals have an increased propensity to ventricular arrhythmias such as torsades de pointes (TdP), which may lead to syncope, seizures and sudden death mainly precipitated by emotional or physical stress. [254] The QT interval on the ECG reflects the depolarization and repolarization phases of the ventricular action potential, which is determined by the concerted interplay of several ion channels. [255] The action potential in human ventricular myocytes can be divided into five distinct phases (phases 0 to 4) during which different ion channels are active. During phase 0, there is an activation of an inward Na^+ current

(I_{Na}), which is responsible for a rapid depolarization of the membrane. Repolarization is much slower and is accomplished in three phases. During phase 1, activation of a repolarizing transient outward K^+ current (I_{TO}) allows K^+ to escape the cell and result in reduction of intracellular voltage. Phase 1 repolarization is achieved rapidly and is followed by phase 2 also called the plateau, which has a much slower repolarization rate. Phase 2 reflects a balance between the depolarizing inward Ca^{2+} current (I_{Ca}) conducted by L-type Ca^{2+} channels and the repolarizing outward K^+ currents, the slow delayed rectifier K^+ current (I_{Ks}) and the rapid delayed rectifier K^+ current (I_{Kr}). Phase 3 repolarization occurs as a result of the predominance of the delayed rectifier K^+ currents, the rapidly activating I_{Kr}, the slowly activating I_{Ks} and the ultra rapid rapidly activating I_{Kur}, after inactivation of L-type Ca^{2+} channels. This repolarization phase ends the action potential and restores resting level membrane potential (phase 4). In phase 4, the Na^+/K^+ ATPase restores the ionic balance, and the inwardly rectifying (I_{Kir}) channels, which allow the escape of K^+ ions, maintain the negative intracellular voltage.

1.2.2.2. Long QT and hERG

Mutations in the genes encoding these ion channels or their accessory subunits are linked to various types of LQTS. [256] One prominent form, LQTS type 2 (LQT2), is due to mutations in the *human ether-a-go-go related gene* (*hERG1*), also known as *KCNH2,* which encodes the Kv11.1 protein α-subunit that underlies the rapidly activating delayed rectifier K^+ current (I_{Kr}). [257] Alternate transcripts of *KCNH2* in the human heart encode two subunits, hERG1a and hERG1b. The major isoform, hERG1a, is a 1,159 amino acid protein contains six transmembrane (TM) domains (S1-S6) with TM helices S1-S4 contributing to the voltage sensor and S5-S6 forming the pore domain. The functional hERG channel is tetrameric and the pore domain from

each of the four subunits forms the ion-conducting pathway. In addition to the membrane-spanning region, the hERG1a has large N- and C-terminal cytosolic domains. hERG1a contains a Per-Arnt-Sim (PAS) domain at the N-terminus and a cyclic nucleotide binding domain (cNBD) at the C-terminus (Figure 1.4B). Regulation of channel function is thought to be through these divergent N- and C-terminal cytosolic domains. The second isoform, hERG1b, has a unique N-terminus as compared to hERG1a in that it lacks the PAS domain, which results in a shorter isoform that is similar to hERG1a except at the N-terminus. [258] While heterotetramers of hERG1a and 1b have been reported to more closely resemble native I_{Kr} than hERG1a homotetramers, the expression levels of hERG1b in adult heart remain in question. In addition, accessory β-subunits including MIRP1 (KCNE2) have been proposed to modulate hERG channel activity but their physiologic role is uncertain. [259]

Genetic analyses have identified over 459 putative hERG mutations, which cause loss-of-function phenotype due to multiple mechanisms such as defective intracellular protein folding and trafficking, altered channel gating and kinetic properties, or altered channel permeability or selectivity. [260,261] Trafficking deficiency has emerged as the most common mechanism for LQT2 disease. [262] Protein trafficking defects are of particular interest since some trafficking-deficient mutants display WT characteristics when normal trafficking is restored. [261]

1.2.2.3. hERG Biosynthesis

As with other polytopic membrane proteins, hERG channel proteins are synthesized in the ER before being exported to the Golgi apparatus and then to the cell surface (Figure 1.4C). During this process, hERG proteins undergo two critical glycosylation steps. [263] The first step occurs in the ER where the immature, newly synthesized hERG protein acquires N-linked core

glycosylation. The second step takes place in the Golgi apparatus where the immature hERG form acquires complex glycosylation. Then, the fully glycosylated mature hERG channel is transported to the cell surface, where it functions. [261] The hERG protein is detected as two characteristic bands on western blot, a core-glycosylated immature band of ~135 kDa and a fully glycosylated mature band of ~155 kDa. [264] The hERG polypeptide contains two sites for N-linked glycosylation at the consensus sequence Asn-X-Ser/Thr, N598 and N629, both of which are located in the extracellular S5-S6 linker. However, hERG is modified by the addition of high mannose oligosaccharides only at the glycosylation site N598 and not at N629. The glycosylation process is not required for assembly of functional hERG channels and their trafficking to the cell surface since the mutant N598Q that is not glycosylated was observed to form functional hERG channels at the cell surface. However, glycosylation plays a role in channel stability once at the plasma membrane since non-glycosylated channels were degraded faster than those that are glycosylated. [263]

1.2.2.3.1. hERG Chaperone System

1.2.2.3.1a. *ERQC Machinery*

Misfolded and incompletely assembled proteins are regularly formed in the ER during protein synthesis. These aberrant proteins are recognized by the ER quality control (ERQC) machinery and retained at the ER so as to undergo chaperone-induced correction or be targeted for proteasomal degradation. [265]

ER-associated and cytoplasmic chaperones comprise one of the main quality control mechanisms. The cytosolic chaperones Hsp70 and Hsp90 are involved in hERG quality control.

Hsp90 is required for hERG folding and hERG proteins that do not interact properly with Hsp90 may be diverted directly into the degradation pathway, while successful protein folding is accompanied by dissociation of the channel-chaperone complexes. In that study, interaction of Hsc/p70 with misfolded hERG was observed suggesting it could be involved, although its function was not tested. [266] Another co-chaperone of Hsp90, FKBP38 is also involved in hERG biogenesis. [267] Work from another group found that Hsp70 specifically stabilized hERG and slowed its degradation. Furthermore, induction of the heat shock response partially rescued the trafficking of several LQT2 mutants of hERG. [268] However, the heat shock response causes upregulation of a number of chaperones and co-chaperones, [109,269,270] and information on which are most effective in assisting hERG is still lacking.

Surprisingly little is known about the degradation of hERG at the ER. It was presumed to be ERAD of incorrectly folded proteins, as polyubiquitinated hERG was detected upon Hsp90 inhibition. [266] Degradation of hERG was then shown to be by proteasomes, to involve dislocation to the cytosol and EDEM recognition of mannose glycans, the outline of a typical ERAD pathway. [271] Mutants of hERG deficient in trafficking were found to accumulate on the ER lumenal chaperones calnexin and calreticulin, where they could potentiate an ER unfolded protein response. [272] However, important mechanisms such as the identity of the E3 Ub-ligase or ligases required, and the possible dislocation pathway, remain to be addressed.

1.3. Objectives and Perspective

Molecular chaperones play a role in both protein folding and degradation. The chaperones assist in the proper folding of transmembrane polytopic ion channels and participate in targeting the misfolded forms for ER-associated degradation (ERAD). Because of the dual function of chaperones, diseases due to misfolding and impaired trafficking of ion channels can be considered to be the result of inefficient chaperone folding activity and/or over activity of the ERAD. An interesting possibility is that manipulation of these chaperones could help alleviate the symptoms of ion channel misfolding diseases through promoting mutant channel folding and thereby rescuing trafficking leading to restored function.

The heat shock protein 70 (Hsc/p70) chaperone has a key role in the quality control of many proteins, and its activity is regulated by a variety of co-chaperones. The overall objective of this thesis is to understand the role of the Hsp70 chaperone system in the quality control of two ion channel misfolding diseases: long QT syndrome type 2 (LQT2), which is a cardiac disorder due to mutations in the potassium channel, human ether-a go-go related gene (hERG) protein, and cystic fibrosis (CF), which is due to mutations in the chloride channel, cystic fibrosis transmembrane conductance regulator (CFTR) protein.

Chapter 2 examines the role of the Hsc/p70 co-chaperones – the human cytosolic type I Hsp40s, DNAJA1, DNAJA2 and DNAJA4 – in hERG folding and degradation in association with the E3 ubiquitin ligase, CHIP. A detailed analysis determined that these DNAJ co-chaperones are key modulators of both the folding and degradation pathways of hERG as demonstrated by their ability to reduce hERG trafficking in a proteasome-dependent manner. Moreover, DNAJA1 is specifically important for hERG folding.

Chapter 3 identifies a novel role of another co-chaperone – the nucleotide exchange factor,

Bag1 – in regulating hERG functional expression, by acting on Hsc/p70. Bag1 induces hERG misfolding and thereby proteasomal degradation by increasing its ubiquitination through the ER-membrane anchored E3 ligase, translocation in renal carcinoma, chromosome 8 gene (TRC8), which cooperates with its cytosolic E2 ubiquitin conjugating enzyme, Ube2g2. This is a novel role for Bag1 in shifting hERG degradation pathway away from CHIP towards other E3 ligases that act independently of Hsc/p70.

Chapter 4 details the role of the Hsp70 chaperone system in CFTR biogenesis. Both DNAJA1 and DNAJA2 are required for CFTR maturation while only DNAJA2 promotes its proteasomal degradation through CHIP. Hsp70 also induces CFTR degradation through CHIP, however, through the lysosomes.

Finally, in chapter 5 the significance of these results is discussed and ideas for future experiments are proposed.

Chapter 2

Mechanisms of Hsp40 co-chaperones in hERG biogenesis

2.1. Abstract

Loss-of-function mutations in the human ether-a-go-go related gene (hERG, or KCNH2) potassium channel are the cause of cardiac long QT syndrome type 2 with heightened risk of arrhythmias. The majority of these mutations interfere with hERG trafficking from its site of synthesis at the endoplasmic reticulum (ER) to its functional location at the cell surface. Instead, the hERG mutants are retained as misfolded proteins and degraded. Cytosolic chaperones are thought to assist the folding of the cytosolic domains of hERG, but the role of the chaperone Hsc70/Hsp70 remains unclear. Here, we identify Hsc70/Hsp70 and the Type 1 Hsp40 co-chaperones as major regulators of hERG trafficking and degradation. Using siRNA knockdown, we find that Hsc70/Hsp70 and DNAJA1 (DJA1/Hdj2) are both necessary for hERG folding and trafficking. However, overexpression of DJA1, DNAJA2 (DJA2) and DNAJA4 (DJA4) inhibited hERG trafficking, by promoting its proteasomal degradation at the ER. Mutants of DJA2 defective in its protein folding function were also ineffective in degradation. The degradation of hERG assisted by the DJAs appeared to be through the E3 ubiquiting ligase CHIP, which depends on interactions with Hsc70/Hsp70. Thus, we propose a novel role of the DJAs in degradation as well as folding, determining the balance of protein quality control.

2.2. Introduction

A key challenge in cell biology is to understand protein folding and the role of chaperones in this process for export from the endoplasmic reticulum (ER). [273] The ER serves as a specialized protein-folding machine where lumenal secreted proteins or transmembrane proteins are transported, processed and folded before being targeted to their final destination. [274] Proteins are exported from the ER for delivery to the Golgi in vesicles formed by the coatamer complex II (COPII) machinery. [275] The molecular mechanisms underlying the protein folding processes at the ER, involving the various ER lumenal and cytosolic chaperone machineries, remain to be fully elucidated. The ER operates a quality control system involved in two competing pathways of folding and degradation. Therefore, the ER-associated folding pathways (ERAF) are counterbalanced by ER-associated degradation (ERAD) pathways, where misfolded proteins are recognized at the ER, retrotranslocated into the cytosol and targeted for proteasomal degradation. [276,277] Various loss-of-function misfolding diseases arise when proteins do not fold properly, fail to incorporate into COPII budding vesicles for export and are recognized by the ERQC machinery and sent for degradation.

Long QT syndrome is a cardiac disorder associated with an increased risk of ventricular arrhythmias that can lead to syncope and sudden death. One prominent form of long QT syndrome, LQT2, is linked to loss-of-function mutations in the human ether-a-go-go-related gene (*hERG1*), also known as *KCNH2*. *hERG* encodes the Kv11.1 protein α-subunit that underlies the rapidly activating delayed rectifier K^+ current (I_{Kr}) in the heart. [257] The hERG α-subunit consists of a cytosolic Per-Arnt-Sim (PAS) domain at the N-terminus, a conserved transmembrane (TM) core with six transmembrane helices, a predicted cyclic nucleotide-binding domain (CNBD) in the cytosol, and a C-terminal coiled-coil (CC) region. The hERG channel,

like other secretory membrane proteins, is integrated into the ER membrane during its synthesis, and is then assembled into tetramers. During insertion, hERG is N-glycosylated, resulting in the core-glycosylated (CG) 135 kDa form. The channel is then exported through the Golgi complex, where it is further fully glycosylated (FG) to the mature 155 kDa form, and eventually inserted into the PM by exocytosis. [258]

Transport of hERG involves both lumenal and cytosolic chaperones that facilitate folding and export from the ER. Chaperone components that are currently thought to significantly affect hERG ERAF pathways include calnexin [278], found in the lumen of the ER, as well as the cytosolic chaperones Hsc70/Hsp70 and Hsp90. [266] Hsp70 and Hsp90 are ATP-dependent chaperones that undergo ATP-regulated cycles of binding to and release of substrate polypeptides. A range of co-chaperones regulates the Hsp70 and Hsp90 ATPase cycles, or link the chaperones to specific activities or locations. In humans, Hsc70 is constitutively expressed and Hsp70 is induced by stress, but is also expressed under normal conditions. [14] Because they often cannot be distinguished experimentally, they will be referred to in general as Hsc/p70.

An early study used the Hsp90-specific inhibitor geldanamycin and found that it prevented hERG maturation and increased its degradation. Transfection of Hsp70 increased the overall expression levels of both the CG and FG hERG without having an effect on trafficking efficiency. In this study they also showed a prolonged interaction of Hsc/p70 and Hsp90 with mutant hERG. Therefore, Hsp90 and possibly Hsc/p70 act as part of hERG quality control at the ER. [266] Another component of hERG quality control at the ER is calnexin whose increased interaction with mutant hERG retains it at the ER and prevents it from further progressing through the secretory pathway. [278] Furthermore, heterologous overexpression of Hsp70 suppressed hERG ubiqitination and increased I_{Kr}. Upregulation of Hsp70 by heat shock

decreased mutant hERG degradation. [268] The latter effect was not observed with Hsp70 expression alone. Because heat shock induces and represses the expression of a number of genes, particularly co-chaperones, the effect on hERG mutants almost certainly involves co-chaperone regulators of Hsc/p70.

To identify potential co-chaperones involved in hERG biogenesis, we initially conducted a proteomics analysis of hERG interactors. This revealed a number of putative hERG-interacting co-chaperones including FKBP38 and DNAJA1 (DJA1). We established the role of the Hsp90 co-chaperone, FKBP38, in hERG biosynthesis. FKBP38 is a membrane-anchored co-chaperone of Hsp90 at the ER and contains a peptidyl-prolyl isomerase activity as well as an Hsp90-binding TPR domain. We found that its knockdown impaired hERG trafficking, in agreement with the importance of co-chaperones. [267] Other co-chaperones were found to be associated with hERG such as DJA1, which is a member of the Hsp40 family. Hsp40 proteins are Hsp70 co-chaperones that activate its ATPase activity and direct Hsp70 towards substrate.

DJA1, and closely related DNAJA2 (DJA2), are the major Type 1 Hsp40 co-chaperones in humans. The Type 1 proteins are the most highly conserved throughout evolution, and are thought to be the most active in assisting protein folding by Hsc/p70. They share a similar architecture with an N-terminal J-domain that activates Hsc/p70 connected by a partially conserved linker to a middle/C-terminal (MC) domain that binds substrate and forms a homodimerization interface. Human DJA1 and DJA2 were found to be functionally distinct despite their homology, and the mechanistic basis for this difference is still under investigation. [26,36,60,61]

It is unknown which Hsp40 co-chaperones are involved in hERG synthesis. Therefore, we tested whether DJA1 and DJA2, being the most abundant cytosolic Hsp40 proteins as well as

Type 1, are part of the chaperone machinery involved in hERG biogenesis. First, we established the importance of Hsc/p70 in hERG folding. Knockdown of Hsc/p70 resulted in decreased hERG trafficking and increased degradation. Next, we showed how DJA1 and DJA2 each contribute to hERG folding or degradation. Knockdown of DJA1 but not DJA2 impaired hERG trafficking, suggesting a specific requirement for DJA1 to support Hsc/p70-mediated folding of hERG. We also identified a role of both DJA1 and DJA2 in regulating the degradation of hERG. The DJAs prolonged hERG association with Hsc70 leading to ubiquitination by an E3 ligase CHIP, and ERAD of hERG.

2.3. Results

2.3.1. Hsc/p70 is essential for hERG folding

To identify the role of Hsc/p70 in hERG biogenesis, we performed combined siRNA knockdown of Hsc70 and Hsp70 in HeLa cells stably expressing hERG with an extracellular HA epitope. There was a 50% decrease in both Hsc70 and Hsp70 upon siRNA transfection. By western blot, we detect the CG immature form of hERG as a 135 kDa band and the FG mature form as a 155 kDa band. The levels of both CG and FG hERG were markedly decreased by Hsc/p70 knockdown, CG hERG to around 70% of the control non-silencing siRNA and FG hERG to around 50% (Figure 2.1A).

The strong effect on the FG form suggested that trafficking was impaired, and pulse-chase experiments were conducted to test this. In this method, a pool of CG hERG is radiolabeled then followed over time by immunoprecipitation. In the control, around 55% of the initial pool of CG is converted into FG over the course of 4.5 h (Figure 2.1B, right graph). The

rest remains in the CG form, ~ 40% (Figure 2.1B, left panel), or gets degraded, ~ 5%. The kinetics and amount of FG hERG formation was substantially lower upon depletion of Hsc/p70 than in controls. There was only ~ 30 % FG formation with Hsc/p70 knockdown, although the turnover of CG hERG was less affected (Figure 2.1B). Altogether, it appears that Hsc/p70 is an essential chaperone for hERG.

2.3.2. DJA1 is the Hsp70 co-chaperone involved in hERG folding

Since DJA1 was identified in our proteomics screen and it works with Hsc/p70, we wanted to determine its role in comparison with DJA2 in hERG biogenesis. Therefore, we started by asking what effect the reduction of DJA expression, by siRNA knockdown, would have on hERG trafficking. The HeLa cell line stably transfected with HA-tagged hERG was used. Knockdown of DJA1 but not DJA2 impaired hERG trafficking, as determined by western blot analysis of FG relative to CG hERG, suggesting a specific requirement for DJA1 to support Hsc70-mediated folding of hERG (Figure 2.2A).

Then we confirmed the effect of DJA1 on hERG biogenesis through pulse-chase experiments. These showed a decrease in the kinetics of FG formation to about 40% of initial CG levels upon depletion of DJA1, as compared to non-silencing control in which there is ~ 55% FG hERG formed (Figure 2.2B). Thus, both western blot and pulse chase results show that DJA1 is important for hERG folding.

2.3.3. DJA proteins inhibit hERG trafficking

Depleting the cells of DJA chaperones resulted in less trafficked hERG with DJA1 siRNA. We then asked what the effect of excess DJA proteins would be on hERG trafficking. Therefore, we transfected myc-tagged DJA1, DJA2 or the lower abundance Type 1 Hsp40 DNAJA4 (DJA4) in HEK293 (GripTite). [60] Overexpression of either one of these Hsp40 proteins resulted in a dramatic reduction in mature FG hERG without affecting the immature CG form as compared to control conditions (Figure 2.3A). DJA2 and DJA4 had a slightly stronger effect than DJA1.

We hypothesized that their effect on inhibiting hERG maturation might be mediated through Hsc/p70 and thereby requires the J-domain. Therefore, we used DJA1 and DJA2 mutant proteins lacking the J-domain. Overexpression of DJA1-ΔJ or DJA2-ΔJ in HEK293 (GripTite) co-transfected with hERG had no effect on hERG trafficking (Figure 2.3B). Thus, the J-domain of these co-chaperones is necessary for the inhibition of hERG maturation, which signifies the importance of the interaction with Hsc70. Nevertheless, overexpressing Hsc70 alone did not have a similar effect as with the DJA proteins (Figure 2.3B), which suggests that the DJAs are required to activate Hsc70 and result in this trafficking inhibition of hERG.

Next, to test whether the DJAs inhibit hERG maturation by inducing its ERAD, we treated HEK293 (GripTite) cells co-transfected with hERG and the DJAs with 25 μM of the specific proteasome inhibitor lactacystin for 24 hours. If the DJAs promote hERG proteasomal degradation, then proteasome inhibition should restore mature hERG levels. Indeed, treatment with lactacystin increased the amount of both FG and CG hERG to similar levels as DMSO vehicle control treated cells, whether they were vector or DJA-transfected (Figure 2.3C).

Therefore, the DJAs seem to inhibit hERG trafficking by inducing its proteasomal degradation at the ER, that is, its ERAD.

2.3.4. DJA2 mutants and hERG trafficking

We then wanted to test whether the folding activity of the DJAs is a requirement for trafficking inhibition and degradation. Therefore, we performed experiments with a range of DJA2 mutants that we constructed and found to have different defects. The mutants were first characterized using our well-established luciferase refolding assays both in vitro and in HEK293 cells. In addition, the mutants were also tested in vitro for the ability to bind substrate and release it in the presence of Hsc70 and ATP. The mutants are shown schematically in Figure 2.4 with a summary of the mechanistic results, and described in detail below.

As previously mentioned, DJA2 has an N-terminal J-domain that is linked through a partially conserved linker to the Type 1 MC domain. [26,36,60,61] The MC domain furthermore contains two zinc finger motifs and a substrate-binding site. This architecture is shared with the well-characterized DnaJ from Escherichia coli and Ydj1 from Saccharomyces cerevisiae. [33,63] The function of DJA2 is expected to depend on structures within the MC domain since mutations or removal of the zinc ions in DnaJ and Ydj1 show the importance of the zinc finger motifs in function. [279-281] The zinc-binding domains were suggested to be required to promote substrate transfer from the DJAs to their Hsp70 partners. [279] A crystal structure of a fragment of the Ydj1 MC region showed that this L-shaped molecule constitutes of three subdomains: a substrate-binding subdomain (middle 1 or m1), a subdomain of unknown function (m2) protruding from the zinc fingers, and a C-terminal subdomain (Figure 2.4). [23] Another crystal structure of Ydj1 revealed a dimerization interface extending from the end of the C-terminal subdomain. [282] DJA2

is expected to have similar domain architecture and Figure 2.4 shows a homology model of DJA2 based on Ydj1 structure. The proximity of the m2 region to the J-domain suggests a functional interaction between them possibly to allow substrate transfer to Hsc70, but up to now there was there was no experimental evidence for this.

After showing that DJA2 overexpression reduces hERG trafficking by inducing its degradation, we used various DJA2 mutants to see whether the folding activity of DJA2 is a requirement for degradation. The constructs used were: DJA2-ΔJ, which lacks the J-domain and could only bind substrate but is unable to release substrate or promote refolding. DJA2-Δm2, which lacks the m2 region; this mutant is non-functional in refolding, yet it binds substrate, but cannot release it. Other experiments showed that the m2 region has a specific role in substrate transfer from DJA2 to Hsc70. DJA122 has the J-domain of DJA1 and the rest of DJA2. It is functional in refolding, substrate binding and release. DJA221, which has the homodimerization domain of DJA1 attached to the rest of DJA2 is non-functional in refolding but can bind substrate and release it (Figure 2.4).

We started by examining the kinetics of hERG trafficking and degradation with pulse chase experiments in HEK293 cells transiently overexpressing both hERG and each of the different DJA2 mutants. Similar to the experiments in HeLa cells, CG hERG is pulse labeled then chased at different time points up to 6 hrs during which it converts into FG, remains as CG or gets degraded. With the vector control the amount of CG decreases to ~ 60% of CG starting material while the amount of FG increased to ~ 35% of initial CG (Figure 2.5A, B) and the rest ~ 5% is degraded. The rate of degradation is the reduction in the total amount of hERG remaining. Upon the transfection of DJA2 the amount of FG formed decreases to 15% while the CG is moderately affected and the amount that is degraded increases to ~25%. This is consistent with

DJA2 increasing hERG degradation. Interestingly, contrary to DJA2 the mutants tested – DJA2-Δm2, DJA-122, DJA-221, and DJA2-ΔJ – were non-functional in reducing hERG trafficking and promoting its degradation (Figure 2.5A, B, C). These results suggest that the m2 region is important for DJA2 degradation functions, exchanging the C-terminal domains is also disruptive, and deleting the J-domain abolishes the DJA2 functions in degradation as well. Furthermore, since most of these mutants were also non-functional in refolding, we can conclude that the requirement for folding is also a requirement for degradation.

2.3.5. The DJA proteins and CHIP reduce hERG stability

After having established that DJA1 and DJA2 reduce hERG trafficking and increase its proteasomal degradation and that these functions require Hsc/p70, we asked which E3 ligase is involved in the process. A first hypothesis was the cytosolic E3 ligase, CHIP, which contacts Hsc/p70 to ubiquitinate substrates bound by the chaperone. Therefore, we decided to test CHIP. We used pulse chase experiments with or without the overexpression of DJA1, DJA2, or CHIP in HEK293 (GripTite) cells. In vector control transfected cells, hERG first appeared as the CG form and a fraction subsequently shifted to the FG form after acquiring complex oligosaccharides around two hours after synthesis (Figure 2.6A). This FG band was still visible after 24 hours of chase time confirming the relative stability of mature hERG. The abundant CG form progressively weakened, apparently due to degradation as well as conversion to the FG form at the cell surface. Measured immediately after radiolabelling (t=0 h), similar quantities of CG hERG were synthesized under control conditions or in the presence of DJA1, DJA2, or CHIP (Figure 2.6A). In control cells, the CG form was reduced to around 30% after 24 h of chase. DJA1 and DJA2 induced a moderate decrease in CG levels relative to control conditions while

CHIP caused the largest decrease in CG hERG at 24 h of chase (Figure 2.6B). The FG form of hERG was most apparent in the control cells, peaking at 4 h of chase at around 16% of the amount of CG hERG present at t=0 (Figure 2.6C) whereas transfection of DJA1 and DJA2 caused a reduction of peak FG hERG levels to about 7% and 9% of initial CG hERG at 4 h chase. The effect of CHIP on FG hERG was not evident until the 4 h chase point and was most noticeable at 10 h of chase. Again, these results correlate with those obtained under steady state conditions where overexpression of the DJAs reduced the expression of the mature FG form of hERG. Overall, these results suggest that the major effect of the DJAs was to prevent the formation of mature hERG, and to increase degradation of the polypeptide by Hsc/p70 complexes with CHIP.

2.4. Discussion

Our results identify the Hsc/Hsp70 chaperone system as an important regulator of hERG trafficking. Although previous work had suggested an involvement of Hsc/p70 [266], its function had not been directly addressed. Our knockdown experiments now demonstrate that Hsc/p70 is indeed necessary for hERG maturation, as well as the Hsp40 co-chaperone DJA1. Interestingly, DJA2 is not required for hERG. Moreover, overexpression of DJA1, DJA2 and DJA4 promoted ERAD of hERG, apparently by the CHIP E3 ubiquitin ligase. The internal mechanisms of the DJAs required to support Hsc/p70-mediated folding are also required for their degradation role. It is possible that polyubiquitination by CHIP is directly or indirectly influenced by Hsp40 co-chaperones.

DJA1 has been studied to some degree, but the other Type I Hsp40s are much less characterized biologically. Early work using purified proteins was unclear about differences

between DJA1 and DJA2 [36], but more recently, we found in vitro evidence of mechanistic and functional differences between the Type I proteins. [60,61] Our above results show that DJA1 is specifically required for hERG maturation, consistent with the idea of functional diversity between the Hsp40 co-chaperones. Furthermore, our results are the first positive identification in live cells of a protein dependent on DJA1. In the only other study at the time our experiments were performed, the activity of the androgen receptor was found to be hyperactivated in a DJA1 knockout mouse [57], and could not be firmly established as a substrate of DJA1. In parallel to our degradation experiments using DJA2, we confirmed using knockdown that DJA2 and not DJA1 was required for luciferase refolding in cells (Figure 2.4, and data from Imad Baaklini and Michael Wong). As well, DJA2 has been shown by another group to support the folding of trimeric G proteins. [283] We expect that more DJA1- and DJA2-dependent proteins will be identified using the powerful knockdown or knockout approach.

While all three DJAs promote degradation of hERG, they differ in efficiency, even accounting for expression levels in transfections. DJA4 and DJA2 are more active in degradation than DJA1. This may be explained by the role of DJA1 in hERG folding, such that a higher expression threshold must be reached before DJA1 has a negative impact, compared to the other DJAs. In addition, there may be intrinsic biochemical or biophysical properties of the DJAs that also contribute, as illustrated by our experiments with DJA2 mutants. Separately, we had found that each mutant had specific characteristics: DJA2-Δm2 defective in the transfer of substrate to Hsp70, DJA-221 in the stability of the C-terminus, and DJA-122 with only a mild decrease refolding function with Hsc70 (Imad Baaklini). However, all of these were less effective than wild-type at inhibiting hERG trafficking, suggesting that each abnormal characteristic impaired the degradation process. Therefore, the wild-type DJAs most likely also differ in some

characteristics, for example affinities of substrate binding or internal flexibility, that underlie their divergent ability to assist both the folding and degradation of different proteins.

The requirement for Hsc70 and/or Hsp70 to assist hERG folding is not unexpected, and had been proposed based on interaction studies with misfolded hERG. [266] However, functional identification of substrates dependent on Hsc70/Hsp70 has been limited due to the lack of reliable inhibitors, in contrast to Hsp90, for which specific inhibitors are widely available. Depletion by siRNA is the best alternative, and although knockdown is not complete, our results were quite clear. Differences between Hsc70 and Hsp70 have been postulated, although the mechanistic basis is still unknown. [284] Because knockdown of Hsc70 alone induces Hsp70 expression to an equivalent level in HeLa and HEK293 cells (data not shown), while Hsp70 can be depleted by siRNA without inducing Hsc70, interpreting individual knockdown results can be difficult. In the future, gene knockouts may provide clearer answers. A mouse having both of its inducible Hsp70 genes knocked out has been generated, with various stress-related phenotypes. [27] MEFs from such a mouse compared with wild-type controls could serve as experimental models. Furthermore, cardiomyocytes from the mice could allow the study of hERG/mERG in a native environment.

Figure 2.1. Hsc/p70 is essential for hERG folding. A, HeLa cells stably expressing hERG were transfected with siRNA duplexes against both Hsc70 and Hsp70, or non-silencing control. CG and FG hERG were detected as 135 kDa and 155 kDa bands, respectively, by western blot, and quantified relative to the amount of each in control cells. Knockdown of Hsc/p70 was confirmed by western blot. B, cells transfected as above were metabolically radiolabelled for 45 min and chased for the indicated times, and lysates were immunoprecipitated using hERG-specific antibodies. CG and FG hERG were detected by SDS-PAGE and autoradiography, and quantified relative to the initial amount of CG hERG. Unless otherwise specified, data are shown as mean ± SD and are representative of at least three independent experiments, * $p<0.05$.

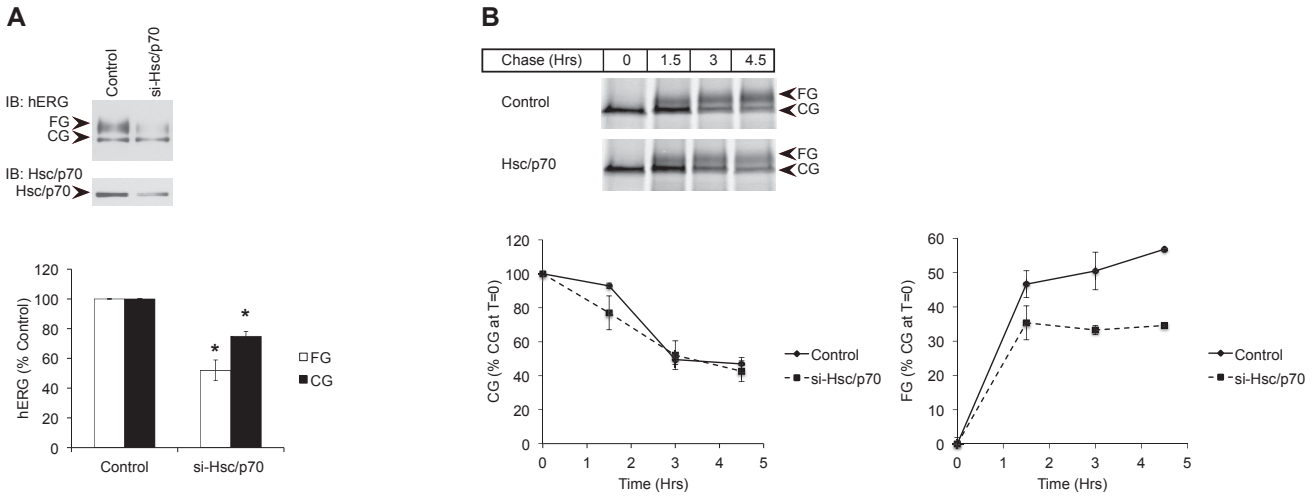
A
Control
si-Hsc/p70
IB: hERG
FG
CG
IB: Hsc/p70
Hsc/p70
hERG (% Control)
120
100
80
60
40
20
0
*
*
FG
CG
Control
si-Hsc/p70
B
Chase (Hrs)
0
1.5
3
4.5
Control
Hsc/p70
FG
CG
CG (% CG at T=0)
Time (Hrs)
Control
si-Hsc/p70
FG (% CG at T=0)
60
50
40
30
20
10
0
Time (Hrs)
Control
si-Hsc/p70

Figure 2.2. DJA1 is the Hsp70 co-chaperone involved in hERG folding. A, HeLa cells stably expressing hERG were transfected with siRNA duplexes against DJA1 or DJA2, or non-silencing control (ns). At the indicated days after transfection, CG and FG hERG were detected by western blot, and quantified relative to the amount of CG hERG in control cells on that day. B, cells were transfected as above with siRNA against DJA2 or non-silencing control. At 3 days after transfection, pulse-chase experiments were performed as in Figure 2.1. Unless otherwise specified, data are shown as mean ± SEM and are representative of at least three independent experiments, * $p<0.05$.

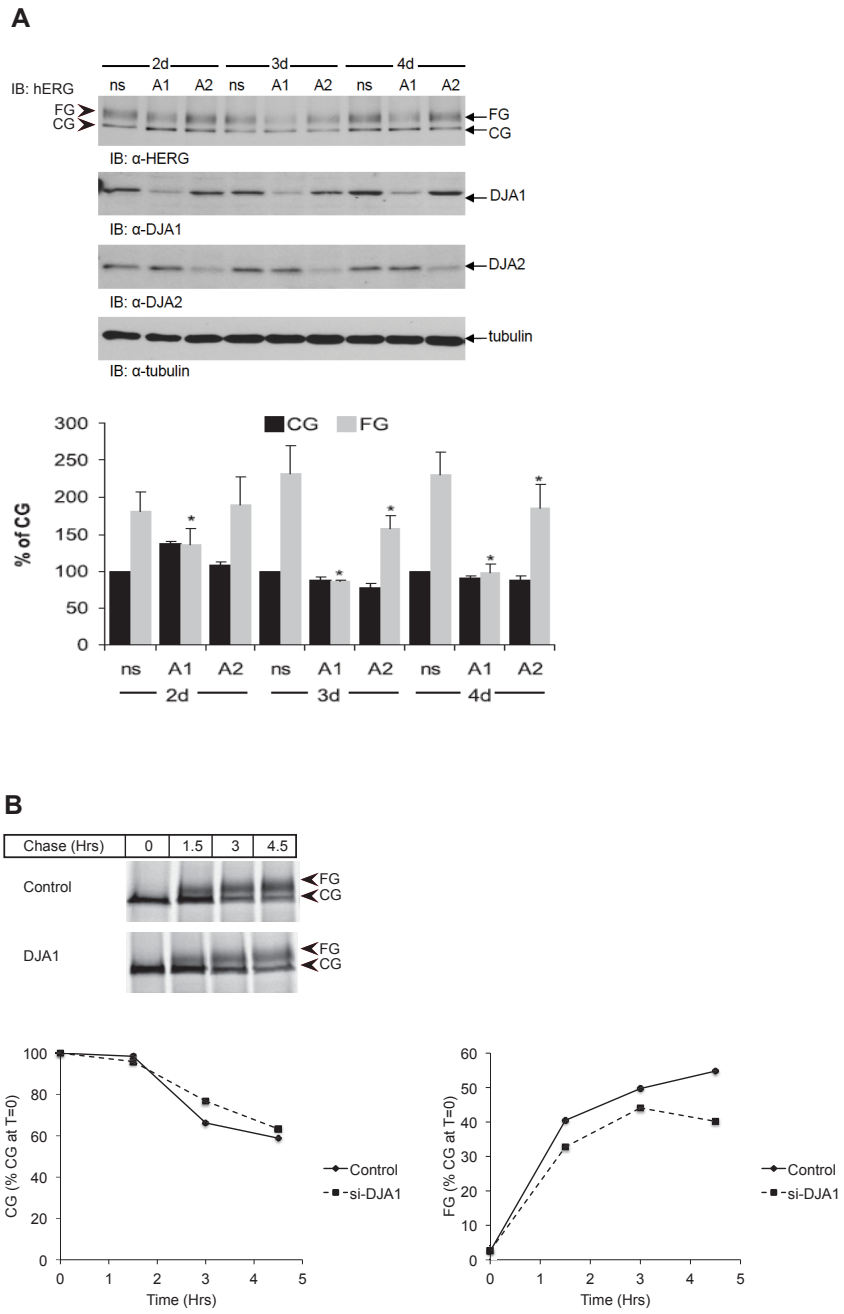
A
2d
3d
4d
IB: hERG
ns
A1
A2
FG
CG
IB: α-HERG
DJA1
IB: α-DJA1
DJA2
IB: α-DJA2
tubulin
IB: α-tubulin
CG
FG
% of CG
300
250
200
150
100
50
0
B
Chase (Hrs)
0
1.5
3
4.5
Control
DJA1
CG (% CG at T=0)
FG (% CG at T=0)
Time (Hrs)
Control
si-DJA1

Figure 2.3. DJA proteins inhibit hERG trafficking. A, HEK293 (GripTite) cells were transiently transfected with hERG and type I Hsp40 co-chaperones DJA1, DJA2 or DJA4, or vector control. CG and FG hERG were detected by western blot, and quantified relative to the amount of CG hERG in control cells. B, cells as above were transfected with hERG and DJA1-ΔJ, DJA2-ΔJ, which are type I Hsp40s lacking the J-domain, or Hsc70, or vector control. C, the experiment in A was performed with the addition of 25 μM of the proteasomal inhibitor, lactacystin, or vehicle control overnight before analysis. Unless otherwise specified, data are shown as mean ± SEM and are representative of at least three independent experiments, * $p<0.05$.

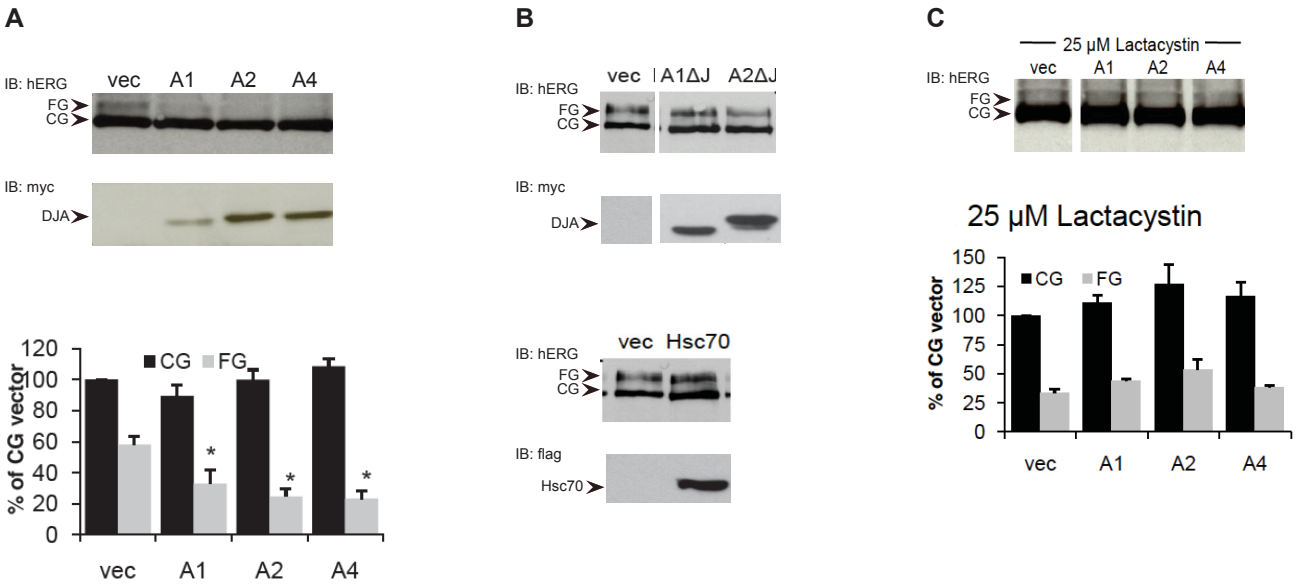
A
IB: hERG
vec
A1
A2
A4
FG
CG
IB: myc
DJA
CG
FG
% of CG vector
120
100
80
60
40
20
0
*
vec
A1
A2
A4
B
IB: hERG
vec
A1ΔJ
A2ΔJ
FG
CG
IB: myc
DJA
vec
Hsc70
IB: hERG
FG
CG
IB: flag
Hsc70
C
25 μM Lactacystin
vec
A1
A2
A4
IB: hERG
FG
CG
25 μM Lactacystin
CG
FG
% of CG vector
150
125
100
75
50
25
0
vec
A1
A2
A4

Figure 2.4. DJA2 mutants and functional defects. Top left, proposed arrangement of domains in DJA2 based on Ref. 13. Top right, a homology model of DJA2 was generated by SwissModel using the middle fragment of Ydj1 (1NLT) as template. The N and C termini, m1 and m2 subdomains, zinc-binding sites (Zn-1 and Zn-2), and partial C-terminal (C-term) dimerization region are marked. The positions of the Δm2 deletion and the C-terminal exchange with DJA1 are indicated by dashed lines. Bottom left, diagram of the domain arrangements in the DJA1 and DJA2 primary sequence, and mutants used in this study. The J domain (J), linker (lk), m1 and m2 sequences, zinc-binding sites (Zn-1 and Zn-2), and C-terminal dimerization sites are marked. Bottom right, summary of the results on refolding of firefly luciferase with Hsc70 in HEK293 cells and with purified proteins.

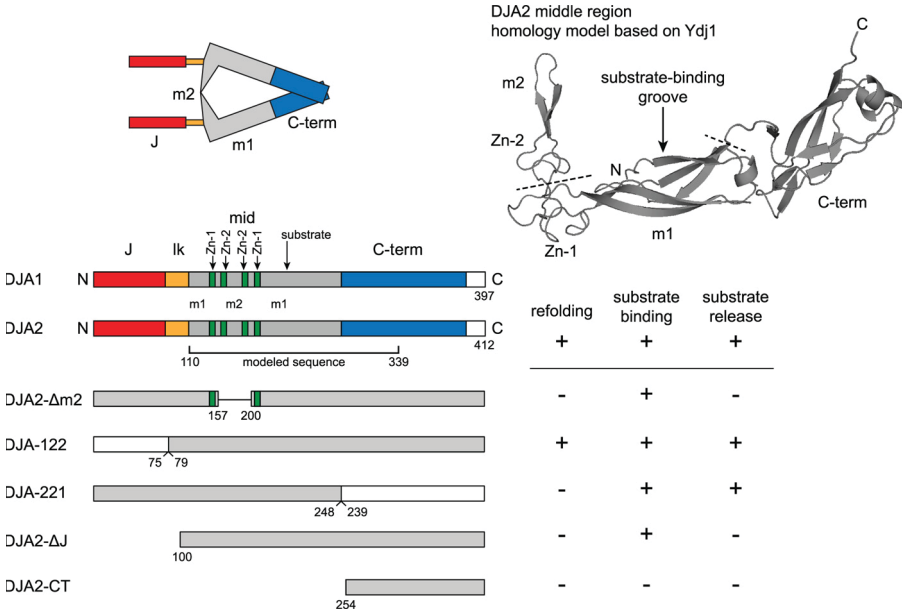
m2
C-term
J
m1
DJA2 middle region
homology model based on Ydj1
C
m2
substrate-binding
groove
Zn-2
N
C-term
m1
Zn-1
mid
J
Ik
Zn-1
Zn-2
Zn-2
Zn-1
substrate
C-term
DJA1
N
C
397
m1
m2
m1
DJA2
N
C
412
110
modeled sequence
339
DJA2-Δm2
157
200
DJA-122
75
79
DJA-221
248
239
DJA2-ΔJ
100
DJA2-CT
254
refolding
substrate binding
substrate release
+
+
+
-
+
-
+
+
+
-
+
+
-
+
-
-
-
-

Figure 2.5. DJA2 mutants and hERG trafficking. A, HEK293 cells were transfected with hERG and wild-type DJA2 or its indicated mutant, or vector control. Pulse-chase experiments were performed as in Figure 2.1. B, quantitation of CG and FG hERG in A, relative to the initial amount of CG hERG. C, the final amounts of CG and FG hERG at 6 h chase in B were plotted as a bar graph. D, Western bot showing expression of DJA mutants. Unless otherwise specified, data are shown as mean ± SD and are representative of at least three independent experiments, ** $p<0.01$ in comparisons with the wild-type DJA2 results.

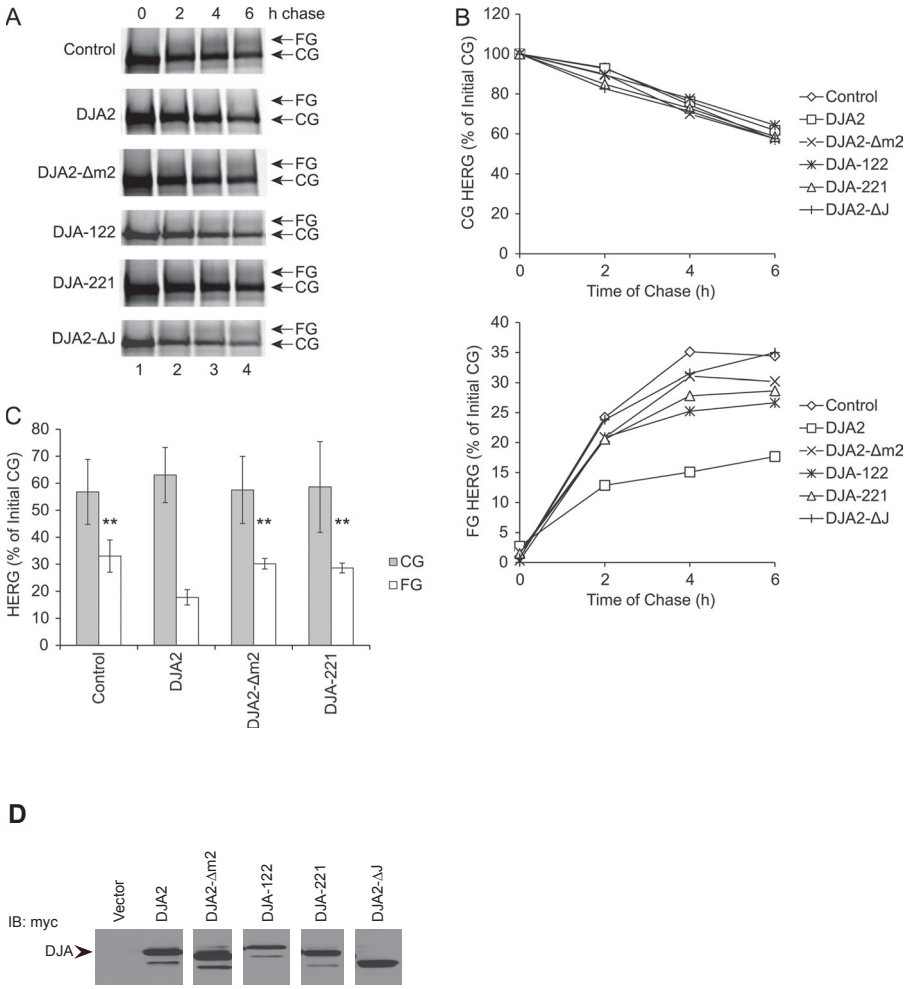
A
0 2 4 6 h chase
Control
DJA2
DJA2-Δm2
DJA-122
DJA-221
DJA2-ΔJ
FG
CG
1 2 3 4
B
CG HERG (% of Initial CG)
Time of Chase (h)
FG HERG (% of Initial CG)
Control
DJA2
DJA2-Δm2
DJA-122
DJA-221
DJA2-ΔJ
C
HERG (% of Initial CG)
**
CG
FG
Control
DJA2
DJA2-Δm2
DJA-221

D
IB: myc
DJA
Vector
DJA2
DJA2-Δm2
DJA-122
DJA-221
DJA2-ΔJ

Figure 2.6. The DJA proteins and CHIP reduce hERG stability. A, HEK293 (GripTite) cells were transiently transfected with hERG and DJA1, DJA2 or CHIP, or vector control. Pulse-chase experiments were performed as in Figure 2.1. B, quantitation of % CG hERG in A, relative to the initial CG amount. C, quantitation of % FG hERG in A, relative to the initial CG amount. Unless otherwise specified, data are shown as mean ± SEM and are representative of at least three independent experiments, * $p<0.05$.

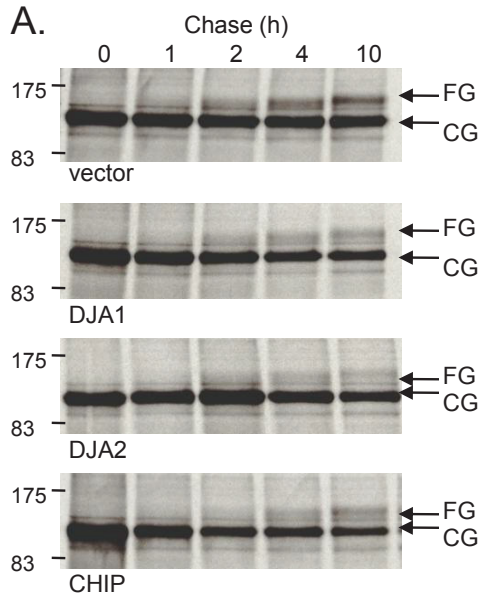
A.
Chase (h)
0
1
2
4
10
175
83
FG
CG
vector
DJA1
DJA2
CHIP

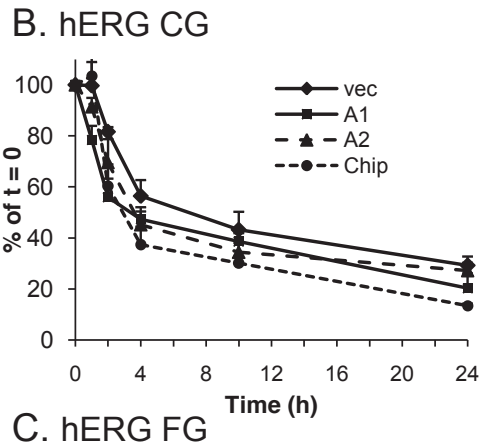
B. hERG CG
% of t = 0
Time (h)
vec
A1
A2
Chip

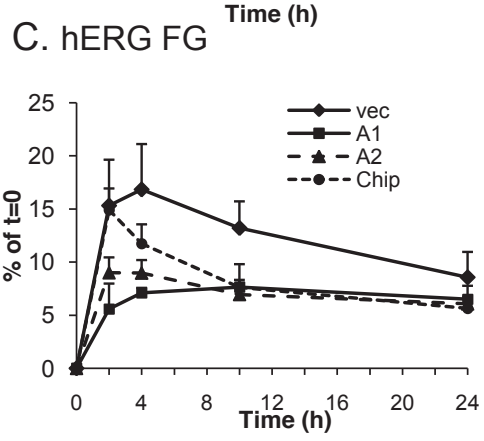
C. hERG FG
% of t=0
Time (h)
vec
A1
A2
Chip

Chapter 3

Bag1 shifts hERG degradation towards the Ube2g2/TRC8 pathway at the ER

3.1. Abstract

Cardiac long QT syndrome type 2 is caused by mutations in the hERG (KCNH2) potassium channel. Many such mutations result in misfolding of the protein, and its retention and degradation at the endoplasmic reticulum (ER), instead of normal trafficking to the cell surface. Molecular chaperones are thought to assist the folding of the hERG cytosolic domains. Here, we identify a novel role of Bag1 in regulating hERG functional expression, by acting on the chaperone Hsp70/Hsc70. Bag1 promotes the degradation of hERG by the ubiquitin-proteasome system, and Bag1 knockdown increases hERG levels and channel activity. As a nucleotide exchange factor for Hsp70/Hsc70, Bag1 decreased the chaperone's interaction with hERG, leading to impaired folding. In addition, Bag1 decreased the involvement of the CHIP E3 ubiquitin ligase in hERG degradation. Instead, hERG degradation is shifted to membrane-associated E3 ligases. The E2 conjugating enzyme Ube2g2 and its partner E3 ligase TRC8 are identified as primarily responsible for CHIP-independent degradation of misfolded hERG. We propose that Bag1 is a key regulator of hERG quality control at the ER, through its modulation of the Hsp70/Hsc70 chaperone essential for folding.

3.2. Introduction

Long QT syndrome is an inherited cardiac disorder characterized by prolongation of the electrocardiogram QT interval due to a delay in ventricular action potential repolarization. This leads to an increased risk of ventricular arrhythmias that can cause syncope, seizures and sudden death. One prominent form of the disease, long QT syndrome type 2 (LQT2), is linked to mutations in the human ether a go-go-related gene type 1 (*HERG1*), also known as *KCNH2*, which encodes the α-subunit of the Kv11.1 channel that conducts the rapid component of the delayed rectifier K^+ current (I_{Kr}) in the heart [257,285].

Molecular genetic studies have identified more than 200 LQT2-associated mutations that result in loss of hERG channel function. The most common mechanism for the loss of function phenotype is impaired hERG trafficking from the endoplasmic reticulum (ER) to the plasma membrane. Mutant channels, which fail to fold properly or form functional tetramers, are recognized by the ER quality control machinery, retained, and sent for ER-associated proteasomal degradation (ERAD) [262,286].

The quality control mechanisms that account for chaperone-mediated hERG folding as well as the selective degradation of misfolded hERG are still poorly understood. The hERG polypeptide contains N- and C-terminal cytosolic domains around a central transmembrane region that tetramerizes to form the channel pore, implicating cytosolic and transmembrane factors in quality control. An early study showed that Hsp90 is necessary for hERG trafficking, and Hsp90 inhibition results in hERG degradation [266]. We found that Hsp70 (and its constitutively expressed form Hsc70, both are normally expressed) is important for hERG biosynthesis, as knockdown of its major co-chaperone DnaJA1/Hdj2 impairs trafficking [287]. The DnaJ-family co-chaperones activate ATP hydrolysis and substrate binding by Hsp70, but

individual DnaJs are biologically distinct [63]. DnaJA2 promotes hERG degradation, by non-productively increasing interactions with Hsp70 and its associated E3 ubiquitin ligase CHIP [30,62,287].

The nucleotide exchange factor (NEF) co-chaperones of Hsp70 counteract the DnaJs. They promote the release of ADP and re-binding of ATP by Hsp70 along with the dissociation of bound substrate. Bag1 is the most well studied and the first to be discovered [79,87,288]. Bag1 can enhance or inhibit chaperone-mediated folding, in a substrate- and concentration-dependent manner [61,96,97,289]. Furthermore, Bag1 has been implicated in proteasomal degradation. The Bag1 isoforms, from alternative translation initiation sites, contain a ubiquitin-like (UBL) domain that interacts with proteasomes; Bag1-Hsp70 complexes could deliver substrates to proteasomes [290]. More recently, Bag1 was reported to increase degradation of polyglutamine-expanded Huntingtin by preventing nuclear accumulation [291]. Also, Bag1 knockdown caused defects in the degradation of reporters recognized by a PEST sequence, the N-end rule and a ubiquitin fusion. Interestingly, the Bag1 function in proteasomal degradation is thought to balance the role of related Bag3 in autophagy [101]. However, the importance of the UBL domain has not been demonstrated, and the mechanisms of Bag1 effects on degradation remain unclear.

Although CHIP promotes hERG degradation, it may not be the only E3 ubiquitin ligase involved, or even the most important. In contrast to soluble CHIP, other ERAD E3 ligases are transmembrane, typically localized to the ER, and do not interact with Hsp70 or other chaperones. The best characterized are HRD1 and gp78, which form complexes with other membrane proteins to recognize, ubiquitinate and dislocate a number of misfolded proteins into the cytosol [154,277,292]. In addition, several other transmembrane E3 ligases are known. RMA1 cooperates with gp78 to degrade mutant CFTR chloride channel [200,201]. TRC8 is involved in

degrading major histocompatibility complex (MHC) class I heavy chain, 3-hydroxy-3-methyl-glutaryl-coenzyme-A (HMG-CoA) reductase, and heme oxygenase, by itself or in combination with gp78 [166,181,293]. The E3 ligases relevant for a particular substrate cannot be predicted and must be empirically addressed. We know very little about the nature of the E3 ligases involved in hERG ERAD – their identities, division of labour, and supporting mechanisms.

To identify key regulators of hERG chaperone-mediated folding and degradation, we addressed the effect of Bag1 on hERG biosynthesis. We found that Bag1 induces hERG misfolding and thereby proteasomal degradation by increasing its ubiquitination through the membrane anchored E3 ligase TRC8, which cooperates with its E2 enzyme Ube2g2. We postulate from our experiments with Bag1 that there is a shift in the hERG degradation pathway away from CHIP towards other E3 ligases that act independently of Hsp70.

3.3. Results

3.3.1. Bag1 regulates hERG expression

Bag1 exists as three isoforms due to alternative translation initiation sites from a single mRNA. These are: Bag1L, Bag1M, and Bag1S which differ in their N-termini, but they all have a C-terminal Hsp70-binding BAG domain and a UBL domain, which was proposed to bind to the proteasome. Bag1L is predominantly nuclear with Bag1M and Bag1S in the cytosol and nucleus [288,290]. The shorter isoforms were most likely to interact through Hsp70 with hERG (Figure 3.1A).

To investigate the role of Bag1 in hERG biogenesis, we performed siRNA knockdown of Bag1, which depletes all isoforms, in Hela cells stably expressing wild-type hERG. We detected hERG by Western blot as two bands: a 135 kDa core-glycosylated (CG) immature form and a

155 kDa fully-glycosylated (FG) mature form that had trafficked through the Golgi. Bag1 knockdown increased the total amount of CG and FG hERG, compared to non-silencing controls (Figure 3.1B). Upon treatment with the proteasome inhibitor MG132, Bag1 knockdown no longer caused a difference in the amounts of hERG (Figure 3.1B), suggesting that the depletion of Bag1 protected hERG from proteasomal degradation.

In the opposite experiment, we overexpressed Bag1M, which results in the expression of both isoforms Bag1M and Bag1S, together with hERG in HEK293 cells. As expected, increased Bag1 levels led to a decrease in both the CG and FG forms of hERG relative to controls. The decrease of total hERG caused by Bag1 was restored by MG132, indicating that it was proteasome dependent (Figure 3.1C). Quantitative RT-PCR ruled out changes in hERG mRNA expression as the basis for the effects of either Bag1 knockdown or overexpression (not shown). Thus, Bag1 appears to promote the proteasomal degradation of hERG.

The FG form of hERG represents the channel in the late secretory pathway but not necessarily in a functional state at the cell surface. To directly test if Bag1 affected functional hERG, we conducted patch clamp measurements of hERG channel currents. As above, HeLa cells stably expressing hERG were depleted of Bag1 by knockdown, and HEK293 cells were transfected with hERG and Bag1. In agreement with the Western blot results, Bag1 knockdown and overexpression caused a substantial increase and decrease, respectively, in hERG tail current density relative to the corresponding controls (Figure 3.1D). Bag1 regulation of degradation may thus be a major determinant of hERG activity.

To address which domains of Bag1 were important for its effects on hERG, two mutants of Bag1M were tested: a deletion mutant (C-Bag1) contained only the BAG domain and lacking the UBL domain; and a point mutant (R237A) unable to bind Hsp70 (Figure 3.1A) [87,294]. When

overexpressed, C-Bag1 behaved identically to wild-type Bag1 in promoting degradation of hERG, whereas Bag1-R237A was ineffective (Figure 3.1C). The expression levels of the Bag1 mutants were adjusted to be comparable to that of wild-type Bag1, and Bag1-R237A generated the same distribution of isoforms as wild-type. We therefore conclude that Bag1 acts on hERG primarily through its activity as a NEF co-chaperone of Hsp70.

3.3.2. Bag1 promotes degradation of immature hERG

Degradation of immature CG hERG is by proteasomes at the ER, whereas mature FG hERG is degraded by the endosome-lysosome pathway [295]. The effects of Bag1 were restored by proteasome inhibition, suggesting that the regulated degradation is mostly of CG hERG. The changes in FG hERG upon Bag1 manipulation were likely due to changes in the amount of CG hERG able to traffic out of the ER. To address this directly, pulse-chase experiments were conducted in HEK293 cells co-expressing hERG and Bag1. Over a 6 h time course, the level of CG hERG decreased to around 60% of the starting amount of total hERG in control cells, and the FG form increased to around 30% of initial hERG (Figure 3.2A). This was consistent with previous results showing relatively inefficient trafficking of hERG [287]. When Bag1 was overexpressed, the final levels of CG and FG hERG were both markedly lower than in the control (Figure 3.2A). Indeed, the final amount of total hERG added to around 90% of initial in the control, and 70% upon Bag1 overexpression. This difference is due to proteasomal degradation as established above, and suggests that the turnover rate of immature hERG is faster upon Bag1 overexpression. The resulting loss of immature hERG would then result in less mature form.

Quality control clearance of mature hERG involves Hsp70 and CHIP [295], and Bag1 could also affect this process, adding to the loss of mature hERG due to ERAD. We therefore performed cycloheximide chase experiments to determine the effects of Bag1 on each form of hERG. Using the same cell lines as above, we found that CG hERG decreased to around 80% of initial levels over 6 h in control cells, and FG hERG remained essentially constant (Figure 3.2B). Bag1 overexpression resulted in a decrease of CG hERG to around 60% and of FG hERG to around 80%, relative to initial amounts (Figure 3.2B). Thus, Bag1 appears to favour both the degradation of CG hERG at the ER and the turnover of FG hERG by lysosomes, but with a proportionally larger effect on the ERAD pathway.

Polyubiquitination by E3 ligases is a key step in selecting proteins to be degraded by proteasomes. It was possible that Bag1 was affecting hERG degradation by regulating the polyubiquitin state of the channel. To address this, hERG was immunoprecipitated and polyubiquitinated forms detected by Western blot, and then quantified with respect to the amount of total hERG. In cells depleted of Bag1 by knockdown, the relative amount of polyubiquitinated hERG was decreased to around 80% of that in control cells (Figure 3.2C). Conversely, the overexpression of Bag1 increased polyubiquitinated hERG by around 50% above the control (Figure 3.2C). These results suggest that Bag1 affects the recognition of hERG by E3 ubiquitin ligases, leading to hERG degradation.

We confirmed the roles of the Bag1 domains in hERG polyubiquitination and turnover by repeating the above experiments with the C-Bag1 and Bag1-R237A mutants. In all of the assays, the effects of C-Bag1 were indistinguishable from those of wild-type Bag1, whereas Bag1-R237A had no effect at all and resembled the controls (Figure 3.2A-C). So, the UBL domain of Bag1 is not involved in regulating hERG degradation, but the Hsp70 interaction is essential.

3.3.3. Bag1 disrupts chaperone complexes with hERG

Because Bag1 is a NEF co-chaperone of Hsp70, it could promote the dissociation of Hsp70 from hERG [87]. Alternatively, complexes containing Bag1 and CHIP, perhaps independent of Hsp70, may direct polyubiquitination of hERG [290]. To test these hypotheses we performed hERG immunoprecipitations (IPs) from cells overexpressing Bag1 or its mutants, and detected co-precipitated Hsp70/Hsc70 and CHIP. In IPs from HEK293 cells transfected with hERG alone, both Hsp70/Hsc70 and CHIP were found complexed with hERG, and no signal for any of these proteins was detected in IPs from untransfected negative controls (Figure 3.3A). Notably, overexpression of Bag1 or C-Bag1 clearly decreased the amount hERG-associated Hsp70/Hsc70 and CHIP to less than 80% of the control, after adjusting for the amount of total hERG in each IP; as expected, Bag1-R237A had no effect (Figure 3.3A). These results support the first hypothesis, that Bag1 disrupts complexes of Hsp70 with hERG, and thereby interactions with the CHIP E3 ligase.

The diminished Hsp70 interaction with hERG suggested that the chaperone would be less able to assist hERG folding. Our previous work indicated that Hsp70 was important for hERG based on the requirement for the DnaJA1 co-chaperone [287]. We confirmed the role of Hsp70 by combined knockdown of Hsp70 and Hsc70. By Western blot detection, the levels of both CG and FG hERG were markedly decreased by Hsp70/Hsc70 knockdown, CG hERG to around 70% of the control and FG hERG to around 50% (Figure 3.3B). The strong effect on the FG form suggested that trafficking was impaired, and pulse-chase experiments were conducted to test this. Indeed, the kinetics and amount of FG hERG formation was substantially lower upon depletion of Hsp70/Hsc70 than in controls, although the turnover of CG hERG was less affected (Figure 3.3C). Altogether, it appears that Hsp70/Hsc70 is an essential chaperone for hERG.

Next, we tested for evidence of hERG misfolding upon Bag1 overexpression and loss of Hsp70 binding, by using limited proteolysis. Total light membrane fractions were prepared from HEK293 cells co-expressing hERG and Bag1, and treated with increasing concentrations of trypsin. In control cells with hERG alone, FG hERG was more resistant to digestion than CG hERG, consistent with a population of immature CG hERG being only partially folded (Figure 3.3D). Upon Bag1 overexpression, CG hERG was even more sensitive to digestion, and could barely be detected at the highest trypsin concentration (Figure 3.3D). FG hERG was also more sensitive with Bag1, although not as dramatically. These results support a mechanism in which the co-chaperone Bag1 regulates Hsp70 interactions with hERG and therefore hERG folding; the misfolding of hERG that results from excess Bag1 leads to polyubiquitination by quality control E3 ligases.

A question is raised by the behavior of CHIP, the only E3 ligase known to be involved in hERG ERAD. We previously showed that CHIP co-expressed with hERG induced its degradation [287], and now confirmed this using knockdowns of CHIP. As predicted, CHIP depletion caused notable increases in both FG and CG hERG compared to controls (Figure 3.3E). The somewhat larger effect on FG hERG was likely a result of the dual function of CHIP in hERG ERAD and clearance from the plasma membrane. However, our results show that although CHIP contributes to hERG degradation, it is dissociated from hERG by the activity of Bag1 and therefore cannot be responsible for the subsequent increase in polyubiquitination of misfolded hERG caused by Bag1. Instead, we propose that some other E3 ligase must be involved, and was likely to be anchored at the ER and dedicated to ERAD.

3.3.4. The E2 conjugating enzyme Ube2g2 functions in hERG ERAD

To identify which E3 ligase might be responsible, we began by addressing the upstream step, which is the E2 conjugating enzyme. The generation of polyubiquitinated substrates requires three enzymes. The ubiquitination system begins with an E1 activating enzyme, which transfers ubiquitin onto an E2 conjugating enzyme that coordinates with an E3 ligase to ubiquitinate the substrate. CHIP and the transmembrane E3 ligases at the ER have U-box and RING finger domains, which bind E2 enzymes and activate the transfer of ubiquitin from the E2 directly onto the substrate [296,297]. While there are many transmembrane E3 ligases, including a number which are uncharacterized or only predicted, only two E2 enzymes are predominantly involved. Ube2g2/Ubc7 does not have a membrane anchor but is known to act with HRD1, TEB4, gp78 and TRC8 [197,199,298,299]. Ube2j1/Ubc6e has a transmembrane anchor and acts with RMA1 and HRD1 [180,200]. Importantly, neither E2 functions with CHIP, which acts with Ube2d1/UbcH5a and Ube2n/Ubc13 among others [297,300].

Depletion of Ube2g2 and Ube2j1 should impair the function of their associated E3 ligases and narrow the set of candidates acting on hERG. In HeLa cell stably expressing hERG, knockdown of Ube2g2 led to a notable increase of about 30% in the CG hERG levels, and the FG form was also increased. In contrast, knockdown of Ube2j1 had no effect on either form of hERG (Figure 3.4A). This indicates that Ube2g2 is solely involved and has no overlapping function with Ube2j1 in hERG ERAD.

We then asked whether the ERAD mediated by Ube2g2 was related to the hERG misfolding caused by excess Bag1. Furthermore, we sought evidence for our proposed

mechanism, that Bag1 caused CHIP dissociation from hERG and favored degradation by Ube2g2-associated E3 ligases. Therefore, experiments were performed in which Bag1 was overexpressed at the same time that CHIP or Ube2g2 was depleted by knockdown. HEK293 cells were co-transfected with hERG, Bag1 and the relevant siRNAs, and the amounts of CG and FG hERG were quantified relative to those in control transfected cells. As established, Bag1 overexpression alone decreased hERG levels and CHIP knockdown increased them. However, CHIP knockdown had no effect on the loss of CG or FG hERG due to Bag1 overexpression (Figure 3.4B). In contrast, Ube2g2 knockdown alone increased hERG amounts, but also upon Bag1 overexpression (Figure 3.4B). Indeed, FG hERG levels were restored close to those in the controls, and CG hERG a bit below. It therefore appears that Bag1 promotes hERG degradation but by shifting the E3 ligase away from CHIP to another that depends on Ube2g2, most probably a transmembrane E3 ligase.

3.3.5. The E3 ligase TRC8 degrades hERG at the ER

We conducted an siRNA screen of various E3 ligases that are interactors of Ube2g2: HRD1, TEB4, gp78 and TRC8. We also included RMA1, which depends on Ube2j1, as a predicted negative control. Of all these, only knockdown of TRC8 led to an increase in CG hERG (Figure 3.5A). Interestingly, MHC class I heavy chain is degraded by TRC8 when induced by cytomegalovirus US2, but by HRD1 when it is misfolded by lack of assembly under normal conditions [180,181], suggesting that quality control of that substrate is by HRD1. In addition, the importance of TRC8 for the degradation of HMG CoA reductase is under debate, as a liver-specific knockout of gp78 in mice restores HMG CoA reductase in contrast to knockout/knockdown studies showing no effect of either gp78 or TRC8 [301,302]. For hERG,

though, depletion of HRD1 or gp78 had no significant effect. Therefore, we postulate that TRC8 is the Ube2g2-associated E3 ligase that is responsible for degradation of misfolded hERG.

3.4. Discussion

Our data suggest a model in which the ERAD pathway by which immature hERG is cleared depends on the degree of hERG misfolding. This in turn depends on how the Hsp70/Hsc70 ATPase cycle, necessary to support hERG folding, is tuned by the NEF Bag1. At least for hERG, endogenous Bag1 appears to be limiting, because Bag1 depletion stabilized the channel. The negative effects of Bag1 could be traced to the dissociation of Hsp70/Hsc70 from hERG, which reduces the ability of the chaperone to promote hERG folding so that more incorrectly folded hERG accumulates. At the same time, the CHIP E3 ubiquitin ligase is less able to modify hERG. Instead, misfolded hERG is selected for degradation by the Ube2g2-linked ER-associated E3 ligase TRC8.

Bag1 is generally thought to promote proteasomal degradation, in contrast to Bag3, which acts in autophagy [101,290,291]. However, the molecular mechanisms that link Bag1 to the ubiquitin-proteasome system have been unclear. Our results show no role for the Bag1 UBL domain in hERG degradation, so the direct interaction between the domain and 26S proteasome does not contribute. We also find that Bag1 reduces the interaction of CHIP with hERG, indicating that Bag1-CHIP complexes are not recruited to the substrate, as is the case for glucocorticoid receptor in the nucleus [303]. Instead, the Bag1 interaction with Hsp70 is required, which causes the release of hERG from Hsp70. Therefore, Bag1 promotes hERG degradation by interfering with its chaperone-mediated folding. This conclusion parallels what has been reported for Bag1 and CFTR in cell-free systems [304]. Moreover, Bag1 favours the recognition of hERG by

quality control E3 ligases other than CHIP, and which are not dependent on the Hsp70 system. From that point of view, CHIP is a relatively inefficient E3 ligase compared to the others at the ER, because its degradation function always competes with the pro-folding activity of Hsp70. Interestingly, for soluble cytosolic proteins, CHIP is also known to not be the only quality control E3 ligase, and others including most prominently UBR1, are also independent of Hsp70 or Hsp90 [305-307]. It is possible that Bag1 similarly shifts the degradation of cytosolic proteins away from CHIP to UBR1.

hERG is now the fourth established substrate of TRC8, after HMG-CoA reductase, MHC class I and heme oxygenase [166,181,293]. TRC8 seems to act on each of these substrates under different circumstances. HMG-CoA reductase is specifically degraded in response to high intracellular cholesterol levels, in a mechanism that involves formation of a complex with Insig-1, Insig-2, AUP1, gp78 and TRC8 leading to degradation of both HMG-CoA reductase and Insig-1 [163,164,299]. MHC class I degradation by TRC8 is also in response to specific disruption by viral US2, but not by US11 [181]. How heme oxygenase degradation is initiated is unknown, but its interaction with TRC8 seems to be through the transmembrane region [293]. We propose that TRC8 recognizes misfolded hERG as a quality control E3 ligase. This mode of action is clearly different from that with HMG-CoA reductase and likely MHC class I-US2, but may account for the degradation of heme oxygenase. Our limited proteolysis data on hERG do not identify a misfolded domain. However, the hERG tetramer is closely packed and most likely cooperatively folded, so it would not be surprising if folding problems in the cytosolic domains cause disruption in the transmembrane regions, and vice versa. We expect that there will be other misfolded proteins cleared from the ER by TRC8.

Cellular regulation of hERG levels has implications for its physiological function. The biosynthetic folding of hERG depends on both the Hsp70 and Hsp90 chaperones, and disruption of these chaperone systems in cardiac muscle could lead to loss of hERG function among other defects. In addition, hERG is found to be upregulated in many cancer types, where it increases proliferation by accelerating cell cycle progression [308]. Inhibitors of Hsp90, and more recently of Hsp70, are being developed as potential therapies in various cancer types [309-311]. It is quite possible that a reduction in overexpressed hERG due to degradation is one of the mechanisms contributing to the anti-oncogenic activity of these inhibitors. The therapeutic advantages of chaperone inhibitors compared to hERG channel blockers will have to be addressed for different cancers.

Figure 3.1. Bag1 regulates hERG expression. A, diagram of Bag1M transfection constructs used in this study. The UBL and BAG domain boundaries are marked with residue numbers, and the position of the R237A mutation disrupting Hsp70 interaction is shown with a star. B, Bag1 knockdown increases hERG levels. HeLa cells stably expressing hERG were transfected with siRNA duplexes against Bag1 (targeting all isoforms) or non-silencing control. CG and FG hERG were detected as 135 kDa and 155 kDa bands, respectively, by western blot, and quantified relative to the amount of each in control cells. Knockdown of Bag1 was confirmed by western blot; the bands corresponding to endogenous Bag1L, Bag1M and Bag1S are marked. Lower panel, the experiment was performed with MG132 treatment. C, Bag1 overexpression decreases hERG levels. HEK293 cells were transfected with hERG and the indicated Bag1 construct or vector control. CG and FG hERG were detected and quantified as above. Bands corresponding to Bag1M, Bag1S and C-Bag1 are marked. Endogenous Bag1 is not visible. Lower panel, the experiment was performed with MG132 treatment (n=1). D, Bag1 regulates cell surface hERG current. HEK293 cells were transfected with hERG, GFP and either Bag1 or vector control. Separately, HEK293 cells were transfected with hERG, siGLO and either siRNA against Bag1 or non-silencing control. Transfected cells were identified fluorescence microscopy. Voltage response curves from patch clamp measurements are shown. Unless otherwise specified, data are shown as mean ± SD and are representative of at least three independent experiments, * $p<0.05$.

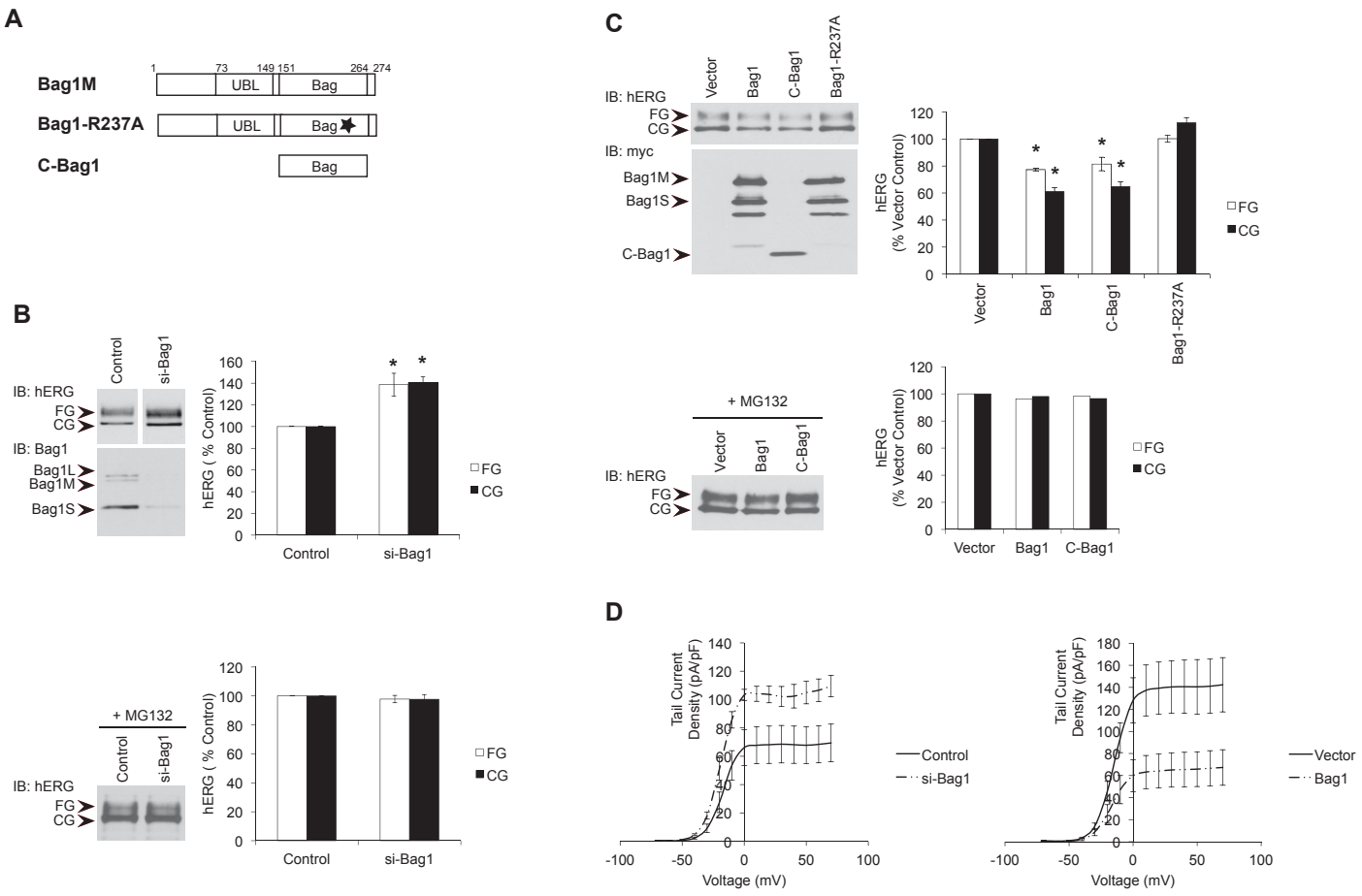
A
Bag1M
Bag1-R237A
C-Bag1
UBL
Bag
1
73
149
151
264
274
B
Control
si-Bag1
IB: hERG
FG
CG
IB: Bag1
Bag1L
Bag1M
Bag1S
hERG (% Control)
Control
si-Bag1
+ MG132
C
Vector
Bag1
C-Bag1
Bag1-R237A
IB: myc
hERG (% Vector Control)
D
Tail Current Density (pA/pF)
Voltage (mV)

Figure 3.2. Bag1 promotes degradation of immature hERG. A, pulse-chase kinetics of hERG upon Bag1 overexpression. HEK293 cells were transfected with hERG and the indicated Bag1 construct or vector control. Cells were metabolically radiolabelled for 45 min and chased for the indicated times, and lysates were immunoprecipitated using hERG-specific antibodies. CG and FG hERG were detected by SDS-PAGE and autoradiography, and quantified relative to the initial amount of CG hERG. B, cycloheximide chase kinetics of hERG upon Bag1 overexpression. HEK293 cells transfected as above were treated with cycloheximide to stop translation for the indicated times. CG and FG hERG were detected by western blot, and quantified relative to the initial amount of each. C, Bag1 affects the amounts of polyubiquitinated hERG. HeLa cells stably expressing hERG were transfected with siRNA against Bag1 or non-silencing control (n=1). In parallel, HEK293 cells were transfected with hERG and the indicated Bag1 construct or vector control. hERG was immunoprecipitated as above, and polyubiquitinated material detected with a ubiquitin-specific antibody. Quantitation of polyubiquitinated hERG was adjusted for the total amount of immunoprecipitated hERG, shown below the ubiquitin blot, and plotted relative to the amount of polyubiquitinated hERG in control cells. Unless otherwise specified, data are shown as mean ± SD and are representative of at least three independent experiments, * $p<0.05$.

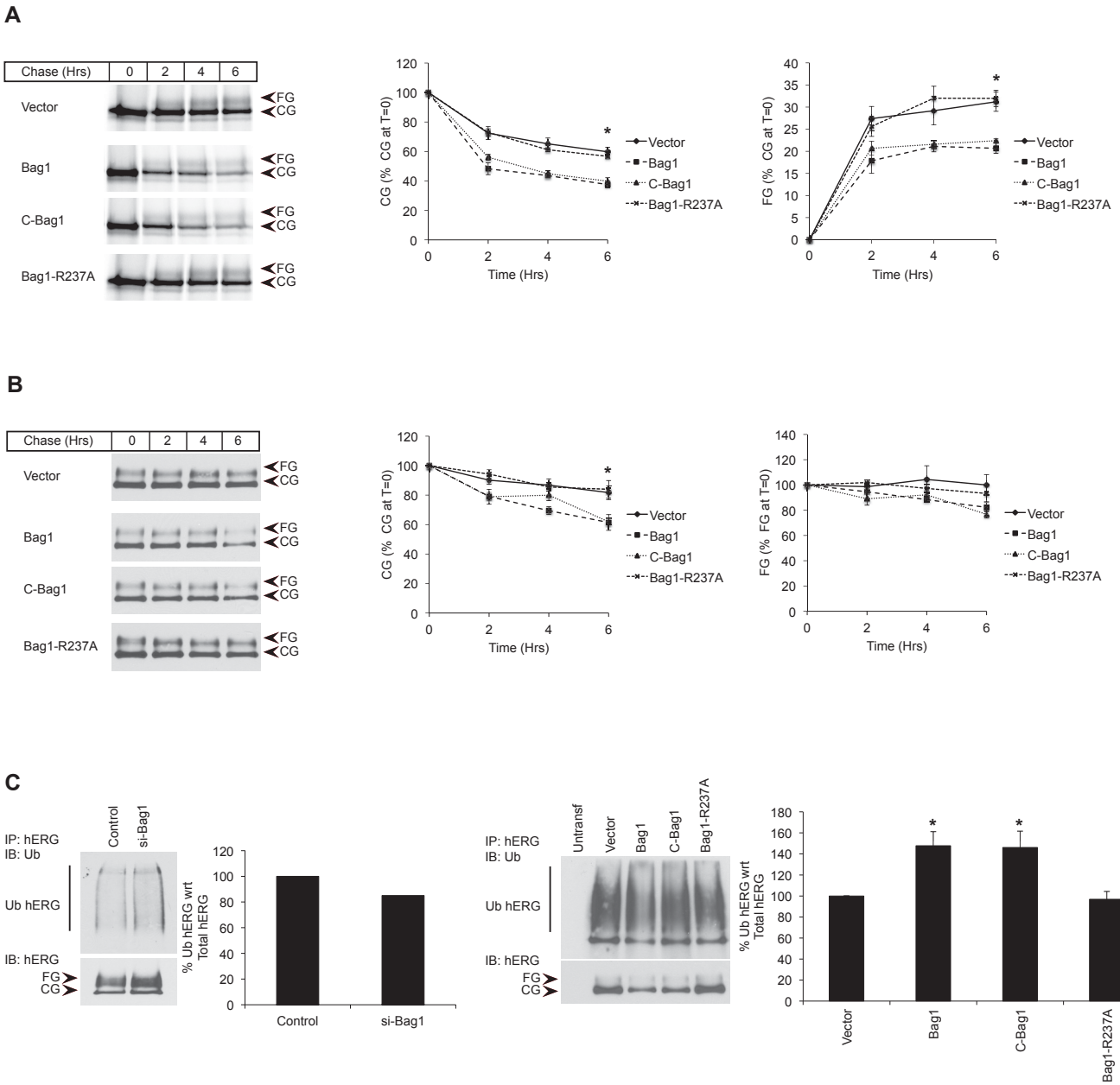
A
Chase (Hrs)
0
2
4
6
Vector
Bag1
C-Bag1
Bag1-R237A
FG
CG
CG (% CG at T=0)
FG (% CG at T=0)
Time (Hrs)
Vector
Bag1
C-Bag1
Bag1-R237A
B
FG (% FG at T=0)
C
IP: hERG
IB: Ub
Ub hERG
IB: hERG
Control
si-Bag1
% Ub hERG wrt Total hERG
Untransf
Vector
Bag1
C-Bag1
Bag1-R237A

Figure 3.3. Bag1 disrupts chaperone complexes with hERG. A, Bag1 affects chaperone complexes. HEK293 cells were transfected with hERG and the indicated Bag1 construct or vector control, and hERG immunoprecipitated as in Figure 3.2. Co-precipitating Hsc70/Hsp70 and CHIP were detected by western blot; Hsc70 and Hsp70 were equally detected by the antibody used here. Quantitation of Hsc70/Hsp70 and CHIP was adjusted for the total amount of immunoprecipitated hERG, and plotted relative to the amounts in the control. B, Hsc70/Hsp70 is necessary for hERG maturation. HeLa cells stably expressing hERG were transfected with siRNA against both Hsc70 and Hsp70, or non-silencing control. CG and FG hERG were detected by western blot, and quantified relative to the amount of each in control cells. C, cells as in B were examined for hERG kinetics by pulse-chase as in Figure 3.2. D, Bag1 induces misfolding of hERG. HEK293 cells were transfected with hERG and either Bag1 or vector control. Total light membrane fractions were isolated and treated with the indicated amounts of trypsin for 10 min at 37°C. CG and FG hERG were detected by western blot and quantified relative to the amount without trypsin treatment (n=1). E. CHIP contributes to hERG degradation. The experiment in B was repected except with siRNA against CHIP. Unless otherwise specified, data are shown as mean ± SD and are representative of at least three independent experiments, * $p<0.05$.

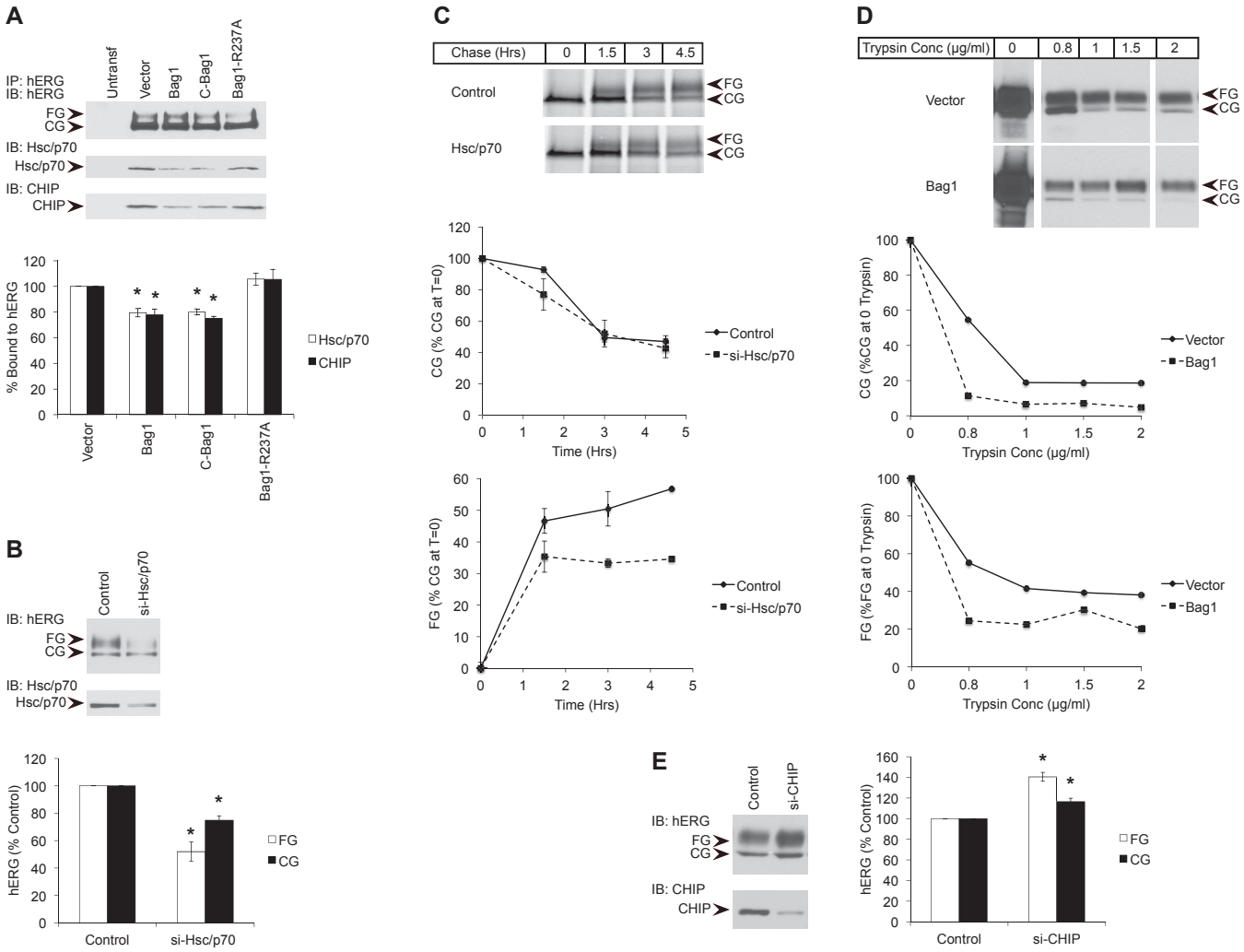
A
IP: hERG
IB: hERG
Untransf
Vector
Bag1
C-Bag1
Bag1-R237A
FG
CG
IB: Hsc/p70
Hsc/p70
IB: CHIP
CHIP
% Bound to hERG
Hsc/p70
CHIP
B
Control
si-Hsc/p70
IB: hERG
IB: Hsc/p70
hERG (% Control)
FG
CG
C
Chase (Hrs)
0
1.5
3
4.5
Control
Hsc/p70
CG (% CG at T=0)
si-Hsc/p70
Time (Hrs)
FG (% CG at T=0)
D
Trypsin Conc (µg/ml)
0
0.8
1
1.5
2
Vector
Bag1
CG (%CG at 0 Trypsin)
Trypsin Conc (µg/ml)
FG (%FG at 0 Trypsin)
E
IB: CHIP
si-CHIP

Figure 3.4. The E2 conjugating enzyme Ube2g2 functions in hERG ERAD. A, HeLa cells stably expressing hERG were transfected with siRNA against the indicated protein, or non-silencing control. Knockdown of the proteins was confirmed by western blot. CG and FG hERG were detected by western blot, and quantified relative to the amount of each in control cells. B, HEK293 cells were transfected with hERG and either Bag1 or vector control, as well as siRNA against Ube2g2 or CHIP or non-silencing control. CG and FG hERG were detected and quantified as above. Unless otherwise specified, data are shown as mean ± SD and are representative of at least three independent experiments, * $p<0.05$.

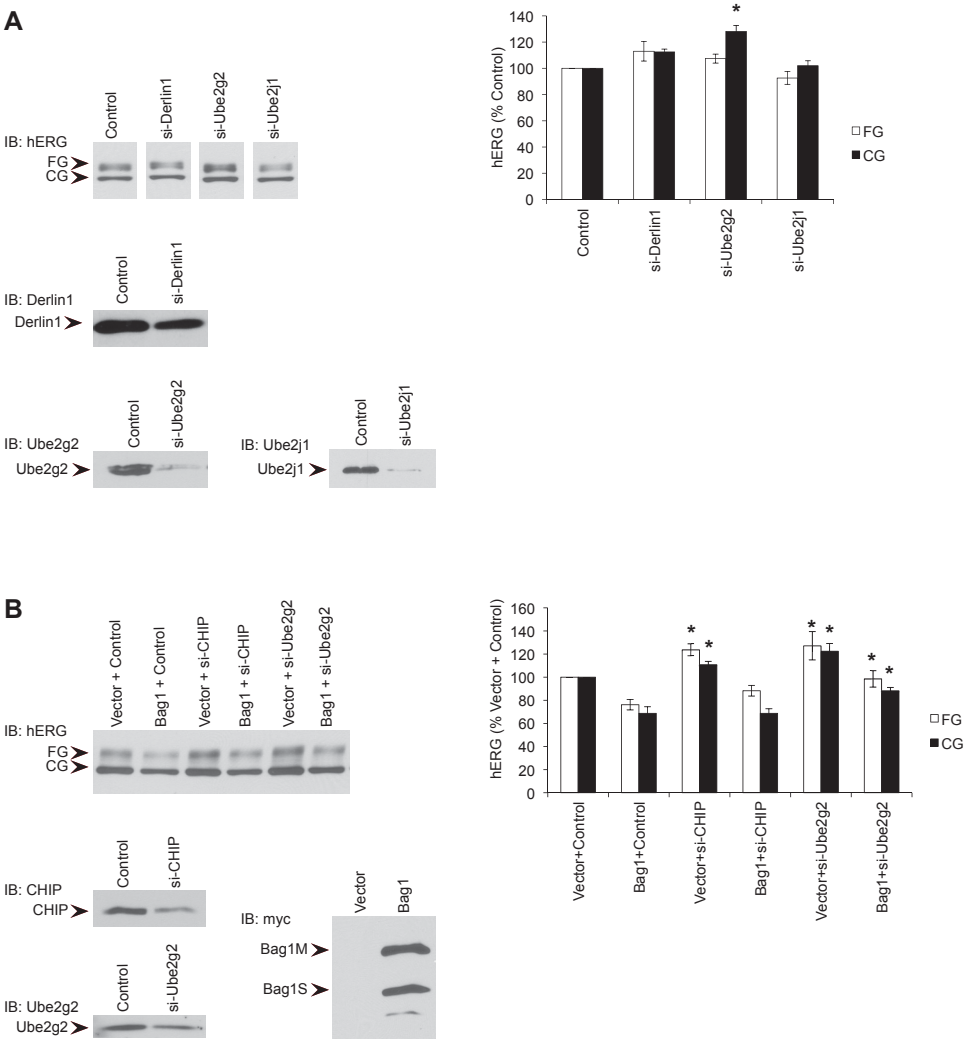
A
Control
si-Derlin1
si-Ube2g2
si-Ube2j1
IB: hERG
FG
CG
IB: Derlin1
Derlin1
IB: Ube2g2
Ube2g2
IB: Ube2j1
Ube2j1
hERG (% Control)
FG
CG
B
Vector + Control
Bag1 + Control
Vector + si-CHIP
Bag1 + si-CHIP
Vector + si-Ube2g2
Bag1 + si-Ube2g2
IB: CHIP
CHIP
IB: myc
Vector
Bag1
Bag1M
Bag1S
hERG (% Vector + Control)
Vector+Control
Bag1+Control
Vector+si-CHIP
Bag1+si-CHIP
Vector+si-Ube2g2
Bag1+si-Ube2g2

Figure 3.5. The E3 ligase TRC8 degrades hERG at the ER. A, HeLa cells stably expressing hERG were transfected with siRNA against the indicated protein, or non-silencing control. Knockdown of the proteins was confirmed by western blot. CG and FG hERG were detected by western blot, and quantified relative to the amount of each in control cells. Unless otherwise specified, data are shown as mean ± SD and are representative of at least three independent experiments, * $p<0.05$.

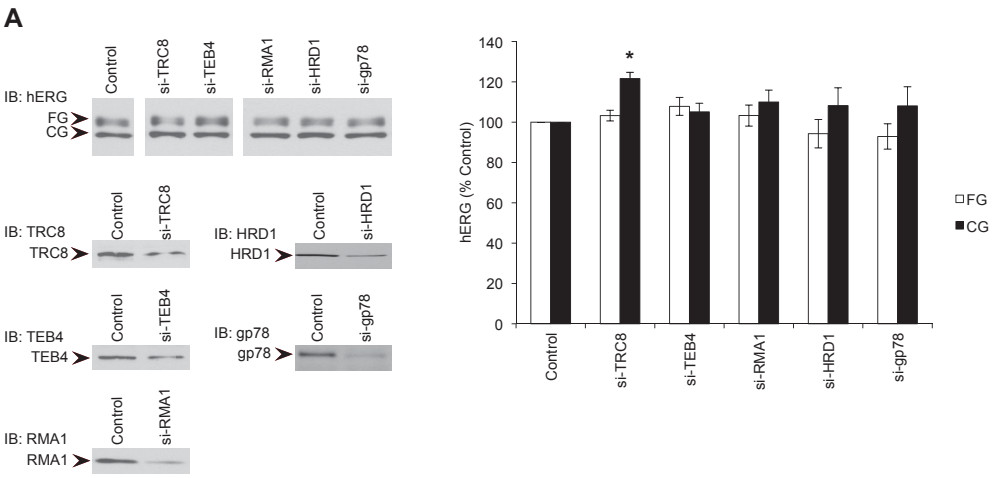
A
Control
si-TRC8
si-TEB4
si-RMA1
si-HRD1
si-gp78
IB: hERG
FG
CG
IB: TRC8
TRC8
IB: HRD1
HRD1
IB: TEB4
TEB4
IB: gp78
gp78
IB: RMA1
RMA1
hERG (% Control)
140
120
100
80
60
40
20
0
*
FG
CG
Control
si-TRC8
si-TEB4
si-RMA1
si-HRD1
si-gp78

Chapter 4

Dual roles of Hsp70 and DNAJA2 in the degradation of CFTR

4.1. Abstract

Loss of function of the cystic fibrosis transmembrane conductance regulator, the CFTR chloride channel, is usually caused by misfolding and degradation of the protein due to mutation. The Hsc70/Hsp70 chaperone system is thought to assist CFTR folding, but also its degradation at both the endoplasmic reticulum (ER) and cell surface. Here, we address how these opposing functions are balanced. We find that the co-chaperone DNAJA2 as well as DNAJA1 is necessary for CFTR, but that Hsc70/Hsp70 restricts the amount of mature CFTR. Overexpressed DNAJA2, but not DNAJA1, specifically caused degradation of CFTR by Hsc70/Hsp70 and the E3 ubiquitin ligase CHIP at the ER. Excess Hsp70 also promoted CFTR degradation, but mostly through the lysosomal pathway. This role of Hsp70 required CHIP, but not complex formation with HOP and Hsp90. Thus, the endogenous levels of DNAJA1 and DNAJA2 appear to be optimized for CFTR. Furthermore, we propose that DNAJA2 is a major determinant of ER-associated degradation of newly synthesized CFTR, whereas Hsp70 is the corresponding determinant of mature CFTR degradation from the cell surface.

4.2. Introduction

Cystic Fibrosis (CF) is an autosomal recessive genetic disease due to loss of function mutations in the cystic fibrosis transmembrane conductance regulator, CFTR (gene ABCC7). CFTR is a Cl^- ion channel located at the apical membrane of polarized epithelial cells lining airways and glands [312,313]. The deletion of the phenylalanine 508 (ΔF508) is the most common CF-causing mutation, which underlies the channel folding defects that impede almost all nascent forms from progressing through the biosynthetic pathway and consequently are degraded at the ER [224]. Therefore, understanding the mechanisms of CFTR biogenesis, folding and degradation is critical for unraveling the molecular basis of CF pathogenesis and the development of new therapeutics.

CFTR is a member of the ATP-binding cassette (ABC) transporter superfamily that contains 1480 amino acid residues and forms five subdomains; two membrane-spanning domains (MSD1 and MSD2) with six transmembrane domains each, two nucleotide-binding domains (NBD1 and NBD2), and a regulatory (R) domain [314]. CFTR synthesis at the endoplasmic reticulum (ER) takes approximately 10 minutes and requires co- and post-translational folding events that involve the cooperative assembly of N- and C-terminal membrane and cytosolic subdomains [232,234,236]. CFTR assembly progresses through the formation of different folding intermediates most of which are destined for the degradation pathway since CFTR folding is inefficient [315].

The F508 residue is located on the surface of NBD1 and is important for proper domain folding [232,233]. Additionally, deletion of F508 is predicted to perturb interaction with NBD2 and with the intracellular loops exposed by MSD1 and MSD2. These contact sites are crucial for

maturation of intact CFTR [232]. Therefore, the great majority of CFTR ΔF508 is unable to fold correctly, and is sent prematurely for ER-associated proteasomal degradation (ERAD) [237].

Molecular chaperones assist the folding and assembly of the cytosolic domains of CFTR. The ATP-dependent Hsc70/Hsp70 and Hsp90 chaperones are thought to be the most important [30,224,240,241]. Hsc70/Hsp70 is activated by the J domains of DNAJ co-chaperones, to support folding but also a variety of other processes [4,63]. Hsc70 and its co-chaperone DNAJA1 (also called DJA1/Hdj2) act early on at the level of the ER to assist co-translational folding of NBD1 [55]. This step is followed by the action of the ER lumenal chaperone, calnexin, which may act after Hsc70 and appears to be critical in the stabilization of MSD2 and NBD2 domains of CFTR [316,317]. N-glycosylation at residues N894 and N900 are required for recruiting calnexin and promoting nascent CFTR folding as well as structurally stabilizing transmembrane regions of MSD2 in the ER membrane [247]. The Hsp90 system is involved probably in the later steps of CFTR folding as Hsp90 inhibition blocks CFTR maturation and accelerates its degradation [241]. In addition, downregulation of the Hsp90 cochaperone Aha1 rescues CFTR ΔF508 allowing its accumulation at the cell surface [240]. The importance of Hsp90 and its co-chaperones in CFTR biogenesis is well established, yet the exact contribution of Hsc70 or Hsp70 and its co-chaperones in the early steps of CFTR biogenesis is still in question.

Molecular chaperones are also involved in CFTR degradation. The cytosolic E3 ubiquitin ligase CHIP interacts with Hsc70/Hsp70 to promote misfolded CFTR ubiquitination and ERAD [104]. In addition to the ER cytosolic Hsc70-CHIP complex, there is an ER membrane-associated complex that involves the E3 ligases RMA1 and gp78 that cooperate to ubiquitinate CFTR [200,201]. Ubiquitinated CFTR is sent for proteasomal degradation through a pathway that involves derlin-1 [200], BAP31 [318], and p97 [319]. It is not entirely clear how CFTR degradation is divided between

the CHIP and RMA1-gp78 E3 machineries. However, RMA1 has been proposed to act co-translationally to sense the folding status and assembly of NBD1 and the R domain while Hsc70-CHIP may act post-translationally after NBD2 synthesis to detect folding defects that involve terminal steps in CFTR assembly [200]. However, binding sites for Hsc70 in NBD1 and NBD2 during folding remain to be determined. The RMA1 E3 ligase complex recognizes misfolded cytosolic domains in CFTR through the help of Hsc70 and a transmembrane ER resident co-chaperone, DNAJB12 [244]. It is not clear which DNAJs promote the binding of Hsc70-CHIP to CFTR leading to degradation. The dual function of Hsc70/Hsp70 in folding and degradation also raises the question as to the extent of its contribution to each of these opposing processes during CFTR biosynthesis.

The Hsc70-CHIP complex also functions in CFTR cell surface quality control by promoting lysosomal degradation of CFTR that is misfolded at the plasma membrane (PM). Hsp90 is also implicated in this function, as well as the co-chaperone HOP which connects Hsp90 with Hsc70/Hsp70 [100]. The mechanisms involved are less clear than for ERAD, but the parallels with ER quality control are notable. However, a similar question arises about the relative contribution of Hsc70/Hsp70 to degradation at the PM compared to the ER, whether CFTR at the PM is maintained by Hsc70/Hsp70, and the role of any of the DNAJ co-chaperones. Furthermore, our previous results found that DJA1 was biologically distinct from its close homolog DNAJA2 (DJA2) in terms of which proteins they assist in folding, but that both could promote CHIP-mediated degradation of the immature hERG potassium channel at the ER [62,287].

Here, we examined the overall importance of the Hsc70/Hsp70 chaperone system for CFTR. Using knockdown and overexpression experiments, we found that both DJA1 and DJA2 are required for CFTR maturation. Remarkably, Hsp70 negatively affected mature CFTR

amounts. We then assessed the roles of DJA1, DJA2 and Hsp70 in ERAD and lysosomal degradation of CFTR. We propose a model in which specific DNAJ activities, or the lack of it, regulate the degradation of CFTR in cells.

4.3. Results

4.3.1. Optimum levels of Hsp70 and DJAs are required for mature CFTR

The Hsp70 chaperone system was expected to be most important for CFTR during its folding at the ER. Thus, we first examined the kinetics of CFTR maturation using radiolabel pulse-chase experiments. HeLa cells, stably expressing CFTR with an external HA epitope tag [100], were labeled with a 15 min pulse and chased for 3 h. In agreement with previous reports, immature core-glycosylated band B CFTR, around 140 kDa, diminished to a low amount compared to its starting level (Figure 4.1A). Mature fully-glycosylated band C CFTR at around 170 kDa rose in amount, representing a substantial amount of the initial band B material, as expected (Figure 4.1A). Hsc70 (gene HSPA8) and Hsp70 (genes HSPA1A and HSPA1B) are the most abundant cytosolic forms of the chaperone family. To address their importance for CFTR, the expression of both was knocked down using a mixture of three siRNA duplexes. The total population of Hsc70 and Hsp70 was depleted to around 50% of non-silencing control (data not shown). Unexpectedly, knockdown of Hsc70/Hsp70 increased the amount of band C CFTR compared to the non-silencing control, while band B was not affected (Figure 4.1A).

The reverse experiment was then conducted. HEK293 cells transiently transfected with HA-tagged CFTR and Hsp70 or vector control, were similarly examined by pulse-chase

experiments. Hsp70 was used because its expression was much higher than that of Hsc70 when co-transfected with CFTR, and at a level comparable to total endogenous Hsc70 and Hsp70 (data not shown). In control experiments, the expected decrease in band B and increase in band C was observed. However, Hsp70 overexpression markedly reduced the amount of band C that appeared during the chase, whereas band B was unaffected (Figure 4.1B). Thus, the knockdown and overexpression results were consistent with each other and both suggested that Hsc70/Hsp70 suppressed mature CFTR levels.

These results were striking, and were further investigated by testing the major DNAJ-family co-chaperones DJA1 and DJA2. Pulse-chase experiments on CFTR were conducted as above with knockdown of either DJA. Depletion of DJA1 clearly decreased the amount of mature band C produced, and remarkably, DJA2 depletion had the same effect (Figure 4.1C). Immature band B was not strongly affected by either knockdown. We then compared the effects of DJA1 or DJA2 overexpression with that of Hsp70. In this case, DJA2 overexpression also decreased band C levels, and caused a small increase in band B over the chase (Figure 4.1D). In contrast, DJA1 had no effect on bands B or C.

The DJA1 and DJA2 results parallel those with the hERG potassium channel [287], but with a different pattern. Knockdown experiments showed that DJA1 was specifically required for mature hERG, and that DJA2 was not. Now, for CFTR, it appears that both DJA1 and DJA2 are important for maturation. Also, the results demonstrate that both DJA1 and DJA2 overexpression promoted hERG ERAD. It is therefore possible that DJA2 specifically has a function to direct CFTR to ERAD. By extension, Hsp70 overexpression could also promote CFTR degradation. The increase in mature CFTR upon Hsp70 knockdown suggests that endogenous cellular levels of the chaperone already favour CFTR degradation. Nevertheless, some level of Hsp70 must be

required for CFTR folding and maturation, as DJA1 and DJA2 are only known to act in coordination with Hsc70/Hsp70. Taken together, we propose that optimum levels of Hsc70/Hsp70 and its DJA co-chaperones are needed for mature CFTR, and that CFTR is highly sensitive to disruption of the chaperone system.

4.3.2. DJA2 promotes ERAD of CFTR

The effects of DJA depletion could be attributed to impaired folding, but the loss of mature CFTR caused by excess DJA2 could be more complex. First, increased ERAD of newly-synthesized CFTR could result in less mature form. Second, the pulse-chase data showed that DJA2 increased immature CFTR levels moderately, so DJA2 could instead be delaying traffic out of the ER. A third possibility is that DJA2 could affect clearance of mature CFTR in lysosomes. To address these questions efficiently, we used HEK293 cells transfected with doxycycline-inducible CFTR, with DJA2 co-expressed under a constitutive promoter. This allowed us to turn on CFTR expression in an environment with a defined pre-existing population of DJA2, compared to vector control. The advantage of the method is that both band B and C can be observed in a single experiment. After 6 h of induction, a large amount of band B CFTR was detectable, along with a clear band C. Cycloheximide (CHX) was then added and over a 3 h chase, band B levels decreased greatly but band C levels only moderately (Figure 4.2A, B). The rate of band B decrease was identical to that observed by pulse-chase (Figure 4.2B), and the starting amount of band C before the chase was around 20% of band B (Figure 4.2A, top left panel). Thus, in its main parameters, the “induction-chase” method recapitulates the pulse-chase in HEK293 cells (Figure 4.1B,D) such that immature CFTR decreases to around 10% of initial amounts over 3 h, and maturation of CFTR is around 20% after induction. Furthermore, during

the CHX chase, band C is in dynamic equilibrium between anterograde trafficking and lysosomal degradation, so effects on both rates can be observed.

As a first experiment, we tested the effect of DJA2 on CFTR. At 6 h of induction, DJA2 overexpression did not greatly change the total amount of band B and C observed. However, during the CHX chase, DJA2 caused a notably steeper decrease in band C levels compared to vector control (Figure 4.2A,B) in overall agreement with the pulse-chase results. A small increase in band B levels was visible but was not significant. To confirm that the effect was specific to the co-chaperone function of DJA2, a deletion mutant lacking the J domain (DJA2-ΔJ) [62] was also tested, with the same results as vector control (Figure 4.2A,B).

We then addressed whether DJA2 promoted ERAD of CFTR by adding the proteasome inhibitor MG132. In control cells, MG132 moderately increased the amounts of both bands B and C (Figure 4.2C). However, when DJA2 was expressed, MG132 restored band C levels to those originally observed in control cells (Figure 4.2D). The increase in band B upon MG132 addition was the same whether vector or DJA2 was transfected (Figure 4.2C,D). For DJA2-ΔJ, only the same increase in band C as for vector control was observed with MG132 (Figure 4.2E). As expected, DJA1 overexpression had no effect on band B or C kinetics (data not shown). These results show that DJA2 promotes degradation of immature CFTR by proteasomes at the ER. The effects of DJA2 on mature band C must then be due to the decrease in immature CFTR available for forward trafficking.

A possible mechanism is that DJA2 directs the binding of Hsc70/Hsp70 complexes with CHIP to CFTR. This would be consistent with the requirement for the J domain shown above, to activate polypeptide binding by Hsc70. We thus examined the induction-chase kinetics of CFTR upon CHIP knockdown. Depletion of CHIP alone modestly increased levels of band C but not

band B during the chase (Figure 4.3A,B), although total levels of both were proportionally higher compared to non-silencing controls. But, when DJA2 was overexpressed to decrease band C amounts, CHIP knockdown restored band C to levels found in vector-transfected non-silencing controls (Figure 4.3A,C). This was very similar to the effect of MG132 upon DJA2 transfection (Figure 4.2D). We conclude that excess DJA2 specifically promotes ERAD of CFTR exclusively through Hsc70-CHIP, leading to impaired forward trafficking.

4.3.3. Hsp70 promotes lysosomal degradation of CFTR

We then investigated the Hsp70 effects on CFTR. Hsp70 overexpression did not change the amounts of band B and C after 6 h of induction, but during the 3 h CHX chase, Hsp70 overexpression led to a clearly faster decline in band C compared to vector control (Figure 4.4A,B). This was similar to the effect of DJA2 above, although Hsp70 had no effect on the kinetics of band B disappearance. Because we had established that DJA2 and CHIP promoted degradation of immature CFTR, it seemed likely that overexpressed Hsp70 acted the same way. However, when we conducted the experiments in the presence of MG132, the proteasome inhibitor had no significant effect on the loss of band C caused by Hsp70 (Figure 4.4A,D). This was opposite to our observations with DJA2. While MG132 resulted in some increase in band B levels on Hsp70 overexpression, the increase was the same as that in vector controls (Figure 4.4C,D). It appeared that Hsp70 suppresses mature CFTR through mechanisms other than ERAD.

Band C levels during the CHX chase depends on its rate of formation from band B, and rate of disappearance due to lysosomal degradation. Because Hsp70 did not change the amounts of band B during the chase, there was no evidence that forward trafficking of CFTR and maturation into band C was slowed. Thus, we addressed the idea that excess Hsp70 directed

mature CFTR to lysosomal degradation. The same experiment was performed but with addition of chloroquine (CQ) to inhibit lysosomal proteases by raising the organellar pH. In vector-transfected cells, CQ did not affect band B as expected, but caused a moderate increase in band C during the chase (Figure 4.4E). When Hsp70 was overexpressed, CQ now prevented the fast decline in band C, and restored band C levels to that in the control cells (Figure 4.4F). Therefore, excess Hsp70 acts primarily to target mature CFTR for lysosomal degradation, and not immature CFTR for ERAD. DJA2, when in excess, works with endogenous levels of Hsc70/Hsp70 to favour ERAD of CFTR.

4.3.4. CHIP but not HOP-Hsp90 is required for mature CFTR degradation

A role for Hsc70/Hsp70 in internalization and lysosomal targeting was previously found for rescued, misfolded CFTR ΔF508 at the PM. siRNA screening showed that Hsc70 but not Hsp70 was required, and that CHIP ubiquitination was the major mechanism. Furthermore, there was evidence of roles for DJA1 and the co-chaperone HOP that links Hsc70/Hsp70 to Hsp90 [100]. Here, our results on wild-type CFTR suggest that Hsp70 is important for its lysosomal targeting, and there was no evidence of a role for DJA1. Hsc70 co-transfection levels in HEK293 were too low for us to make reliable conclusions. Thus, the involvement of CHIP and HOP in Hsp70-directed lysosomal degradation was examined.

As a first approach, we took advantage of a recent report of a phosphorylation site in Hsc70/Hsp70 within its C-terminal binding motif for tetratricopeptide-repeat domain co-chaperones, including CHIP and HOP. In particular, the phosphorylation at T636 on Hsp70

impaired CHIP binding, as well as the phosphomimic mutant T636D [320]. However, direct effects on Hsp70-mediated degradation were not addressed by that work, as cell proliferation related to kinase activity was mostly examined. We constructed the Hsp70 T636D mutant and tested its co-chaperone interactions by co-IP from HEK293 cells. Both wild-type and T636D mutant were recovered in similar amounts using the FLAG tag, but there was a clear loss of CHIP and HOP binding to the mutant, with about 40% remaining compared to wild-type Hsp70 (Figure 4.5A). Consistent with the decreased HOP interaction, co-precipitating Hsp90 was also markedly reduced with the mutant. Hsp110 was also detected, as a negative control, which binds to the N-terminal ATPase domain of Hsp70 [321,322], and its interaction was unaffected (Figure 4.5A). Hsp70-T636D thus appears to be uncoupled both from CHIP and the Hsp90 chaperone system.

To rule out any intrinsic functional defects in Hsp70 T636D, its chaperone activity was confirmed. We previously showed that in HEK293 cells, the model reporter firefly luciferase denatured by heat shock could be refolded to around 20% of initial activity by endogenous Hsc70/Hsp70 and DJA2, and that refolding could be enhanced to around 50% of initial by overexpression of Hsp70 [62,310]. The Hsp70-T636D mutant when overexpressed resulted in an identical refolding yield to wild-type Hsp70 (Figure 4.5B). Therefore, any effects of Hsp70-T636D must be due to its loss of interactions and not to other biochemical defects.

When Hsp70 T636D was overexpressed in CFTR induction-chase experiments, the decline in band C was weak compared to that with wild-type Hsp70 (Figure 4.5C,D). The rate of decrease was still greater than with vector control (Figure 4.5D), which may be due to the partial loss of CHIP and HOP-Hsp90 binding to the Hsp70 mutant. The presence of MG132 did not significantly change the kinetics of band C with Hsp70-T636D, and the increase in band B was the same as that with vector control (Figure 4.5E and 4.4C). CQ treatment caused some increase

in band C, as expected (Figure 4.5F). It appears that the co-chaperone interactions are important for degradation of mature CFTR.

Next, the roles of CHIP and HOP were directly investigated by knockdown. As reported above, CHIP knockdown increased band C somewhat during the CHX chase (Figure 4.3A,B), but HOP knockdown had no visible effect on either band of CFTR (Figure 4.6A,B). Combined Hsp70 overexpression and CHIP knockdown was tested, and notably, band C amounts were restored to those in controls (Figure 4.6C,D). Again, HOP knockdown had no effect, indicating that Hsp70 effects were exclusively through CHIP. As a further test, Hsp70-T636D was overexpressed, and as predicted CHIP knockdown only marginally increased band C levels, with HOP knockdown being ineffective (Figure 4.6C,E). Therefore, we conclude that excess Hsp70 suppresses mature CFTR amounts by promoting ubiquitination by CHIP, leading to degradation in lysosomes. Moreover, Hsp70 complexes with HOP and Hsp90 appear not to be involved.

4.4. Discussion

Taken together, these results outline a dual role of the Hsp70 chaperone system in the degradation of immature and mature CFTR. These quality control activities are on top of the chaperone requirement for CFTR folding and trafficking, and depend on the expression levels of specific chaperone components. Our model has three key points: First, not only DJA1, but also DJA2 is necessary for CFTR maturation, and by extension Hsc70/Hsp70 is also important. Second, DJA2 has a unique role in inducing the degradation of immature CFTR, through Hsc70/Hsp70 and CHIP. Third, Hsp70 in excess promotes lysosomal targeting and degradation of mature CFTR, again through CHIP. The model raises interesting questions about how CFTR

may be recognized differently by the chaperones, and how chaperone manipulation could be usefully pursued.

The degradation role of Hsp70 has the most important implications for the understanding of cystic fibrosis. The knockdown data suggest that only a fraction of endogenous Hsc70 and Hsp70 is necessary for CFTR folding and trafficking, supported by endogenous levels of DJA1 and DJA2. Because Hsc70 and Hsp70 are highly abundant in cells [4], their levels are also unlikely to be limiting for the folding of CFTR ΔF508. Instead, the excess endogenous Hsc70/Hsp70 may naturally restrict the population of mature CFTR, wild-type and ΔF508, by favouring lysosomal degradation. Moreover, excess Hsc70/Hsp70 does not strongly promote ERAD of CFTR, so acts primarily on the mature form. Cellular concentrations of Hsc70/Hsp70 are substantially higher than its DJA partners, and it is possible that the imbalance contributes to CFTR degradation. In any case, Hsc70/Hsp70 is a promising drug target for cancer therapies, and there has been recent progress in developing novel small molecules that modulate different aspects of its mechanism. [310,311] The use of such an agent at low doses to achieve partial inhibition could be a promising therapeutic approach to preserve CFTR ΔF508 at the PM in cystic fibrosis patients.

CFTR is now the first protein identified to require both DJA1 and DJA2 for folding. These DNAJs are biochemically distinct, which underlies their different abilities to support Hsc70-mediated folding of various proteins. [60-62] As already mentioned, we demonstrated that DJA1 but not DJA2 was required for the hERG channel. [287] DJA1 is also specifically required for Activation-Induced Deaminase [58], and for proper regulation of the Androgen Receptor [57]. Oppositely, we found that DJA2 but not DJA1 is necessary for luciferase refolding [62]. DJA2 is also known to be important for signaling through certain trimeric G proteins [283]. These studies suggest that each DJA may be optimal for Hsc70-mediated folding of certain types of structures,

and it would be expected that some substrates would contain structures of both types so that both DJAs are required. We believe that CFTR will be only the first example of other proteins dependent on DJA1 and DJA2. As DJA1 interacts with the CFTR NBD1 during its synthesis [55], an intriguing speculation is that DJA2 acts at a later step, perhaps on NBD2.

The results on CHIP-mediated ERAD of CFTR also show that DJA2 and DJA1 are not interchangeable. This is more unexpected than specific requirements for folding. The simplest model would be that any DNAJ could promote ubiquitination by CHIP-Hsc70 complexes, as folding of the substrate is not required. However, our previous data had some indications that the process was more complex. Although both DJAs promoted hERG degradation, DJA2 was more effective than DJA1, and another co-chaperone DNAJA4 still more [287]. Furthermore, in a study of DJA2 mutants with different mechanistic defects, all mutants, which could not promote luciferase refolding, were also unable to drive hERG degradation [62]. Finally, the ER-anchored co-chaperone DNAJB12 promotes CFTR degradation through the RMA1 pathway and not through CHIP [244]. Thus, while the exact roles of DNAJs in ERAD are still to be determined, conformational changes in the substrate related to those during folding are likely to be involved. The DJAs are harder to target pharmacologically than Hsc70 or Hsp70 because they do not have enzymatic activities, and high-resolution structural information is lacking. Our results suggest that overall, Hsc70 and Hsp70 have the most potential for research into future therapies.

Figure 4.1. Optimum levels of Hsp70 and DJAs are required for mature CFTR. A, HeLa cells stably expressing externally HA-tagged CFTR were transfected with siRNA against both Hsc70 and Hsp70, or non-silencing control. Cells were metabolically radiolabelled for 15 min and chased for the indicated times, and lysates were immunoprecipitated using HA-specific antibodies. CFTR bands B and C were detected by SDS-PAGE and autoradiography at 140 kDa and 170 kDa, respectively, and quantified by image phosphor analysis relative to the initial amount of band B CFTR. B, HEK293 cells were transfected with HA-tagged CFTR and either Hsp70 or vector control, and analyzed by pulse-chase as above. C, HeLa cells as above were transfected with siRNA against DJA1, DJA2 or non-silencing control, and analyzed by pulse-chase. D, HEK293 were transfected with CFTR and either DJA2 or vector control, and analyzed by pulse-chase. Unless otherwise specified, data are shown as mean ± SD and are representative of at least three independent experiments, * $p<0.05$, ** $p<0.01$, ***$p<0.001$.

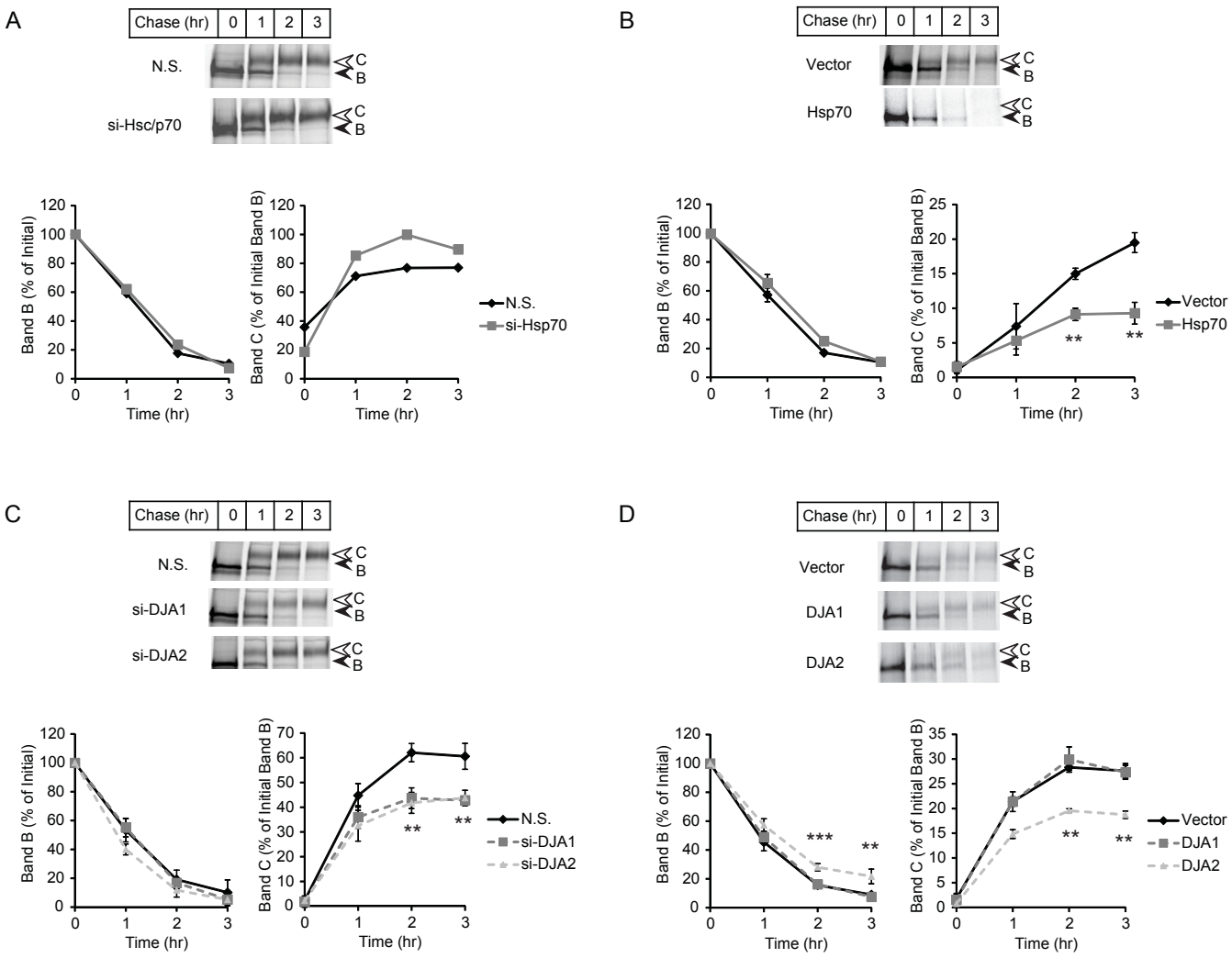
A
Chase (hr) 0 1 2 3
N.S.
si-Hsc/p70
C
B
Band B (% of Initial)
Band C (% of Initial Band B)
Time (hr)
N.S.
si-Hsp70
B
Vector
Hsp70
Vector
Hsp70
**
C
Chase (hr) 0 1 2 3
N.S.
si-DJA1
si-DJA2
N.S.
si-DJA1
si-DJA2
**
D
Chase (hr) 0 1 2 3
Vector
DJA1
DJA2
***
**
Vector
DJA1
DJA2

Figure 4.2. DJA2 promotes ERAD of immature CFTR. A, HEK293 Tet-On 3G cells were transfected with HA-tagged CFTR under an inducible TRE-Tight promoter, and either DJA2 or DJA2-ΔJ under CMV promoters, or vector control. CFTR expression was induced by 1 μg/mL doxycycline for 6 h, then 50 μg/mL cycloheximide was added and cells were analyzed at the indicated chase times. One set of experiments were performed with the addition of 20 μM MG132 at the same time as cycloheximide, and another set with vehicle control added. CFTR bands B and C were detected by western blot (representative images are shown) quantified by chemiluminescent detection and a digital camera. B, quantitation of A comparing DJA2 and DJA2-ΔJ overexpression, with amounts of bands B and C plotted relative to their initial amounts upon addition of cycloheximide. C, comparison of MG132 treatment with control. D, comparison of DJA2 overexpression and MG132 treatment with control. E, comparison of DJA2-ΔJ overexpression and MG132 treatment with control. Unless otherwise specified, data are shown as mean ± SD and are representative of at least three independent experiments.

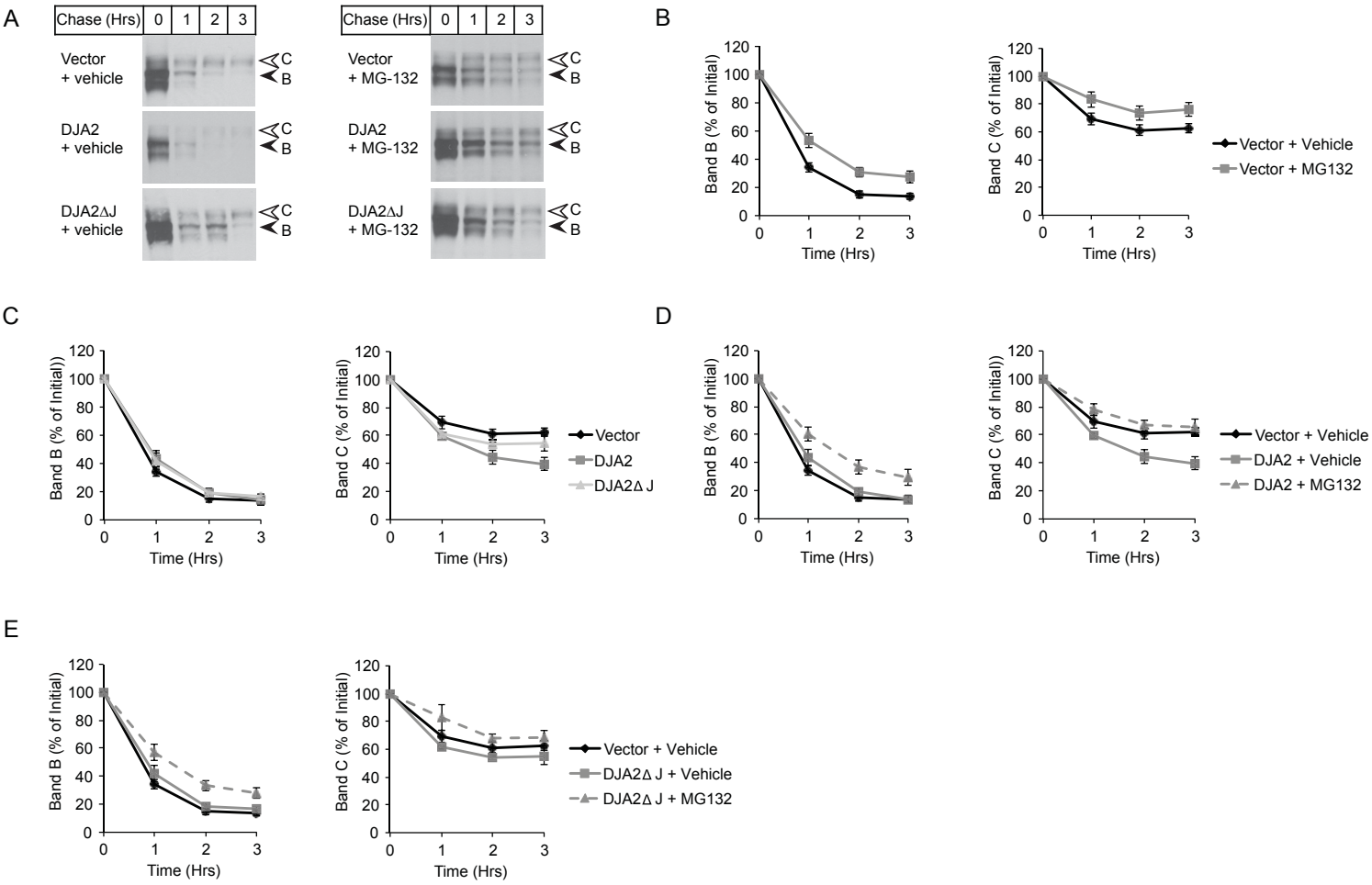
A
Chase (Hrs)
0
1
2
3
Vector + vehicle
DJA2 + vehicle
DJA2ΔJ + vehicle
Vector + MG-132
DJA2 + MG-132
DJA2ΔJ + MG-132
C
B
B
Band B (% of Initial)
Time (Hrs)
Band C (% of Initial)
Vector + Vehicle
Vector + MG132
C
Band B (% of Initial))
Band C (% of Initial)
Vector
DJA2
DJA2Δ J
D
Band B (% of Initial)
Band C (% of Initial))
Vector + Vehicle
DJA2 + Vehicle
DJA2 + MG132
E
Band B (% of Initial)
Band C (% of Initial)
Vector + Vehicle
DJA2Δ J + Vehicle
DJA2Δ J + MG132

Figure 4.3. DJA2 promotes CFTR degradation through CHIP. A, HEK293 Tet-On cells were transfected with inducible CFTR and overexpressed DJA2 as in Figure 4.2, and either siRNA against CHIP or non-silencing control. CFTR expression was induced and chased with cycloheximide as in Figure 4.2. B, quantitation of A comparing CHIP knockdown with control. C, comparison of DJA2 and CHIP knockdown with control. Unless otherwise specified, data are shown as mean ± SD and are representative of at least three independent experiments, * $p<0.05$, ** $p<0.01$.

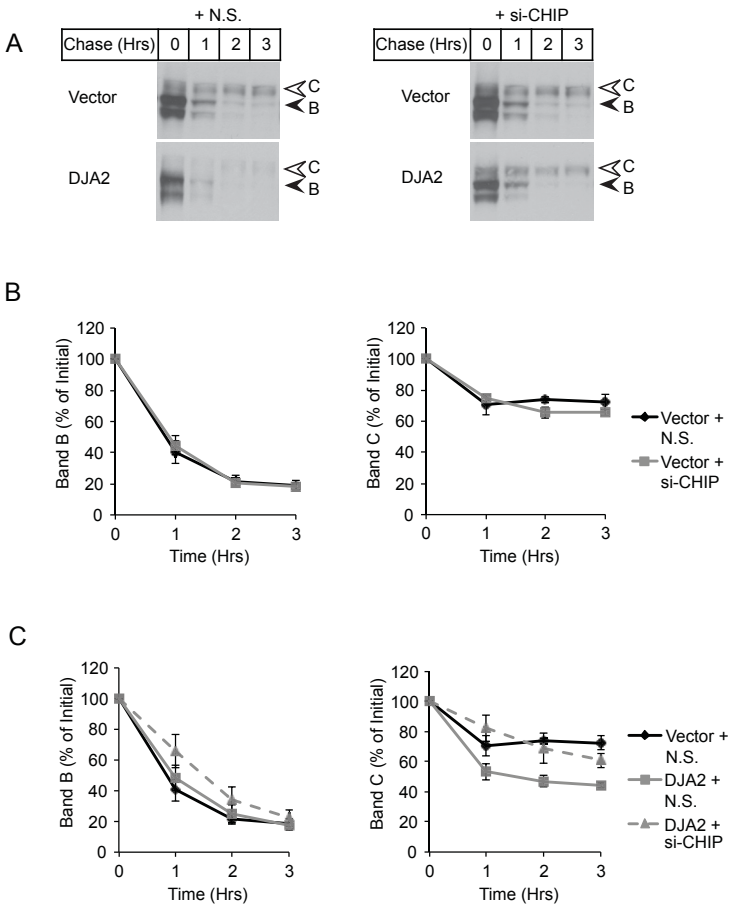
A
+ N.S.
+ si-CHIP
Chase (Hrs)
0
1
2
3
Vector
DJA2
C
B
B
Band B (% of Initial)
Band C (% of Initial)
Time (Hrs)
Vector + N.S.
Vector + si-CHIP
C
DJA2 + N.S.
DJA2 + si-CHIP

Figure 4.4. Hsp70 promotes lysosomal degradation of mature CFTR. A, HEK293 Tet-On cells were transfected with inducible CFTR and overexpressed Hsp70, and then CFTR expression was induced and chased with cycloheximide as in Figure 4.2. One set of experiments were performed with the addition of 20 μM MG132 at the same time as cycloheximide, another set with 200 μM chloroquine (CQ), and a control set with vehicle. B, quantitation of A comparing Hsp70 overexpression with control. C, comparison of MG132 treatment with control. D, comparison of Hsp70 overexpression and MG132 treatment with control. E, comparison of CQ treatment with control. D, comparison of Hsp70 overexpression and CQ treatment with control. Unless otherwise specified, data are shown as mean ± SD and are representative of at least three independent experiments, * $p<0.05$, ** $p<0.01$, ***$p<0.001$.

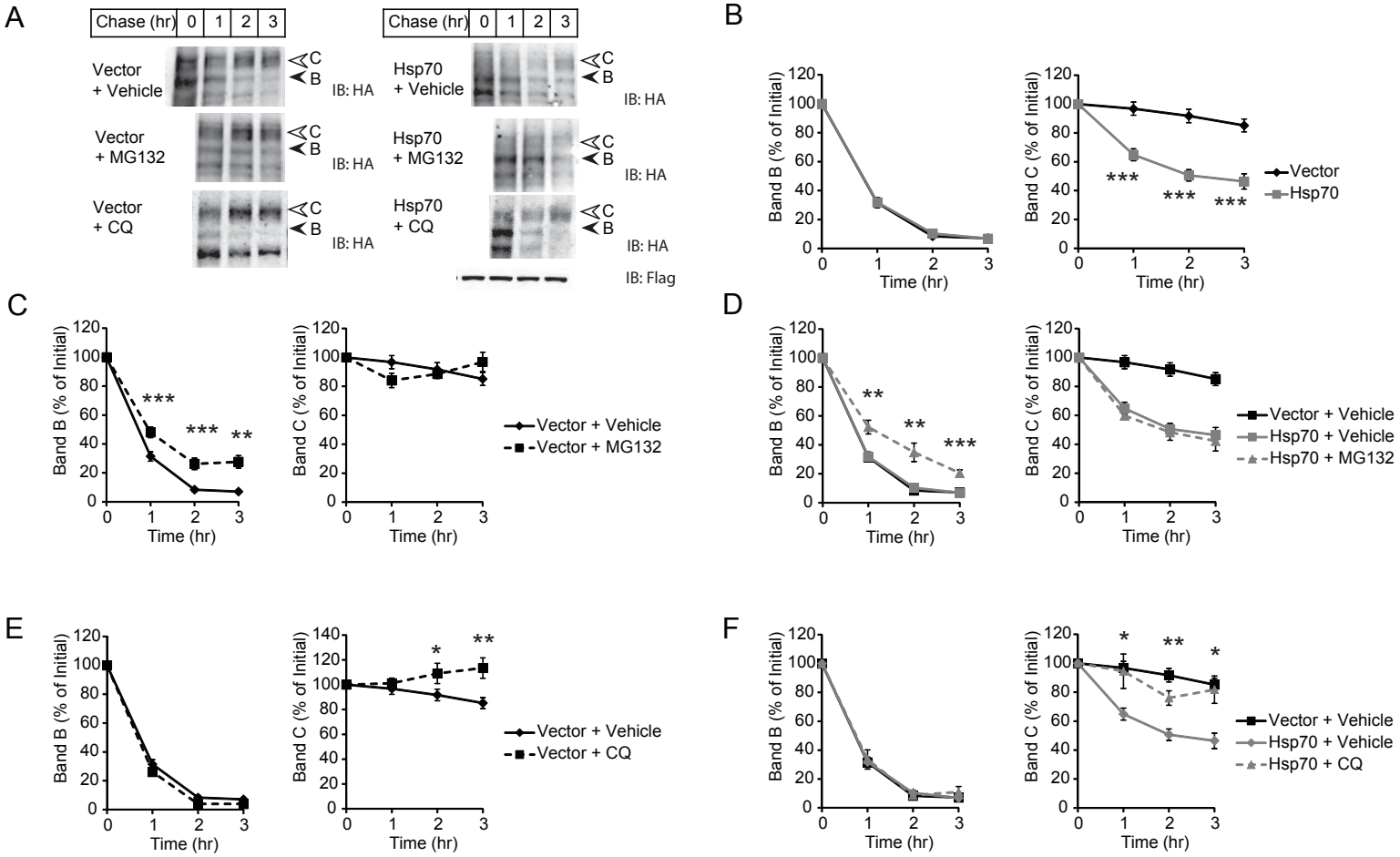
A
Chase (hr) 0 1 2 3
Vector + Vehicle
Vector + MG132
Vector + CQ
Hsp70 + Vehicle
Hsp70 + MG132
Hsp70 + CQ
C
B
IB: HA
IB: Flag
B
Band B (% of Initial)
Band C (% of Initial)
Time (hr)
Vector
Hsp70
C
Band B (% of Initial)
Band C (% of Initial)
Time (hr)
Vector + Vehicle
Vector + MG132
D
Band B (% of Initial)
Band C (% of Initial)
Time (hr)
Vector + Vehicle
Hsp70 + Vehicle
Hsp70 + MG132
E
Band B (% of Initial)
Band C (% of Initial)
Time (hr)
Vector + Vehicle
Vector + CQ
F
Band B (% of Initial)
Band C (% of Initial)
Time (hr)
Vector + Vehicle
Hsp70 + Vehicle
Hsp70 + CQ

Figure 4.5. Hsp70-T636D is ineffective at promoting degradation. A, HEK293 cells were transfected with FLAG-tagged Hsp70 or Hsp70-T636D, or vector control. Cells were lysed and immunoprecipitated with FLAG-specific antibodies, and samples analyzed by western blot for the indicated proteins. The amounts of co-precipitated proteins were quantified and adjusted to the amounts of Hsp70 and Hsp70-T636D recovered. The amounts bound to Hsp70-T636D were then plotted as a percentage of the amounts bound to wild-type Hsp70. B, HEK293 cells were transfected with firefly luciferase and either Hsp70 or Hsp70-T636D, or vector control. Cells were treated with cycloheximide and heat shocked at 45°C for 1 h to denature the luciferase, then allowed to recover at 37°C for the indicated times. Luciferase enzymatic activity was measured in cell lysates to monitor refolding, and plotted relative to the initial activity before heat shock. Refolding with Hsp70-T636D was significantly above that with vector, but not different from that with Hsp70. C, HEK293 Tet-On cells were transfected with inducible CFTR and overexpressed Hsp70 or Hsp70-T636D, and then CFTR expression was induced and chased with cycloheximide in the presence of MG132 or CQ or control, as in Figure 4.2. D, quantitation of C comparing Hsp70 with Hsp70-T636D. E, comparison of Hsp70-T636D and MG132 with control. F, comparison of Hsp70-T636D and CQ with control. Unless otherwise specified, data are shown as mean ± SD and are representative of at least three independent experiments, * $p<0.05$, ** $p<0.01$, *** $p<0.001$.

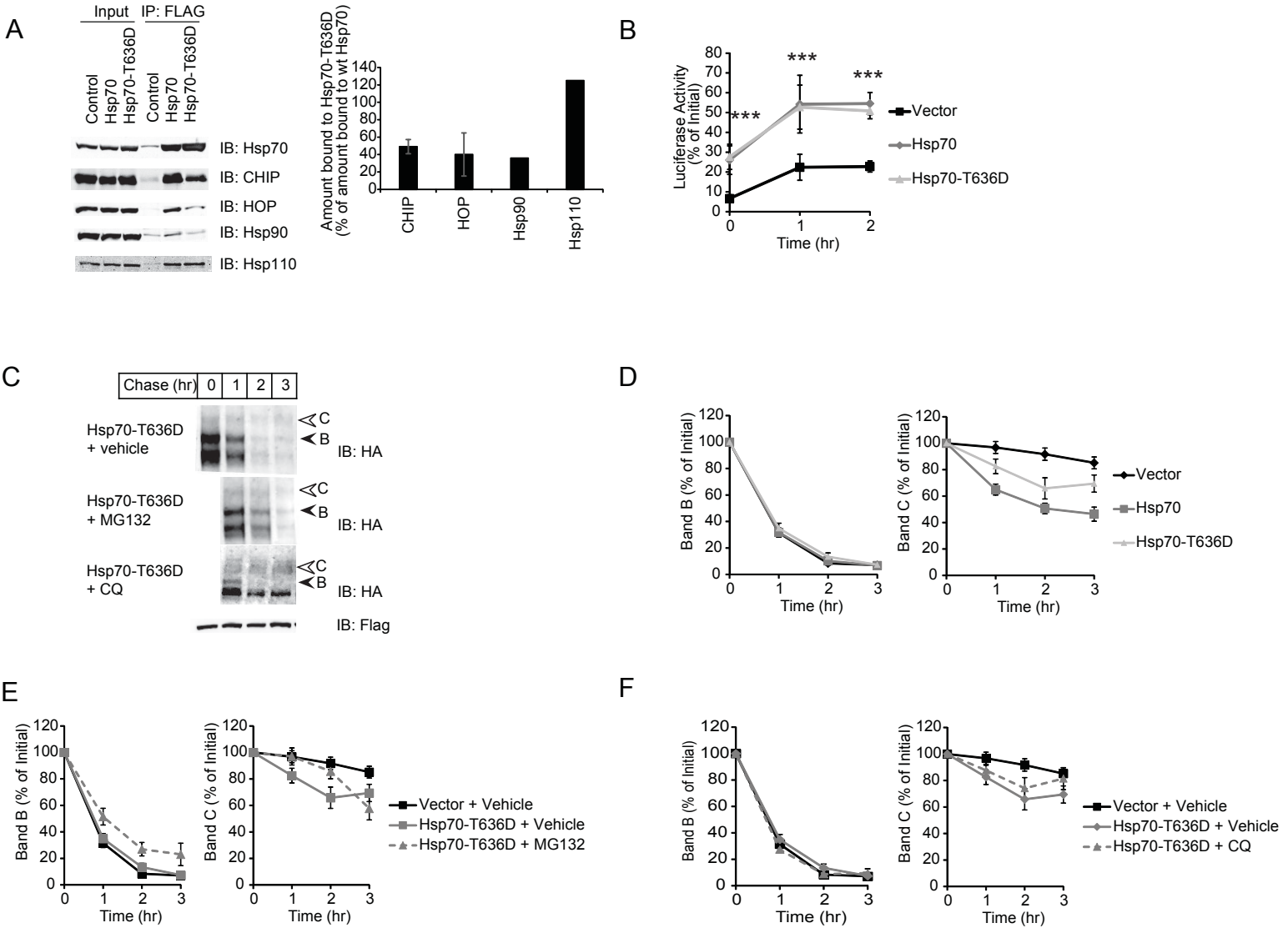
A
Input
IP: FLAG
Control
Hsp70
Hsp70-T636D
Control
Hsp70
Hsp70-T636D
IB: Hsp70
IB: CHIP
IB: HOP
IB: Hsp90
IB: Hsp110
Amount bound to Hsp70-T636D (% of amount bound to wt Hsp70)
CHIP
HOP
Hsp90
Hsp110
B
Luciferase Activity (% of Initial)
***
***
***
Time (hr)
Vector
Hsp70
Hsp70-T636D
C
Chase (hr)
0
1
2
3
Hsp70-T636D + vehicle
Hsp70-T636D + MG132
Hsp70-T636D + CQ
C
B
IB: HA
IB: Flag
D
Band B (% of Initial)
Band C (% of Initial)
Time (hr)
Vector
Hsp70
Hsp70-T636D
E
Band B (% of Initial)
Band C (% of Initial)
Time (hr)
Vector + Vehicle
Hsp70-T636D + Vehicle
Hsp70-T636D + MG132
F
Band B (% of Initial)
Band C (% of Initial)
Time (hr)
Vector + Vehicle
Hsp70-T636D + Vehicle
Hsp70-T636D + CQ

Figure 4.6. CHIP but not HOP-Hsp90 is required for mature CFTR degradation. A, HEK293 Tet-On cells were transfected with inducible CFTR, and either siRNA against HOP or non-silencing control, and then CFTR expression was induced and chased with cycloheximide as in Figure 4.2. B, quantitation of A comparing HOP knockdown with control. C, the experiment in A was expanded to include overexpressed Hsp70 or Hsp70-T636D, and siRNA against CHIP or HOP or non-silencing control. D, comparison of Hsp70 overexpression and CHIP or HOP knockdown with control. E, comparison of Hsp70-T636D overexpression and CHIP or HOP knockdown with control. Unless otherwise specified, data are shown as mean ± SD and are representative of at least three independent experiments, * $p<0.05$.

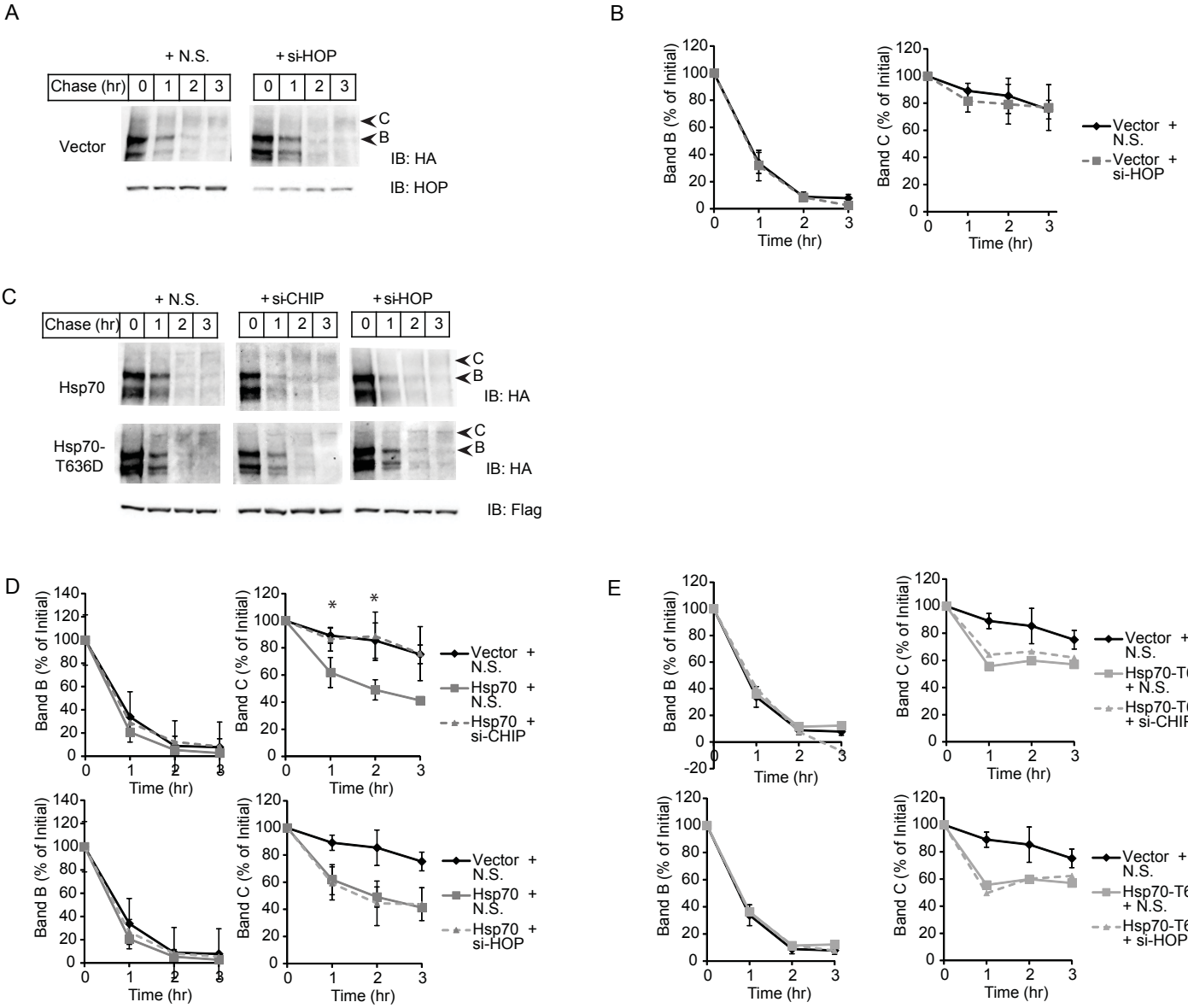
A
+ N.S.
+ si-HOP
Chase (hr)
0 1 2 3
0 1 2 3
Vector
C
B
IB: HA
IB: HOP
B
Band B (% of Initial)
Band C (% of Initial)
Time (hr)
Vector + N.S.
Vector + si-HOP
C
+ N.S.
+ si-CHIP
+ si-HOP
Hsp70
Hsp70-T636D
IB: HA
IB: Flag
D
Band B (% of Initial)
Band C (% of Initial)
Time (hr)
Vector + N.S.
Hsp70 + N.S.
Hsp70 + si-CHIP
Hsp70 + si-HOP
E
Band B (% of Initial)
Band C (% of Initial)
Time (hr)
Vector + N.S.
Hsp70-T636D + N.S.
Hsp70-T636D + si-CHIP
Hsp70-T636D + si-HOP

Chapter 5

General Discussion

5.1. HSP40 co-chaperones are regulators of hERG biogenesis

In the first study, we demonstrated the importance of the Hsc/p70 chaperone system in hERG biogenesis. First, we showed that Hsc/p70 is critical for proper hERG folding and trafficking across the secretory pathway. Then, we identified the type I Hsp40, DJA1 that interacts with Hsc/p70 to promote its folding activity. While only DJA1 was involved in hERG folding, all the other type I Hsp40s, namely DJA1, DJA2, and DJA4, promoted hERG proteasomal degradation through the E3 ubiquitin ligase CHIP. We carried our research further to demonstrate the internal mechanisms by which the DJAs promote folding and degradation, and we showed that whatever is required for degradation function of the DJA2 is also required for the folding.

In luciferase refolding experiments from our lab, we showed that the folding activity of DJA2 is dependent upon specific internal structures in the middle/C-terminal domain: that is, the presence of an intact m2 region and the C-terminal dimerization interface, which cannot be interchanged with that of DJA1. Is this also applicable for the folding activity of DJA1 with regard to hERG? We expect the function of DJA1 in hERG folding to be impaired in case any of the internal structures is deleted or replaced. Pure protein experiments found that the m2 region

of DJA1 as well as that of DJA2 was necessary for the transfer of substrate from the co-chaperones onto Hsc70 [62], and this is most likely a universal requirement for DJA function. The homodimerization region is important to maintain the conformation of both DJAs. Another point we raised in that same study is the point at which DJA1 or DJA2 transfer substrate after inducing Hsc/p70 ATPase activity. Using a non-hydrolyzable ATP mimetic and ATP transition state analogues, we demonstrated that DJA2 substrate release might be coupled to the actual ATP hydrolysis step while that of DJA1 might occur at a later stage of the ATPase reaction. This distinction between DJA1 and DJA2 substrate release could be one of the underlying mechanism that reflect the difference between these two co-chaperones in hERG folding.

The question remains as to which domains of hERG are dependent on the chaperones for their folding. It is logical to assume that both cytosolic domains, the PAS and cNBD, depend on chaperone function, but it seems that the cNBD requires the chaperone system more than the PAS domain. We tried unsuccessfully to purify the cNBD by constructing different truncations and expressing them in bacteria (data not shown). However, the PAS domain was purified and its structure solved by crystallography [323], suggesting that it is not as dependent on the human chaperones as the cNBD, which formed aggregates in bacteria in our trials. While there are no reports of purified hERG cNBD from other groups, structures of the cNBD from the closely related mouse EAG1 (ether-a-go-go) channel have recently been solved. [324,325] Small differences in protein sequence between the hERG and EAG1 domains may explain their different abilities to fold.

We illustrated the importance of the Hsc/p70 system in hERG biogenesis and we identified the co-chaperones at play, but to what extent are the Hsp90 system and its co-chaperones required as well? Hsp90 was shown to be critical for hERG folding using inhibitor

experiments. [266] However, none of its co-chaperones were tested. Nonetheless, we tested Aha1 and p23, both of which were shown to be involved in CFTR biogenesis, and in siRNA knockdown experiments we found no significant effect of these co-chaperones on hERG trafficking. This also underscores the different effects chaperones have on different substrates and emphasizes the need to test substrates case by case.

5.2. Bag1 shifts the hERG ERAD pathway to TRC8-Ube2g2

After identifying the players involved in hERG biosynthesis in the first part of the Hsc/p70 cycle, we focused on the second part, which involves the NEFs. We showed that the NEF, Bag1, promotes hERG proteasomal degradation by inhibiting the pro-folding action of Hsc/p70 and therefore inducing hERG misfolding. hERG degradation however, does not seem to be through the already characterized degradation pathway that involves Hsc/p70 and CHIP, but rather through an ER-associated E3 ligase, TRC8, whose function is independent of Hsc/p70. Figure 5.1A demonstrates a model of hERG folding and degradation pathways and the players involved in each of these processes.

There could be two types of hERG degradation, as part of the quality control or regulated degradation, both of which may be due to TRC8 either directly or indirectly. As part of the quality control, TRC8 could be somehow recognizing misfolding in the hERG domains and promoting its ubiquitination and ultimately degradation. Alternatively, TRC8 could be affecting hERG indirectly by controlling cholesterol levels in the cell through regulated ERAD of HMG-CoAR. HMG-CoAR catalyzes the conversion of HMG CoA to mevalonate, a rate-limiting step

Figure 5.1. Model of hERG or CFTR biogenesis. A, Model of hERG ERAD and trafficking depending on its folding. DJA1 assists hERG folding by Hsc70 and subsequently Hsp90 together with FKBP38, resulting in traffic to the cell surface and channel function. DJA2 promotes hERG degradation by inappropriate complex formation with the Hsc70-dependent E3 ubiquitin ligase CHIP. Bag1 interferes with hERG folding by inducing the release of Hsc70, leading to degradation by Hsc70-independent E3 ligases TRC8 and its partner E2 ubiquitin conjugating enzyme Ube2g2. B, Model of CFTR proteasomal degradation at the ER and lysosomal degradation at the plasma membrane and its trafficking. The top panel shows the mechanisms of chaperone folding and degradation at the ER. DNAJA1, DNAJA2 and Hsp70, then HOP, Hsp90, p23 and FKBP38 assist CFTR folding (middle to right). If CFTR is properly folded it trafficks to cell surface whereas if it improperly folded it is bound by DNAJA2 and Hsp70, polyubiquitinated by E3 ligase CHIP, and directed for proteasomal degradation (ERAD, middle to the left). Chaperone-independent E3 ligases RMA1 and gp78 also direct degradation of CFTR. The bottom panel shows the quality control at the cell surface where functional mature CFTR may be recognized by DNAJA1, Hsp70 and Hsp90 together with HOP. Hsp70 and CHIP promote polyubiquitination, and targeting to lysosomes for degradation. (Figure 5.1B adapted from [30])

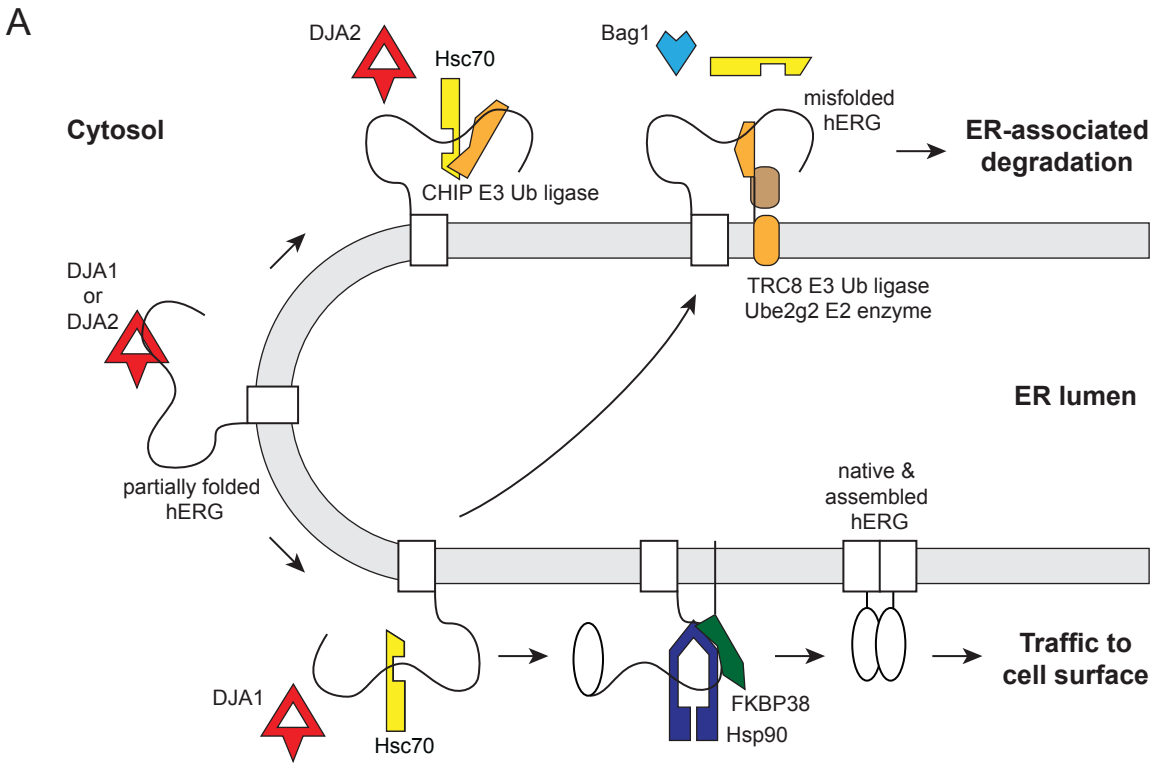
A
DJA2
Hsc70
Bag1
misfolded
hERG
Cytosol
ER-associated
degradation
CHIP E3 Ub ligase
DJA1
or
DJA2
TRC8 E3 Ub ligase
Ube2g2 E2 enzyme
ER lumen
partially folded
hERG
native &
assembled
hERG
Traffic to
cell surface
DJA1
Hsc70
FKBP38
Hsp90

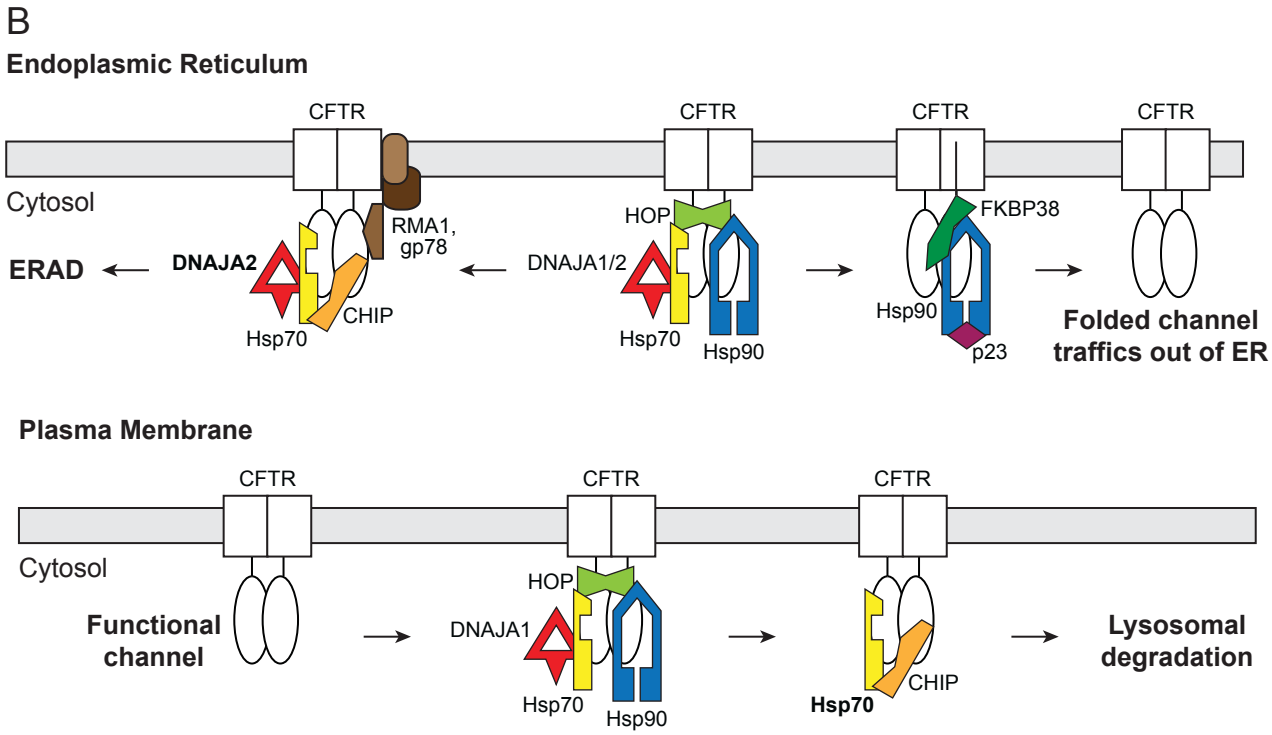
B
Endoplasmic Reticulum
CFTR
CFTR
CFTR
CFTR
Cytosol
RMA1,
gp78
HOP
FKBP38
ERAD
DNAJA2
DNAJA1/2
CHIP
Hsp70
Hsp70
Hsp90
Hsp90
p23
Folded channel
traffics out of ER
Plasma Membrane
CFTR
CFTR
CFTR
Cytosol
HOP
Functional
channel
DNAJA1
CHIP
Hsp70
Hsp90
Hsp70
Lysosomal
degradation

in cholesterol synthesis. Protein folding/trafficking can be directly or indirectly affected by cholesterol and acute depletion of cholesterol from the ER membrane inhibits ER to Golgi transport of secretory membrane proteins. [326] Furthermore, there is evidence that intracellular cholesterol distribution specifically affects hERG. Decreasing ER cholesterol levels with simvastatin, which inhibits HMG-CoA reductase activity, or shifting cholesterol to the endosomes/lysosomes with imipramine, results in a decrease in mature hERG. [327] Therefore, cholesterol levels within the cell are important for hERG trafficking and reducing the levels of cholesterol through inhibiting HMG-CoAR activity, whether by inducing it degradation through TRC8 or by blocking it with a drug, leads to less hERG trafficking and increased ERAD. Finally, TRC8 itself was originally postulated to contain a sterol-sensing element [182], although its function has not been established, and it is possible that cholesterol specifically inhibits TRC8 recognition of hERG.

To distinguish between these two kinds of hERG degradation, further experiments could be performed. We propose co-IP experiments to show a direct interaction with hERG and TRC8. TRC8WT or RING finger mutant or deletion constructs could be used. The WT TRC8 is expected to promote hERG degradation while the ones lacking E3 ligase activity would have no effect. All of these proteins are expected to interact with hERG, but we might be able to see it more clearly with the mutant and ΔRING TRC8 since these would be acting as hERG traps that are unable to degrade it, but would remain bound to it instead. Another critical potential experiment would be to knock down TRC8 with the overexpression of Bag1 to promote hERG misfolding. In such a case, where Bag1 is inducing hERG misfolding, if TRC8 is indeed the main E3 ligase at the ER involved in hERG quality control, then the depletion of TRC8 should inhibit hERG degradation. Finally TRC8 knockdown could be tested with the trafficking

deficient LQT2 hERG mutants, which are expected to be more severe misfolded. These experiments can then be performed upon manipulation of ER cholesterol, such as by statin inhibition of HMG-CoAR.

We showed that Bag1 is involved in hERG ERAD, but another potential NEF that would be interesting to test is Bag3. Bag3 has been shown to be involved in autophagy and lysosomal degradation, but what effect would it have on hERG is unknown. Finally, an important question to address is whether all NEFs are equivalent with regard to hERG or, like the DJAs, each have a specialized function that differs from the other. Indeed knockdown of Hsp110 appeared to have an opposite effect on hERG biosynthesis than Bag1 knockdown (data not shown). In order to understand the involvement of each of these NEFs, there should be a systematic study that makes use of knockdown (or knockout) and overexpression experiments of each of these co-chaperones.

5.3. DNAJA2 and Hsp70 are determinants of CFTR degradation

In the final study, we investigated the role of the Hsc/p70 system in CFTR synthesis. Hsc/p70 has a dual role in CFTR folding and degradation at the ER and cell surface. First, we showed that Hsc/p70 requires both DJA1 and DJA2 to promote CFTR folding, but when present in excess, Hsc/p70 promotes CFTR proteasomal and lysosomal degradation through CHIP. DJA2 is also involved in CFTR ERAD as well. Figure 5.1B demonstrates a model of CFTR folding and degradation pathways, both at the ER and cell surface, along with the players involved in each of these processes.

Although we characterized the involvement of the Hsc/p70 and its co-chaperones in WT CFTR biogenesis, there is question as to whether these pathways would be also applicable for ΔF508 CFTR. Therefore, similar approaches should be used to assess the role Hsc/p70 chaperone machinery in relation to the mutant. However, comparative proteomics suggested that the same chaperones and co-chaperones were associated with ΔF508 CFTR as with the WT. [240,328] Thus, the mutant is likely to differ only in the amounts of Hsc/p70, DJA1 and DJA2 required for its folding and possible rescue compared to WT.

From these experiments, we can predict that Hsp70 partial inhibiton to a level comparable to that of the knockdown would be useful for CF patients. However, a major challenge in developing Hsp70 inhibitors is specificity. Various inhibitors were designed and tested including the adenosine-derived inhibitor, VER-155008, which inhibits Hsp70 chaperone activity through targeting its ATP-binding domain. [329] Another compound that also inhibits Hsp70 ATPase activity by binding to the ATP-binding site is apoptozole. MKT-077, YK5, and myricetin are yet other Hsp70 inhibitors that bind to different allosteric sites in the NBD of Hsp70. [310,330,331] In addition, a compound that inhibits Hsp70 chaperone activity through targeting its SBD is phenylacetylenylsulfonamide (PES, also known as pifithrin-μ). [332] Among all these Hsp70 inhibitors, only apoptozole was tested for CFTR. This study showed that apoptozole moderately rescues ΔF508 CFTR trafficking to the cell surface and increases its chloride activity by inhibiting Hsc/p70, which leads to inhibition of CHIP binding and thus a decrease in ΔF508 CFTR ubiquitination and degradation. [333] The other compounds remain to be tested for their effect on CFTR biogenesis and the questions over their specificity, mechanism of action and potency in cells remain to be answered.

It is possible that CFTR stabilization, especially restoration of the ΔF508 mutant, will be moderate even at the optimal condition for an individual Hsp70 inhibitor. As indicated by recent reports, a combination of therapeutic strategies is more promising than one alone. [334-336] Therefore, different Hsp70 inhibitors with different mechanisms of action could be used together in CF therapy to provide Hsp70 inhibition that is optimized to increase functional CFTR at the plasma membrane. Furthermore, Hsp70 inhibitors could be used together with other small molecule correctors of ΔF508-CFTR trafficking. These compounds stabilize CFTR structurally, and therefore would be promising in combination with Hsp70 inhibition to block the degradation but not folding of CFTR. They stabilize the ΔF508 mutant NBD1 interactions with the other parts of CFTR, but act on different parts of the structure. [336-345] How Hsp70 recognizes CFTR is not known and some correctors may be more effective than others, if their mode of CFTR stabilization already decreases Hsp70 binding, or even dependence on Hsp70 for folding. The most promising corrector that could be used in combination with the Hsp70 inhibitors is VX-809 (Lumacaftor), which is in clinical trials as a combination therapy with a channel potentiator. [342-345] Others will be VRT-325, corr-4a and 15jf, which on their own provide less rescue of ΔF508 CFTR trafficking than VX-809. [337-340]

5.4. Hsc70 and Hsp70

The role of Hsc/p70 chaperones in ion-channel protein misfolding diseases is complicated because of their opposing effects in promoting folding or assisting degradation at the ER. Their roles in protein quality control at the plasma membrane are just beginning to be studied. However, Hsc/p70 are expected to have different mechanisms of action at the ER compared to the plasma membrane for different ion channels. In the case of ΔF508 CFTR, loss

of CHIP function does not result in channel trafficking to the cell surface but inhibits its internalization from the plasma membrane. An additional level of complexity in understanding Hsc/p70 role in ion-channel misfolding diseases is added because of the potential biological differences between these two chaperones. Hsc70 and Hsp70 were reported to have opposite effects on the trafficking of the human epithelial sodium channel expressed in Xenopus oocytes, and some evidence of this is found in mammalian cells. [284,346] Also, Hsp70 but not Hsc70 was suggested to protect hERG from degradation. [268] However, there is no known biochemical basis for these differences. The origin of these reported biological differences in knockdown experiments could be due to differences in Hsc70 and Hsp70 expression levels in different cell lines. It is noteworthy to mention that in these relevant studies [100,268,347-349] Hsc70 knockdown induces Hsp70 expression and not vice versa (observed in our own experiments) so in order to get full effects both should be silenced. However, the differences found in overexpression experiments, which mask any endogenous expression variations, suggest that the chaperones are indeed biologically distinct . Hsc70 and Hsp70 are remarkably identical with 87% sequence identity and 94% similarity. It is possible, though, that even small differences in amino acid sequence could cause variations in structure, biochemical properties or post-translational modifications, which in turn may result in significant biological functional differences. Furthermore, Hsc70 and Hsp70 might interact with different subsets of co-chaperones that modulate their activity although there is so far no evidence for exclusive co-chaperone interaction with Hsc70 or Hsp70. However, it is possible that some co-chaperones might preferentially interact with one versus another due to differences in binding affinities or abundance in the cell.

Addressing the roles of Hsc/p70 in folding and degradation is central to understanding how these chaperones could influence different ion channels involved in protein misfolding diseases. Another point that needs to be addressed also is the overlapping or opposing functions of the HSP40s and NEFs as their role in protein misfolding diseases is largely uncharacterized. Therefore, primarily knockdown followed by overexpression experiments should be used to systematically address these questions.

5.5. Small molecule inhibitors of Hsc/p70

Development of new specific Hsc/p70 inhibitors are promising as useful novel therapies for various protein misfolding diseases. Small molecule activators of Hsc/p70 are also possible, although the one reported has not been tested in mammalian cells. [350] Drug therapy combined with manipulation of chaperone levels could be also a powerful approach to influence CFTR or hERG biosynthesis and thus rescue CF or LQT2 phenotypes. However, a concern to be addressed is that Hsc/p70 inhibitors could affect several targets thus improving one disease while worsening the other. For example, Hsc/p70 inhibition might decrease ΔF508 CFTR degradation through CHIP while also preventing hERG folding through Hsc/p70 leading to LQT2 susceptibility in CF affected individuals. Some of these problems could be addressed during drug testing with prioritization of the most affected organ-systems in addition to the main tissue being treated. In other cases, enhanced Hsc/p70 function might have positive effects on mutant channels in affected individuals. While specific DJAs will still be needed, they may synergize with Hsc/p70 activators to stabilize the mutants. Furthermore, such activators may have greater effects on mutant channels than on WT forms, which are more stably folded to begin with. Thus,

doses of activators may be found which rescue mutant channels, without overly promoting the degradation role of Hsc/p70 on other proteins.

Finally, an optimal situation would be to target the specific tissue affected due to the genetic disease with small molecules that would enhance (or inhibit if necessary) the chaperone function in those cells. However, the specificity required for this process is not yet available, but novel approaches in drug delivery are supposed to address this challenge. Thus, there is a potential of developing both drugs that inhibit or stimulate Hsc/p70 functions with each having their own benefits depending on the physiological system that is targeted.

Chapter 6

Experimental Procedures

6.1. Chemicals and Reagents

Unless otherwise stated, all chemical reagents were from Sigma-Aldrich Canada or BioShop Canada. Restriction enzymes and other recombinant DNA reagents were from New England Biolabs, Invitrogen, and Stratagene. The following commercially available antibodies were used: Bag1 (Santa Cruz), CFTR (M3A7) (Millipore), CHIP (Sigma), Derlin-1 (Sigma), DJA1 (Thermo Fisher Scientific), Flag (M2) (Sigma, Mississauga, ON), GFP (JL-8) (BD Living Colours, Clontech), Goat anti-rabbit IgG conjugated HRP (Jackson ImmunoReseach Laboratory), Goat anti-mouse IgG conjugated HRP (Sigma), Gp78 (Abcam), Hemagglutinin (HA.11) (Covance), hERG (Almone labs), His-tag (Bioshop), HRD1 (Abcam), Hsc70 (StressMarq), Hsp70 (StressMarq), Hsc/Hsp70 (Stressgen), Luciferase (Sigma), myc (9E10) (Santa Cruz), RMA1 (Abcam), TRC8 (Abcam), Tubulin (Sigma-Aldrich), Ube2j1 (Abcam), Ube2g2 (Abcam), Ub (P4D1) (Santa Cruz). Additional antibodies specific for DJA1 and DJA2 were raised in rabbits against the synthetic peptides LVDFDPNQER and PEVPNIIGET. [60] Protein G Agarose Fast Flow beads were from EMD Millipore (Canada). The Express Protein labelling mix, [35S]- used for pulse chase studies was from Perkin Elmer (Boston, MA).

6.2. Plasmids

hERG-pcDNA3 with HA tag inserted after residue 443 in the extracellular S1-S2 loop was a kind gift from Eckhard Ficker. [266] CFTR-pcDNA with HA tag was kindly provided by John Hanrahan. pTRE-Tight CFTR was generated as follows CFTR-3HA was cloned from pcDNA into pTRE-TIGHT using KpnI on the 5' end and Not I on the 3' end. Sequences of DJA1, DJA2, and DJA4 were inserted into pcDNA3.1 myc-His C (Invitrogen) as described previously [60] as were DJA1- and DJA2-ΔJ (amino acids 98-397 and 100-412, respectively). To generate the DJA2-Δm2 construct, the m2 fragment from residue 158 to 199 of DJA2 was removed by PCR and replaced with an EcoRI site encoding Glu-Phe. The mutant was constructed in pPROEX-HTa and subcloned into pcDNA3.1 myc-His as BamHI-NotI fragments. For DJA-221 construction, the EcoRV site at amino acids Asp-299/Ile-300 of DJA1 was removed by silent mutation. EcoRV sites were reintroduced in DJA1 by silent mutation at Asp-238/Ile-239, and in DJA2 at Asp-247/Ile-248. The sequences encoding the N-terminal fragments were exchanged as BamHI-EcoRV fragments in pPROEX-HTa and subcloned into pcDNA3.1 as BamHI-NotI fragments. DJA-122 was constructed as follows: a BamHI site was inserted into DJA1 by point mutation at Gly-75/Gly-76, mutating it to encode Gly-75/Ser-76. A BamHI site was inserted by silent mutation into DJA2 at Gly-78/Ser-79. DJA1 and DJA2 were re-inserted into pPROEX-HTa as SalI-NotI fragments to remove the BamHI site before the open reading frame. The C-terminal fragments were exchanged as BamHI-NotI fragments in pPROEX-HTa and subcloned into pcDNA3.1 as KpnI-NotI fragments. Hsp70 was amplified by PCR from pSV-Hsp70 [351] and inserted with an N-terminal FLAG tag into pcDNA3.1. Myc-tagged CHIP was a kind gift from Jörg Höhfeld. [66]

6.3. siRNAs

All siRNA duplexes were from Dharmacon/Thermo Fisher Scientific with the following target sequences:

- DNAJA1

5’-GTGAAGGACTGTAATCATA (Dharmacon Custom siRNA Designer) in the 3’ UTR

ON-Target plus siRNA - SmartPool

5’-GGACAUACAGCUCGUUGAA

5’-GAUAGGACCUGGAAUGGUU

5’-GAUCAGUCCUAAAGAUAGA

5’-UAUCGUAGACCAUAUGAAA

- DNAJA2

5’-CCACAAAGCTTTACATCTT (Dharmacon Custom siRNA Designer) in the 3’ UTR

ON-Target plus siRNA - SmartPool

5’-CUGAGAAGCGUGAGUUAUA

5’-GGAUGCCGCAGUAUCGUAA

5’-GACGUCAGAUUGUGGUGAA

5’-GAGAGGACAUGAUGCAUCC

- Hsc70 (HSPA8)

ON-Target plus siRNA - SmartPool

5’-CGUAAUACCACCAUUCCUA

5’-GAUAACAACCUGCUUGGCA

5’-GACCUUCACUACCUAUUCU

5’-UGAAACUGCUGGUGGAGUC

- Hsp70 (HSPA1B)

5’-CCGAUAUGUUCAUUAGAAUUU (Dharmacon Custom siRNA Designer)

ON-Target plus siRNA - SmartPool

5’-GAUCAACGACGGAGACAAG

5’-GCUCCGACCUGUUCCGAAG

5’-GUCAAGAGGUCAUCUCGUG

5’-GCGAGAGGGUGUCAGCCAA

- Hsp70 (HSPA1A)

5’-GCUUCAAGACUUUGCAUUUUU (Dharmacon Custom siRNA Designer)

- CHIP (STUB1)

ON-Target plus siRNA - SmartPool

5’-CGCUGGUGGCCGUGUAUUA

5’-GUGGAGGACUACUGAGGUU

5’-GAAGGAGGUUAUUGACGCA

5’-UGGAAGAGUGCCAGCGAAAA

- Derlin-1

ON-Target plus siRNA - SmartPool

5’-CAACAAUCAUAUUCACGUA

5’-GAGAGACCCUCAUACGCUA

5’-CAAUUAUGUUGCACGUACA

5’-GGGCCAGGGCUUUCGACUU

- Ube2j1

ON-Target plus siRNA - SmartPool

5’-GCUCUUAUAUUCCGACGAA

5’-GAGUAUAAGGACAGCAUUA

5’-GAUGUCCUGUUGCCUUUAA

5’-GCCAUAGGUUCUCUAGAUU

- Ube2g2

ON-Target plus siRNA - SmartPool

5’-GAUGGGAGAGUCUGCAUUU

5’-GAGCUAACGUGGAUGCGUC

5’-GCGAUGACCGGGAGCAGUU

5’-CCACUUGAUUACCCGUUAA

- HRD1 (SYVN1)

ON-Target plus siRNA - SmartPool

5’-GGAAAGGCCUCCAGCUCCU

5’-CAACAUGAACACCCUGUAU

5’-GAGAAGAGAUGGUGACUGG

5’-UCAUCAAGGUUCUGCUGUA

- gp78 (AMFR)

ON-Target plus siRNA - SmartPool

5’-GCAAGGAUCGAUUUGAAUA

5’-GGACGUAUGUCUAUUACAC

5’-GAAUUCGUCGGCACAAGAA

5’-GUAAAUACCGCUUGCUGUG

- TRC8 (RNF139)

ON-Target plus siRNA - SmartPool

5’-UGACAGGCGUCUUGGCUUU

5’-GGGAGCCGCUUACAAGAAA

5’-AGAGAGACUUUACUGUUUA

5’-GGGAAAAGCUUGACGAUUA

- RMA1 (RNF5)

ON-Target plus siRNA - SmartPool

5’-GGCCAUGUCUUCAUCAGUG

5’-GCAAGAGUGUCCAGUAUGU

5’-UCAAUGCCCAUGAGCCUUU

5’GCGCGACCUUCGAAUGUAA

- Bag1

ON-Target plus siRNA - SmartPool

5’-CGAGUGAGGUGUAGCAGAA

5’-ACACUGAUCCUGCCAGAAA

5’-AAGCACGACCUUCAUGUUA

5’-GAAUAAAGAGCUUACUGGA

- Control non-silencing

ON-Target plus non-targeting siRNA Pool

5’-UGGUUUACAUGUCGACUAA

5’-UGGUUUACAUGUUGUGUGA

5’-UGGUUUACAUGUUUUCUGA

5’-UGGUUUACAUGUUUUCCUA

- siGLO transfection indicator was from Dharmacon/Thermo Fisher Scientific

6.4. Cell Culture

HeLa and HEK293 cells were cultured in Dulbecco's modified Eagle's medium (DMEM), high glucose and glutamine (Gibco-Invitrogen), supplemented with 10% fetal bovine serum, 1 mM sodium pyruvate, 100 units/ml Penicillin and 100 μg/ml Streptomycin. The cells were cultured at 37°C in 5% CO_2. Plasmid transfections were carried out using Lipofectamine 2000 (Invitrogen).

For western blots, unless otherwise indicated, cells were lysed two days after transient transfection of plasmid, or three days after transfection of siRNA. For hERG experiments, cells were washed two times with cold PBS and incubated in lysis buffer (0.5 % Nonidet P-40, 75 mM NaCl, and 50 mM Tris, pH 8) plus a protease inhibitor cocktail (Roche) for a minimum of 15 minutes, or alternatively in PBS containing 1% Triton X-100 under identical conditions. For CFTR experiments, cells were lysed in PBS containing 1% Triton X-100, 0.5% sodium deoxycholate, and 0.1% SDS. Cells were homogenized by pipetting on ice with occasional vortexing. Detergent insoluble material was sedimented at 16,000 x g for 20 minutes after which the resulting supernatant was collected and the protein concentration was determined by Bradford or bicinchonic acid assays (Pierce). Equal amounts of lysate were loaded on gels within one experiment for analysis by standard SDS-PAGE and electro-transfer to nitrocellulose, and the quality of transfer confirmed by Ponceau Red staining. Western blots were decorated with primary and secondary antibodies under recommended conditions, and visualized using ECL, ECL Plus or ECL Prime reagent (GE Healthcare) on film or for quantitation by a FluorChem HD2 digital camera and the FluorChem HD2 software (Alpha Innotech).

For immunoprecipitations, HeLa and HEK293 cells were lysed in in PBS containing 1% Triton X-100, the lysates were adjusted to identical protein concentrations and volumes, and then antibody and Protein G-Agarose Fast Flow (EMD Millipore) were added to the lysates for incubation overnight at 4 °C. The beads were washed with PBS containing 0.1% Triton X-100 and eluted with SDS-PAGE loading buffer.

To detect polyubiquitinated hERG, N-Ethylmaleimide (NEM) (Sigma-Aldrich) was added to lysis and wash buffers, then IPed samples using anti-hERG Ab were run on SDS-PAGE and blotted with anti-Ub Ab (Santa Cruz).

6.4.1. Plasmid and siRNA Transfection

Typical plasmid transfections in HEK293 cells used 18 μg total DNA per 10 cm dish containing $4x10^6$ cells. 6 μg of hERG or CFTR plasmid were used together with 12 μg of plasmid for the relevant chaperone, co-chaperone, or empty vector, and 18 μl Lipofectamine 2000. The exceptions were the pulse chase experiments with CFTR and DJA1 or DJA2 overexpression, where cells were transfected with 6 μg CFTR and 6 μg DJA1/DJA2.

Typical siRNA transfection 50 nM final siRNA concentration per 10 cm dish containing $3x10^6$ cells transfected with 20 μl oligofectamine.

6.4.2. Pulse-chase Experiments

HEK293 cells or HeLa cells stably expressing hERG or CFTR were transfected in 10 cm dish, and distributed into 6 cm dishes following the transfection. Two days after transfection, the cells were starved for 1 h in DMEM lacking amino acids and serum, then labeled for 30 min for

hERG and 20 min for CFTR with 100 μCi [^{35}S]-methionine/cysteine labelling mix (Perkin Elmer). The cells were washed with PBS and incubated with regular medium for the indicated times, and then lysed and immunoprecipitated as above with antibody against hERG (Almone labs) or CFTR (Millipore). SDS-PAGE autoradiograms were analyzed by phosphorimager.

6.4.3. Limited Proteolysis

HEK293 cells transiently transfected with 6 μg hERG and 12 μg vector/Bag1 were collected from 4 x 10 cm dishes (with 4x10^6 cells) in PBS-1 mM Ca^{2+} + 1 mM Mg^{2+}, washed 3 times with PBS-Ca/Mg then once with sucrose washing solution (0.25 M sucrose, 10 mM HEPES, 1 mM EDTA, pH 6.8 with 1M Tris) then resuspended in homogenization solution (0.25 M sucrose, 10 mM HEPES, 1mM EDTA, 10 μg/ml proteinase inhibitors cocktail, 1 mM DTT). They were then subjected to pressure using the N_2 homogenization bomb. This was followed by different rounds of centrifugation: first for 5 min at 4000 rpm, then for 10 min at 9000 rpm, and a final ultracentrifugation step for 1 h at 23,000 rpm. The microsomal palette was collected and resuspended in resuspension solution (0.25 M sucrose, 10 mM HEPES, 1 mM EDTA, pH 7.6 with 1 M Tris). The microsomal preparation was digested for 10 min in 37°C water bath with different concentrations of trypsin (Worthington) and the reaction was inhibited with trypsin inhibitor (Sigma Aldrich). Then the samples were run on SDS-PAGE and blotted for hERG.

6.4.4. Doxycycline Induction Experiments

HEK293 Tet-On 3G cells were transfected with 6 μg of pTRE-Tight CFTR and 12 μg of chaperone plasmid or control vector per 10 cm dish containing 4x10^6 cells, and distributed into

12 well dishes. One day after transfection, the cells were treated with 1 μg/ml doxycycline for 6 h to induce CFTR expression, and then with 50 μg/ml cycloheximide. Cells were lysed at the indicated times after cycloheximide addition and analysed by western blot for CFTR.

6.4.5. Patch Clamp Experiments

Cells were plated in the perfusion chamber of an inverted microscope (Zeiss Axiovert S100TV) and perfused using a gravity-based flow system (1-2 mL/min) containing a Tyrodes solution (composition, mM: NaCl 135; KCl 5; $CaCl_2$ 1; $MgCl_2$ 1; Glucose 10; 4-(2-hydroxyethyl)-1-piperazineethanesulfonic acid (HEPES) 5; pH to 7.4 with NaOH; 300 mOsm). Borosilicate glass pipettes (Warner Instruments, Hamden, CT) were made using a microprocessor-controlled, multi-stage puller (P97, Sutter Instruments). Tips with resistances that fell between 1.5-3 MΩ were backfilled using an internal solution (composition, mM: KCl 135; ethylene glycol tetraacetic acid (EGTA) 5; $MgCl_2$ 1; HEPES 10; pH to 7.2 with KOH; 300 mOsm). All experiments were performed at room temperature (21 °C-22 °C).

All voltage-clamp experiments were performed under the whole-cell configuration. Currents were recorded using an Axon Instruments headstage (CV 203BU), attached to an Axopatch 200B amplifier (Axon Instruments, USA), and displayed on a computer using pClamp 10.2/Digidata 1440A software (Axon Instruments, USA). Data was sampled at 20 kHz (every 50 μs) and filtered at 2 kHz.

Prior to the formation of a multi-GΩ seal, currents were corrected for pipette (fast) capacitance. To determine whole-cell capacitance, capacitive currents were elicited by a 30 ms, 10 mV depolarizing pulse from a holding potential of -80 mV at 2 Hz after a whole-cell environment was formed. A minimum requirement for data collection was that access resistance

was below 10 MΩ. All currents were corrected for whole-cell capacitance, series resistance, and compensated to 80% using the Axopatch 200B amplifier.

hERG currents were elicited via a two component step protocol. The first component utilized depolarizing steps (7 s) from −80 mV to +70 mV in 10 mV intervals, and the second component stepped to −50 mV (2 s). The second component activated hERG tail currents that are presented in current-voltage (I-V) relationships. Finally, the membrane was clamped back to −80 mV holding potential for 1 s before the next depolarizing step.

All currents were analyzed in Clampfit 10.2. All data are represented as mean ± standard error mean (S.E.M.) in I-V relationships generated from Graphpad Prism 5.

6.5. Densitometry and Statistical Analysis

Densitometric analysis was carried out using the digital imagine program ImageJ (National Institutes of Health). Paired t tests were used to compare groups of data to determine significance.

References

1 Vabulas, R. M., Raychaudhuri, S., Hayer-Hartl, M. & Hartl, F. U. Protein folding in the cytoplasm and the heat shock response. *Cold Spring Harbor perspectives in biology* **2**, a004390, doi:10.1101/cshperspect.a004390 (2010).

2 Balch, W. E., Morimoto, R. I., Dillin, A. & Kelly, J. W. Adapting proteostasis for disease intervention. *Science* **319**, 916-919, doi:10.1126/science.1141448 (2008).

3 Gregersen, N., Bross, P., Vang, S. & Christensen, J. H. Protein misfolding and human disease. *Annual review of genomics and human genetics* **7**, 103-124, doi:10.1146/annurev.genom.7.080505.115737 (2006).

4 Hartl, F. U., Bracher, A. & Hayer-Hartl, M. Molecular chaperones in protein folding and proteostasis. *Nature* **475**, 324-332, doi:nature10317 [pii]10.1038/nature10317 (2011).

5 Lee, S., Sowa, M. E., Choi, J. M. & Tsai, F. T. The ClpB/Hsp104 molecular chaperone-a protein disaggregating machine. *Journal of structural biology* **146**, 99-105, doi:10.1016/j.jsb.2003.11.016 (2004).

6 Bakthisaran, R., Tangirala, R. & Rao, C. M. Small heat shock proteins: Role in cellular functions and pathology. *Biochimica et biophysica acta*, doi:10.1016/j.bbapap.2014.12.019 (2014).

7 Bukau, B. & Horwich, A. L. The Hsp70 and Hsp60 chaperone machines. *Cell* **92**, 351-366 (1998).

8 Hartl, F. U. Molecular chaperones in cellular protein folding. *Nature* **381**, 571-579, doi:10.1038/381571a0 (1996).

9 Flynn, G. C., Pohl, J., Flocco, M. T. & Rothman, J. E. Peptide-binding specificity of the molecular chaperone BiP. *Nature* **353**, 726-730, doi:10.1038/353726a0 (1991).

10 Rudiger, S., Buchberger, A. & Bukau, B. Interaction of Hsp70 chaperones with substrates. *Nature structural biology* **4**, 342-349 (1997).

11 Szabo, A. *et al.* The ATP hydrolysis-dependent reaction cycle of the Escherichia coli Hsp70 system DnaK, DnaJ, and GrpE. *Proceedings of the National Academy of Sciences of the United States of America* **91**, 10345-10349 (1994).

12 Buchberger, A., Schroder, H., Hesterkamp, T., Schonfeld, H. J. & Bukau, B. Substrate shuttling between the DnaK and GroEL systems indicates a chaperone network promoting protein folding. *Journal of molecular biology* **261**, 328-333, doi:10.1006/jmbi.1996.0465 (1996).

13 Hartl, F. U. & Hayer-Hartl, M. Molecular chaperones in the cytosol: from nascent chain to folded protein. *Science* **295**, 1852-1858, doi:10.1126/science.1068408 (2002).

14 Daugaard, M., Rohde, M. & Jaattela, M. The heat shock protein 70 family: Highly homologous proteins with overlapping and distinct functions. *FEBS letters* **581**, 3702-3710, doi:10.1016/j.febslet.2007.05.039 (2007).

15 Mayer, M. P. & Bukau, B. Hsp70 chaperones: cellular functions and molecular mechanism. *Cellular and molecular life sciences : CMLS* **62**, 670-684, doi:10.1007/s00018-004-4464-6 (2005).

16 Palleros, D. R., Reid, K. L., Shi, L., Welch, W. J. & Fink, A. L. ATP-induced protein-Hsp70 complex dissociation requires K+ but not ATP hydrolysis. *Nature* **365**, 664-666, doi:10.1038/365664a0 (1993).
17 Schmid, D., Baici, A., Gehring, H. & Christen, P. Kinetics of molecular chaperone action. *Science* **263**, 971-973 (1994).
18 Flaherty, K. M., DeLuca-Flaherty, C. & McKay, D. B. Three-dimensional structure of the ATPase fragment of a 70K heat-shock cognate protein. *Nature* **346**, 623-628, doi:10.1038/346623a0 (1990).
19 Zhu, X. *et al.* Structural analysis of substrate binding by the molecular chaperone DnaK. *Science* **272**, 1606-1614 (1996).
20 Vogel, M., Mayer, M. P. & Bukau, B. Allosteric regulation of Hsp70 chaperones involves a conserved interdomain linker. *The Journal of biological chemistry* **281**, 38705-38711, doi:10.1074/jbc.M609020200 (2006).
21 Swain, J. F. *et al.* Hsp70 chaperone ligands control domain association via an allosteric mechanism mediated by the interdomain linker. *Molecular cell* **26**, 27-39, doi:10.1016/j.molcel.2007.02.020 (2007).
22 Qian, Y. Q., Patel, D., Hartl, F. U. & McColl, D. J. Nuclear magnetic resonance solution structure of the human Hsp40 (HDJ-1) J-domain. *Journal of molecular biology* **260**, 224-235, doi:10.1006/jmbi.1996.0394 (1996).
23 Li, J., Qian, X. & Sha, B. The crystal structure of the yeast Hsp40 Ydj1 complexed with its peptide substrate. *Structure* **11**, 1475-1483 (2003).
24 Kityk, R., Kopp, J., Sinning, I. & Mayer, M. P. Structure and dynamics of the ATP-bound open conformation of Hsp70 chaperones. *Molecular cell* **48**, 863-874, doi:10.1016/j.molcel.2012.09.023 (2012).
25 Bertelsen, E. B., Chang, L., Gestwicki, J. E. & Zuiderweg, E. R. Solution conformation of wild-type E. coli Hsp70 (DnaK) chaperone complexed with ADP and substrate. *Proceedings of the National Academy of Sciences of the United States of America* **106**, 8471-8476, doi:10.1073/pnas.0903503106 (2009).
26 Young, J. C. Mechanisms of the Hsp70 chaperone system. *Biochemistry and cell biology = Biochimie et biologie cellulaire* **88**, 291-300, doi:10.1139/o09-175 (2010).
27 Hunt, C. R. *et al.* Genomic instability and enhanced radiosensitivity in Hsp70.1- and Hsp70.3-deficient mice. *Molecular and cellular biology* **24**, 899-911 (2004).
28 Liberek, K., Marszalek, J., Ang, D., Georgopoulos, C. & Zylicz, M. Escherichia coli DnaJ and GrpE heat shock proteins jointly stimulate ATPase activity of DnaK. *Proceedings of the National Academy of Sciences of the United States of America* **88**, 2874-2878 (1991).
29 Schroder, H., Langer, T., Hartl, F. U. & Bukau, B. DnaK, DnaJ and GrpE form a cellular chaperone machinery capable of repairing heat-induced protein damage. *The EMBO journal* **12**, 4137-4144 (1993).
30 Young, J. C. The role of the cytosolic HSP70 chaperone system in diseases caused by misfolding and aberrant trafficking of ion channels. *Disease models & mechanisms* **7**, 319-329, doi:10.1242/dmm.014001 (2014).
31 Pellecchia, M., Szyperski, T., Wall, D., Georgopoulos, C. & Wuthrich, K. NMR structure of the J-domain and the Gly/Phe-rich region of the Escherichia coli DnaJ chaperone. *Journal of molecular biology* **260**, 236-250, doi:10.1006/jmbi.1996.0395 (1996).

32 Genevaux, P., Schwager, F., Georgopoulos, C. & Kelley, W. L. Scanning mutagenesis identifies amino acid residues essential for the in vivo activity of the Escherichia coli DnaJ (Hsp40) J-domain. *Genetics* **162**, 1045-1053 (2002).
33 Qiu, X. B., Shao, Y. M., Miao, S. & Wang, L. The diversity of the DnaJ/Hsp40 family, the crucial partners for Hsp70 chaperones. *Cellular and molecular life sciences : CMLS* **63**, 2560-2570, doi:10.1007/s00018-006-6192-6 (2006).
34 Cheetham, M. E. & Caplan, A. J. Structure, function and evolution of DnaJ: conservation and adaptation of chaperone function. *Cell stress & chaperones* **3**, 28-36 (1998).
35 Terada, K., Kanazawa, M., Bukau, B. & Mori, M. The human DnaJ homologue dj2 facilitates mitochondrial protein import and luciferase refolding. *The Journal of cell biology* **139**, 1089-1095 (1997).
36 Terada, K. & Mori, M. Human DnaJ homologs dj2 and dj3, and bag-1 are positive cochaperones of hsc70. *The Journal of biological chemistry* **275**, 24728-24734, doi:10.1074/jbc.M002021200 (2000).
37 Hafizur, R. M., Yano, M., Gotoh, T., Mori, M. & Terada, K. Modulation of chaperone activities of Hsp70 and Hsp70-2 by a mammalian DnaJ/Hsp40 homolog, DjA4. *Journal of biochemistry* **135**, 193-200 (2004).
38 Hohfeld, J., Minami, Y. & Hartl, F. U. Hip, a novel cochaperone involved in the eukaryotic Hsc70/Hsp40 reaction cycle. *Cell* **83**, 589-598 (1995).
39 Minami, Y., Hohfeld, J., Ohtsuka, K. & Hartl, F. U. Regulation of the heat-shock protein 70 reaction cycle by the mammalian DnaJ homolog, Hsp40. *The Journal of biological chemistry* **271**, 19617-19624 (1996).
40 Hageman, J. *et al.* A DNAJB chaperone subfamily with HDAC-dependent activities suppresses toxic protein aggregation. *Molecular cell* **37**, 355-369, doi:10.1016/j.molcel.2010.01.001 (2010).
41 Kazemi-Esfarjani, P. & Benzer, S. Genetic suppression of polyglutamine toxicity in Drosophila. *Science* **287**, 1837-1840 (2000).
42 Fayazi, Z. *et al.* A Drosophila ortholog of the human MRJ modulates polyglutamine toxicity and aggregation. *Neurobiology of disease* **24**, 226-244, doi:10.1016/j.nbd.2006.06.015 (2006).
43 Chuang, J. Z. *et al.* Characterization of a brain-enriched chaperone, MRJ, that inhibits Huntingtin aggregation and toxicity independently. *The Journal of biological chemistry* **277**, 19831-19838, doi:10.1074/jbc.M109613200 (2002).
44 Westhoff, B., Chapple, J. P., van der Spuy, J., Hohfeld, J. & Cheetham, M. E. HSJ1 is a neuronal shuttling factor for the sorting of chaperone clients to the proteasome. *Current biology : CB* **15**, 1058-1064, doi:10.1016/j.cub.2005.04.058 (2005).
45 Mastrogiacomo, A. *et al.* Cysteine string proteins: a potential link between synaptic vesicles and presynaptic Ca2+ channels. *Science* **263**, 981-982 (1994).
46 Braun, J. E. & Scheller, R. H. Cysteine string protein, a DnaJ family member, is present on diverse secretory vesicles. *Neuropharmacology* **34**, 1361-1369 (1995).
47 Brown, H. *et al.* Cysteine string protein (CSP) is an insulin secretory granule-associated protein regulating beta-cell exocytosis. *The EMBO journal* **17**, 5048-5058, doi:10.1093/emboj/17.17.5048 (1998).
48 Kyle, B. D., Ahrendt, E., Braun, A. P. & Braun, J. E. The large conductance, calcium-activated K+ (BK) channel is regulated by cysteine string protein. *Scientific reports* **3**, 2447, doi:10.1038/srep02447 (2013).

49 Ahrendt, E., Kyle, B., Braun, A. P. & Braun, J. E. Cysteine string protein limits expression of the large conductance, calcium-activated K(+) (BK) channel. *PloS one* **9**, e86586, doi:10.1371/journal.pone.0086586 (2014).

50 Zhang, Y. Q. *et al.* Identification of CSPalpha clients reveals a role in dynamin 1 regulation. *Neuron* **74**, 136-150, doi:10.1016/j.neuron.2012.01.029 (2012).

51 Sharma, M. *et al.* CSPalpha knockout causes neurodegeneration by impairing SNAP-25 function. *The EMBO journal* **31**, 829-841, doi:10.1038/emboj.2011.467 (2012).

52 Donnelier, J. & Braun, J. E. CSPalpha-chaperoning presynaptic proteins. *Frontiers in cellular neuroscience* **8**, 116, doi:10.3389/fncel.2014.00116 (2014).

53 Ungewickell, E. *et al.* Role of auxilin in uncoating clathrin-coated vesicles. *Nature* **378**, 632-635, doi:10.1038/378632a0 (1995).

54 Walsh, P., Bursac, D., Law, Y. C., Cyr, D. & Lithgow, T. The J-protein family: modulating protein assembly, disassembly and translocation. *EMBO reports* **5**, 567-571, doi:10.1038/sj.embor.7400172 (2004).

55 Meacham, G. C. *et al.* The Hdj-2/Hsc70 chaperone pair facilitates early steps in CFTR biogenesis. *The EMBO journal* **18**, 1492-1505, doi:10.1093/emboj/18.6.1492 (1999).

56 Cintron, N. S. & Toft, D. Defining the requirements for Hsp40 and Hsp70 in the Hsp90 chaperone pathway. *The Journal of biological chemistry* **281**, 26235-26244, doi:10.1074/jbc.M605417200 (2006).

57 Terada, K. *et al.* A type I DnaJ homolog, DjA1, regulates androgen receptor signaling and spermatogenesis. *The EMBO journal* **24**, 611-622, doi:10.1038/sj.emboj.7600549 (2005).

58 Orthwein, A. *et al.* Optimal functional levels of activation-induced deaminase specifically require the Hsp40 DnaJa1. *The EMBO journal* **31**, 679-691, doi:10.1038/emboj.2011.417 (2012).

59 Schmidt, U. *et al.* Essential role of the unusual DNA-binding motif of BAG-1 for inhibition of the glucocorticoid receptor. *The Journal of biological chemistry* **278**, 4926-4931, doi:10.1074/jbc.M212000200 (2003).

60 Bhangoo, M. K. *et al.* Multiple 40-kDa heat-shock protein chaperones function in Tom70-dependent mitochondrial import. *Molecular biology of the cell* **18**, 3414-3428, doi:10.1091/mbc.E07-01-0088 (2007).

61 Tzankov, S., Wong, M. J., Shi, K., Nassif, C. & Young, J. C. Functional divergence between co-chaperones of Hsc70. *The Journal of biological chemistry* **283**, 27100-27109, doi:10.1074/jbc.M803923200 (2008).

62 Baaklini, I. *et al.* The DNAJA2 substrate release mechanism is essential for chaperone-mediated folding. *The Journal of biological chemistry* **287**, 41939-41954, doi:10.1074/jbc.M112.413278 (2012).

63 Kampinga, H. H. & Craig, E. A. The HSP70 chaperone machinery: J proteins as drivers of functional specificity. *Nature reviews. Molecular cell biology* **11**, 579-592, doi:10.1038/nrm2941 (2010).

64 Kabbage, M. & Dickman, M. B. The BAG proteins: a ubiquitous family of chaperone regulators. *Cellular and molecular life sciences : CMLS* **65**, 1390-1402, doi:10.1007/s00018-008-7535-2 (2008).

65 Luders, J., Demand, J. & Hohfeld, J. The ubiquitin-related BAG-1 provides a link between the molecular chaperones Hsc70/Hsp70 and the proteasome. *The Journal of biological chemistry* **275**, 4613-4617 (2000).

66 Arndt, V., Daniel, C., Nastainczyk, W., Alberti, S. & Hohfeld, J. BAG-2 acts as an inhibitor of the chaperone-associated ubiquitin ligase CHIP. *Molecular biology of the cell* **16**, 5891-5900, doi:10.1091/mbc.E05-07-0660 (2005).
67 Lee, J. H. *et al.* Bis, a Bcl-2-binding protein that synergizes with Bcl-2 in preventing cell death. *Oncogene* **18**, 6183-6190, doi:10.1038/sj.onc.1203043 (1999).
68 Jiang, Y., Woronicz, J. D., Liu, W. & Goeddel, D. V. Prevention of constitutive TNF receptor 1 signaling by silencer of death domains. *Science* **283**, 543-546 (1999).
69 Kalia, S. K. *et al.* BAG5 inhibits parkin and enhances dopaminergic neuron degeneration. *Neuron* **44**, 931-945, doi:10.1016/j.neuron.2004.11.026 (2004).
70 Vos, M. J., Hageman, J., Carra, S. & Kampinga, H. H. Structural and functional diversities between members of the human HSPB, HSPH, HSPA, and DNAJ chaperone families. *Biochemistry* **47**, 7001-7011, doi:10.1021/bi800639z (2008).
71 Goeckeler, J. L., Stephens, A., Lee, P., Caplan, A. J. & Brodsky, J. L. Overexpression of yeast Hsp110 homolog Sse1p suppresses ydj1-151 thermosensitivity and restores Hsp90-dependent activity. *Molecular biology of the cell* **13**, 2760-2770, doi:10.1091/mbc.02-04-0051 (2002).
72 Oh, H. J., Chen, X. & Subjeck, J. R. Hsp110 protects heat-denatured proteins and confers cellular thermoresistance. *The Journal of biological chemistry* **272**, 31636-31640 (1997).
73 Oh, H. J., Easton, D., Murawski, M., Kaneko, Y. & Subjeck, J. R. The chaperoning activity of hsp110. Identification of functional domains by use of targeted deletions. *The Journal of biological chemistry* **274**, 15712-15718 (1999).
74 Raynes, D. A. & Guerriero, V., Jr. Inhibition of Hsp70 ATPase activity and protein renaturation by a novel Hsp70-binding protein. *The Journal of biological chemistry* **273**, 32883-32888 (1998).
75 Kabani, M., Beckerich, J. M. & Brodsky, J. L. Nucleotide exchange factor for the yeast Hsp70 molecular chaperone Ssa1p. *Molecular and cellular biology* **22**, 4677-4689 (2002).
76 Kabani, M., McLellan, C., Raynes, D. A., Guerriero, V. & Brodsky, J. L. HspBP1, a homologue of the yeast Fes1 and Sls1 proteins, is an Hsc70 nucleotide exchange factor. *FEBS letters* **531**, 339-342 (2002).
77 Shomura, Y. *et al.* Regulation of Hsp70 function by HspBP1: structural analysis reveals an alternate mechanism for Hsp70 nucleotide exchange. *Molecular cell* **17**, 367-379, doi:10.1016/j.molcel.2004.12.023 (2005).
78 Takayama, S. *et al.* Cloning and functional analysis of BAG-1: a novel Bcl-2-binding protein with anti-cell death activity. *Cell* **80**, 279-284 (1995).
79 Hohfeld, J. & Jentsch, S. GrpE-like regulation of the hsc70 chaperone by the anti-apoptotic protein BAG-1. *The EMBO journal* **16**, 6209-6216, doi:10.1093/emboj/16.20.6209 (1997).
80 Takayama, S. *et al.* BAG-1 modulates the chaperone activity of Hsp70/Hsc70. *The EMBO journal* **16**, 4887-4896, doi:10.1093/emboj/16.16.4887 (1997).
81 Zeiner, M., Gebauer, M. & Gehring, U. Mammalian protein RAP46: an interaction partner and modulator of 70 kDa heat shock proteins. *The EMBO journal* **16**, 5483-5490, doi:10.1093/emboj/16.18.5483 (1997).
82 Packham, G., Brimmell, M. & Cleveland, J. L. Mammalian cells express two differently localized Bag-1 isoforms generated by alternative translation initiation. *The Biochemical journal* **328 (Pt 3)**, 807-813 (1997).

83 Takayama, S. *et al.* Expression and location of Hsp70/Hsc-binding anti-apoptotic protein BAG-1 and its variants in normal tissues and tumor cell lines. *Cancer research* **58**, 3116-3131 (1998).
84 Yang, X. *et al.* Human BAG-1/RAP46 protein is generated as four isoforms by alternative translation initiation and overexpressed in cancer cells. *Oncogene* **17**, 981-989, doi:10.1038/sj.onc.1202032 (1998).
85 Zeiner, M., Niyaz, Y. & Gehring, U. The hsp70-associating protein Hap46 binds to DNA and stimulates transcription. *Proceedings of the National Academy of Sciences of the United States of America* **96**, 10194-10199 (1999).
86 Alberti, S., Esser, C. & Hohfeld, J. BAG-1--a nucleotide exchange factor of Hsc70 with multiple cellular functions. *Cell stress & chaperones* **8**, 225-231 (2003).
87 Sondermann, H. *et al.* Structure of a Bag/Hsc70 complex: convergent functional evolution of Hsp70 nucleotide exchange factors. *Science* **291**, 1553-1557, doi:10.1126/science.291.5508.1553 (2001).
88 El Mourabit, H. *et al.* The PDZ domain of TIP-2/GIPC interacts with the C-terminus of the integrin alpha5 and alpha6 subunits. *Matrix biology : journal of the International Society for Matrix Biology* **21**, 207-214 (2002).
89 Liman, J. *et al.* Interaction of BAG1 and Hsp70 mediates neuroprotectivity and increases chaperone activity. *Molecular and cellular biology* **25**, 3715-3725, doi:10.1128/MCB.25.9.3715-3725.2005 (2005).
90 Aveic, S., Pigazzi, M. & Basso, G. BAG1: the guardian of anti-apoptotic proteins in acute myeloid leukemia. *PloS one* **6**, e26097, doi:10.1371/journal.pone.0026097 (2011).
91 Kermer, P. *et al.* Bag1 is a regulator and marker of neuronal differentiation. *Cell death and differentiation* **9**, 405-413, doi:10.1038/sj/cdd/4400972 (2002).
92 Naishiro, Y. *et al.* BAG-1 accelerates cell motility of human gastric cancer cells. *Oncogene* **18**, 3244-3251, doi:10.1038/sj.onc.1202661 (1999).
93 Takahashi, N. *et al.* BAG-1M, an isoform of Bcl-2-interacting protein BAG-1, enhances gene expression driven by CMV promoter. *Biochemical and biophysical research communications* **286**, 807-814, doi:10.1006/bbrc.2001.5473 (2001).
94 Song, J., Takeda, M. & Morimoto, R. I. Bag1-Hsp70 mediates a physiological stress signalling pathway that regulates Raf-1/ERK and cell growth. *Nature cell biology* **3**, 276-282, doi:10.1038/35060068 (2001).
95 Knee, D. A., Froesch, B. A., Nuber, U., Takayama, S. & Reed, J. C. Structure-function analysis of Bag1 proteins. Effects on androgen receptor transcriptional activity. *The Journal of biological chemistry* **276**, 12718-12724, doi:10.1074/jbc.M010841200 (2001).
96 Knapp, R. T. *et al.* BAG-1 diversely affects steroid receptor activity. *The Biochemical journal* **441**, 297-303, doi:10.1042/BJ20111456 (2012).
97 Knapp, R. T. *et al.* Hsp70 cochaperones HspBP1 and BAG-1M differentially regulate steroid hormone receptor function. *PloS one* **9**, e85415, doi:10.1371/journal.pone.0085415 (2014).
98 Elliott, E., Tsvetkov, P. & Ginzburg, I. BAG-1 associates with Hsc70.Tau complex and regulates the proteasomal degradation of Tau protein. *The Journal of biological chemistry* **282**, 37276-37284, doi:10.1074/jbc.M706379200 (2007).
99 Tsukahara, F. & Maru, Y. Bag1 directly routes immature BCR-ABL for proteasomal degradation. *Blood* **116**, 3582-3592, doi:10.1182/blood-2009-10-249623 (2010).

100 Okiyoneda, T. *et al.* Peripheral protein quality control removes unfolded CFTR from the plasma membrane. *Science* **329**, 805-810, doi:10.1126/science.1191542 (2010).
101 Gamerdinger, M. *et al.* Protein quality control during aging involves recruitment of the macroautophagy pathway by BAG3. *The EMBO journal* **28**, 889-901, doi:10.1038/emboj.2009.29 (2009).
102 Young, J. C., Barral, J. M. & Ulrich Hartl, F. More than folding: localized functions of cytosolic chaperones. *Trends in biochemical sciences* **28**, 541-547, doi:10.1016/j.tibs.2003.08.009 (2003).
103 Connell, P. *et al.* The co-chaperone CHIP regulates protein triage decisions mediated by heat-shock proteins. *Nature cell biology* **3**, 93-96, doi:10.1038/35050618 (2001).
104 Meacham, G. C., Patterson, C., Zhang, W., Younger, J. M. & Cyr, D. M. The Hsc70 co-chaperone CHIP targets immature CFTR for proteasomal degradation. *Nature cell biology* **3**, 100-105, doi:10.1038/35050509 (2001).
105 Pearl, L. H. & Prodromou, C. Structure and mechanism of the Hsp90 molecular chaperone machinery. *Annual review of biochemistry* **75**, 271-294, doi:10.1146/annurev.biochem.75.103004.142738 (2006).
106 Dittmar, K. D. & Pratt, W. B. Folding of the glucocorticoid receptor by the reconstituted Hsp90-based chaperone machinery. The initial hsp90.p60.hsp70-dependent step is sufficient for creating the steroid binding conformation. *The Journal of biological chemistry* **272**, 13047-13054 (1997).
107 Kim, Y. E., Hipp, M. S., Bracher, A., Hayer-Hartl, M. & Hartl, F. U. Molecular chaperone functions in protein folding and proteostasis. *Annual review of biochemistry* **82**, 323-355, doi:10.1146/annurev-biochem-060208-092442 (2013).
108 Young, J. C. Hsp90: a specialized but essential protein-folding tool. *The Journal of Cell Biology* **154**, 267-274, doi:10.1083/jcb.200104079 (2001).
109 Ryno, L. M. *et al.* Characterizing the altered cellular proteome induced by the stress-independent activation of heat shock factor 1. *ACS chemical biology* **9**, 1273-1283, doi:10.1021/cb500062n (2014).
110 Stebbins, C. E. *et al.* Crystal structure of an Hsp90-geldanamycin complex: targeting of a protein chaperone by an antitumor agent. *Cell* **89**, 239-250 (1997).
111 Prodromou, C. *et al.* Identification and structural characterization of the ATP/ADP-binding site in the Hsp90 molecular chaperone. *Cell* **90**, 65-75 (1997).
112 Ali, M. M. *et al.* Crystal structure of an Hsp90-nucleotide-p23/Sba1 closed chaperone complex. *Nature* **440**, 1013-1017, doi:10.1038/nature04716 (2006).
113 Li, J., Soroka, J. & Buchner, J. The Hsp90 chaperone machinery: conformational dynamics and regulation by co-chaperones. *Biochimica et biophysica acta* **1823**, 624-635, doi:10.1016/j.bbamcr.2011.09.003 (2012).
114 Shiau, A. K., Harris, S. F., Southworth, D. R. & Agard, D. A. Structural Analysis of E. coli hsp90 reveals dramatic nucleotide-dependent conformational rearrangements. *Cell* **127**, 329-340, doi:10.1016/j.cell.2006.09.027 (2006).
115 Vaughan, C. K. *et al.* Structure of an Hsp90-Cdc37-Cdk4 complex. *Molecular cell* **23**, 697-707, doi:10.1016/j.molcel.2006.07.016 (2006).
116 Southworth, D. R. & Agard, D. A. Client-loading conformation of the Hsp90 molecular chaperone revealed in the cryo-EM structure of the human Hsp90:Hop complex. *Molecular cell* **42**, 771-781, doi:10.1016/j.molcel.2011.04.023 (2011).

117 Kirschke, E., Goswami, D., Southworth, D., Griffin, P. R. & Agard, D. A. Glucocorticoid receptor function regulated by coordinated action of the Hsp90 and Hsp70 chaperone cycles. *Cell* **157**, 1685-1697, doi:10.1016/j.cell.2014.04.038 (2014).
118 Young, J. C., Obermann, W. M. & Hartl, F. U. Specific binding of tetratricopeptide repeat proteins to the C-terminal 12-kDa domain of hsp90. *The Journal of biological chemistry* **273**, 18007-18010 (1998).
119 Scheufler, C. *et al.* Structure of TPR domain-peptide complexes: critical elements in the assembly of the Hsp70-Hsp90 multichaperone machine. *Cell* **101**, 199-210, doi:10.1016/S0092-8674(00)80830-2 (2000).
120 Barral, J. M., Broadley, S. A., Schaffar, G. & Hartl, F. U. Roles of molecular chaperones in protein misfolding diseases. *Seminars in cell & developmental biology* **15**, 17-29, doi:10.1016/j.semcdb.2003.12.010 (2004).
121 Brychzy, A. *et al.* Cofactor Tpr2 combines two TPR domains and a J domain to regulate the Hsp70/Hsp90 chaperone system. *The EMBO journal* **22**, 3613-3623, doi:10.1093/emboj/cdg362 (2003).
122 Young, J. C., Agashe, V. R., Siegers, K. & Hartl, F. U. Pathways of chaperone-mediated protein folding in the cytosol. *Nature reviews. Molecular cell biology* **5**, 781-791, doi:10.1038/nrm1492 (2004).
123 Dittmar, K. D., Demady, D. R., Stancato, L. F., Krishna, P. & Pratt, W. B. Folding of the glucocorticoid receptor by the heat shock protein (hsp) 90-based chaperone machinery. The role of p23 is to stabilize receptor.hsp90 heterocomplexes formed by hsp90.p60.hsp70. *The Journal of biological chemistry* **272**, 21213-21220 (1997).
124 Young, J. C. & Hartl, F. U. Polypeptide release by Hsp90 involves ATP hydrolysis and is enhanced by the co-chaperone p23. *The EMBO journal* **19**, 5930-5940, doi:10.1093/emboj/19.21.5930 (2000).
125 Panaretou, B. *et al.* Activation of the ATPase activity of hsp90 by the stress-regulated cochaperone aha1. *Molecular cell* **10**, 1307-1318 (2002).
126 McLaughlin, S. H. *et al.* The co-chaperone p23 arrests the Hsp90 ATPase cycle to trap client proteins. *Journal of molecular biology* **356**, 746-758, doi:10.1016/j.jmb.2005.11.085 (2006).
127 Olzmann, J. A., Kopito, R. R. & Christianson, J. C. The mammalian endoplasmic reticulum-associated degradation system. *Cold Spring Harbor perspectives in biology* **5**, doi:10.1101/cshperspect.a013185 (2013).
128 Guerriero, C. J. & Brodsky, J. L. The delicate balance between secreted protein folding and endoplasmic reticulum-associated degradation in human physiology. *Physiological reviews* **92**, 537-576, doi:10.1152/physrev.00027.2011 (2012).
129 Ruggiano, A., Foresti, O. & Carvalho, P. Quality control: ER-associated degradation: protein quality control and beyond. *J Cell Biol* **204**, 869-879, doi:10.1083/jcb.201312042 (2014).
130 Braakman, I. & Hebert, D. N. Protein folding in the endoplasmic reticulum. *Cold Spring Harbor perspectives in biology* **5**, a013201, doi:10.1101/cshperspect.a013201 (2013).
131 Aebi, M., Bernasconi, R., Clerc, S. & Molinari, M. N-glycan structures: recognition and processing in the ER. *Trends in biochemical sciences* **35**, 74-82, doi:10.1016/j.tibs.2009.10.001 (2010).
132 Lederkremer, G. Z. Glycoprotein folding, quality control and ER-associated degradation. *Current opinion in structural biology* **19**, 515-523, doi:10.1016/j.sbi.2009.06.004 (2009).

133 Gonzalez, D. S., Karaveg, K., Vandersall-Nairn, A. S., Lal, A. & Moremen, K. W. Identification, expression, and characterization of a cDNA encoding human endoplasmic reticulum mannosidase I, the enzyme that catalyzes the first mannose trimming step in mammalian Asn-linked oligosaccharide biosynthesis. *The Journal of biological chemistry* **274**, 21375-21386 (1999).
134 Tremblay, L. O. & Herscovics, A. Cloning and expression of a specific human alpha 1,2-mannosidase that trims Man9GlcNAc2 to Man8GlcNAc2 isomer B during N-glycan biosynthesis. *Glycobiology* **9**, 1073-1078 (1999).
135 Olivari, S. *et al.* EDEM1 regulates ER-associated degradation by accelerating de-mannosylation of folding-defective polypeptides and by inhibiting their covalent aggregation. *Biochemical and biophysical research communications* **349**, 1278-1284, doi:10.1016/j.bbrc.2006.08.186 (2006).
136 Hosokawa, N. *et al.* EDEM1 accelerates the trimming of alpha1,2-linked mannose on the C branch of N-glycans. *Glycobiology* **20**, 567-575, doi:10.1093/glycob/cwq001 (2010).
137 Hirao, K. *et al.* EDEM3, a soluble EDEM homolog, enhances glycoprotein endoplasmic reticulum-associated degradation and mannose trimming. *The Journal of biological chemistry* **281**, 9650-9658, doi:10.1074/jbc.M512191200 (2006).
138 Hosokawa, N., Kamiya, Y., Kamiya, D., Kato, K. & Nagata, K. Human OS-9, a lectin required for glycoprotein endoplasmic reticulum-associated degradation, recognizes mannose-trimmed N-glycans. *The Journal of biological chemistry* **284**, 17061-17068, doi:10.1074/jbc.M809725200 (2009).
139 Hosokawa, N., You, Z., Tremblay, L. O., Nagata, K. & Herscovics, A. Stimulation of ERAD of misfolded null Hong Kong alpha1-antitrypsin by Golgi alpha1,2-mannosidases. *Biochemical and biophysical research communications* **362**, 626-632, doi:10.1016/j.bbrc.2007.08.057 (2007).
140 Bernasconi, R., Pertel, T., Luban, J. & Molinari, M. A dual task for the Xbp1-responsive OS-9 variants in the mammalian endoplasmic reticulum: inhibiting secretion of misfolded protein conformers and enhancing their disposal. *The Journal of biological chemistry* **283**, 16446-16454, doi:10.1074/jbc.M802272200 (2008).
141 Hosokawa, N. *et al.* Human XTP3-B forms an endoplasmic reticulum quality control scaffold with the HRD1-SEL1L ubiquitin ligase complex and BiP. *The Journal of biological chemistry* **283**, 20914-20924, doi:10.1074/jbc.M709336200 (2008).
142 Christianson, J. C., Shaler, T. A., Tyler, R. E. & Kopito, R. R. OS-9 and GRP94 deliver mutant alpha1-antitrypsin to the Hrd1-SEL1L ubiquitin ligase complex for ERAD. *Nature cell biology* **10**, 272-282, doi:10.1038/ncb1689 (2008).
143 Bernasconi, R., Galli, C., Calanca, V., Nakajima, T. & Molinari, M. Stringent requirement for HRD1, SEL1L, and OS-9/XTP3-B for disposal of ERAD-LS substrates. *J Cell Biol* **188**, 223-235, doi:10.1083/jcb.200910042 (2010).
144 Sato, T. *et al.* STT3B-dependent posttranslational N-glycosylation as a surveillance system for secretory protein. *Molecular cell* **47**, 99-110, doi:10.1016/j.molcel.2012.04.015 (2012).
145 Bhamidipati, A., Denic, V., Quan, E. M. & Weissman, J. S. Exploration of the topological requirements of ERAD identifies Yos9p as a lectin sensor of misfolded glycoproteins in the ER lumen. *Molecular cell* **19**, 741-751, doi:10.1016/j.molcel.2005.07.027 (2005).

146 Eletto, D., Dersh, D. & Argon, Y. GRP94 in ER quality control and stress responses. *Seminars in cell & developmental biology* **21**, 479-485, doi:10.1016/j.semcdb.2010.03.004 (2010).
147 Weekes, M. P. *et al.* Proteomic plasma membrane profiling reveals an essential role for gp96 in the cell surface expression of LDLR family members, including the LDL receptor and LRP6. *Journal of proteome research* **11**, 1475-1484, doi:10.1021/pr201135e (2012).
148 Carvalho, P., Stanley, A. M. & Rapoport, T. A. Retrotranslocation of a misfolded luminal ER protein by the ubiquitin-ligase Hrd1p. *Cell* **143**, 579-591, doi:10.1016/j.cell.2010.10.028 (2010).
149 Cormier, J. H., Tamura, T., Sunryd, J. C. & Hebert, D. N. EDEM1 recognition and delivery of misfolded proteins to the SEL1L-containing ERAD complex. *Molecular cell* **34**, 627-633, doi:10.1016/j.molcel.2009.05.018 (2009).
150 Mueller, B., Lilley, B. N. & Ploegh, H. L. SEL1L, the homologue of yeast Hrd3p, is involved in protein dislocation from the mammalian ER. *The Journal of cell biology* **175**, 261-270, doi:10.1083/jcb.200605196 (2006).
151 Mueller, B., Klemm, E. J., Spooner, E., Claessen, J. H. & Ploegh, H. L. SEL1L nucleates a protein complex required for dislocation of misfolded glycoproteins. *Proceedings of the National Academy of Sciences of the United States of America* **105**, 12325-12330, doi:10.1073/pnas.0805371105 (2008).
152 Iida, Y. *et al.* SEL1L protein critically determines the stability of the HRD1-SEL1L endoplasmic reticulum-associated degradation (ERAD) complex to optimize the degradation kinetics of ERAD substrates. *The Journal of biological chemistry* **286**, 16929-16939, doi:10.1074/jbc.M110.215871 (2011).
153 Klemm, E. J., Spooner, E. & Ploegh, H. L. Dual role of ancient ubiquitous protein 1 (AUP1) in lipid droplet accumulation and endoplasmic reticulum (ER) protein quality control. *The Journal of biological chemistry* **286**, 37602-37614, doi:10.1074/jbc.M111.284794 (2011).
154 Christianson, J. C. *et al.* Defining human ERAD networks through an integrative mapping strategy. *Nature cell biology* **14**, 93-105, doi:10.1038/ncb2383 (2012).
155 Cattaneo, M. *et al.* SEL1L and HRD1 are involved in the degradation of unassembled secretory Ig-mu chains. *Journal of cellular physiology* **215**, 794-802, doi:10.1002/jcp.21364 (2008).
156 Gardner, R. G. *et al.* Endoplasmic reticulum degradation requires lumen to cytosol signaling. Transmembrane control of Hrd1p by Hrd3p. *J Cell Biol* **151**, 69-82 (2000).
157 Carvalho, P., Goder, V. & Rapoport, T. A. Distinct ubiquitin-ligase complexes define convergent pathways for the degradation of ER proteins. *Cell* **126**, 361-373, doi:10.1016/j.cell.2006.05.043 (2006).
158 Denic, V., Quan, E. M. & Weissman, J. S. A luminal surveillance complex that selects misfolded glycoproteins for ER-associated degradation. *Cell* **126**, 349-359, doi:10.1016/j.cell.2006.05.045 (2006).
159 Pearce, M. M., Wormer, D. B., Wilkens, S. & Wojcikiewicz, R. J. An endoplasmic reticulum (ER) membrane complex composed of SPFH1 and SPFH2 mediates the ER-associated degradation of inositol 1,4,5-trisphosphate receptors. *The Journal of biological chemistry* **284**, 10433-10445, doi:10.1074/jbc.M809801200 (2009).

160 Pearce, M. M., Wang, Y., Kelley, G. G. & Wojcikiewicz, R. J. SPFH2 mediates the endoplasmic reticulum-associated degradation of inositol 1,4,5-trisphosphate receptors and other substrates in mammalian cells. *The Journal of biological chemistry* **282**, 20104-20115, doi:10.1074/jbc.M701862200 (2007).
161 Lu, J. P., Wang, Y., Sliter, D. A., Pearce, M. M. & Wojcikiewicz, R. J. RNF170 protein, an endoplasmic reticulum membrane ubiquitin ligase, mediates inositol 1,4,5-trisphosphate receptor ubiquitination and degradation. *The Journal of biological chemistry* **286**, 24426-24433, doi:10.1074/jbc.M111.251983 (2011).
162 Jo, Y., Sguigna, P. V. & DeBose-Boyd, R. A. Membrane-associated ubiquitin ligase complex containing gp78 mediates sterol-accelerated degradation of 3-hydroxy-3-methylglutaryl-coenzyme A reductase. *The Journal of biological chemistry* **286**, 15022-15031, doi:10.1074/jbc.M110.211326 (2011).
163 Song, B. L., Sever, N. & DeBose-Boyd, R. A. Gp78, a membrane-anchored ubiquitin ligase, associates with Insig-1 and couples sterol-regulated ubiquitination to degradation of HMG CoA reductase. *Molecular cell* **19**, 829-840, doi:10.1016/j.molcel.2005.08.009 (2005).
164 Hartman, I. Z. *et al.* Sterol-induced dislocation of 3-hydroxy-3-methylglutaryl coenzyme A reductase from endoplasmic reticulum membranes into the cytosol through a subcellular compartment resembling lipid droplets. *The Journal of biological chemistry* **285**, 19288-19298, doi:10.1074/jbc.M110.134213 (2010).
165 Cao, J. *et al.* Ufd1 is a cofactor of gp78 and plays a key role in cholesterol metabolism by regulating the stability of HMG-CoA reductase. *Cell metabolism* **6**, 115-128, doi:10.1016/j.cmet.2007.07.002 (2007).
166 Jo, Y., Lee, P. C., Sguigna, P. V. & DeBose-Boyd, R. A. Sterol-induced degradation of HMG CoA reductase depends on interplay of two Insigs and two ubiquitin ligases, gp78 and Trc8. *Proceedings of the National Academy of Sciences of the United States of America* **108**, 20503-20508, doi:10.1073/pnas.1112831108 (2011).
167 Lee, J. P. *et al.* The TRC8 ubiquitin ligase is sterol regulated and interacts with lipid and protein biosynthetic pathways. *Molecular cancer research : MCR* **8**, 93-106, doi:10.1158/1541-7786.MCR-08-0491 (2010).
168 Lee, J. N., Song, B., DeBose-Boyd, R. A. & Ye, J. Sterol-regulated degradation of Insig-1 mediated by the membrane-bound ubiquitin ligase gp78. *The Journal of biological chemistry* **281**, 39308-39315, doi:10.1074/jbc.M608999200 (2006).
169 Flury, I. *et al.* INSIG: a broadly conserved transmembrane chaperone for sterol-sensing domain proteins. *The EMBO journal* **24**, 3917-3926, doi:10.1038/sj.emboj.7600855 (2005).
170 Gardner, R. G., Shearer, A. G. & Hampton, R. Y. In vivo action of the HRD ubiquitin ligase complex: mechanisms of endoplasmic reticulum quality control and sterol regulation. *Molecular and cellular biology* **21**, 4276-4291, doi:10.1128/MCB.21.13.4276-4291.2001 (2001).
171 Theesfeld, C. L. & Hampton, R. Y. Insulin-induced gene protein (INSIG)-dependent sterol regulation of Hmg2 endoplasmic reticulum-associated degradation (ERAD) in yeast. *The Journal of biological chemistry* **288**, 8519-8530, doi:10.1074/jbc.M112.404517 (2013).

172 Foresti, O., Ruggiano, A., Hannibal-Bach, H. K., Ejsing, C. S. & Carvalho, P. Sterol homeostasis requires regulated degradation of squalene monooxygenase by the ubiquitin ligase Doa10/Teb4. *eLife* **2**, e00953, doi:10.7554/eLife.00953 (2013).
173 Gill, S., Stevenson, J., Kristiana, I. & Brown, A. J. Cholesterol-dependent degradation of squalene monooxygenase, a control point in cholesterol synthesis beyond HMG-CoA reductase. *Cell metabolism* **13**, 260-273, doi:10.1016/j.cmet.2011.01.015 (2011).
174 Yoshida, Y. *et al.* Fbs2 is a new member of the E3 ubiquitin ligase family that recognizes sugar chains. *The Journal of biological chemistry* **278**, 43877-43884, doi:10.1074/jbc.M304157200 (2003).
175 Yoshida, Y. *et al.* E3 ubiquitin ligase that recognizes sugar chains. *Nature* **418**, 438-442, doi:10.1038/nature00890 (2002).
176 Hirsch, C., Blom, D. & Ploegh, H. L. A role for N-glycanase in the cytosolic turnover of glycoproteins. *The EMBO journal* **22**, 1036-1046, doi:10.1093/emboj/cdg107 (2003).
177 Willey, R. L., Maldarelli, F., Martin, M. A. & Strebel, K. Human immunodeficiency virus type 1 Vpu protein induces rapid degradation of CD4. *Journal of virology* **66**, 7193-7200 (1992).
178 Margottin, F. *et al.* A novel human WD protein, h-beta TrCp, that interacts with HIV-1 Vpu connects CD4 to the ER degradation pathway through an F-box motif. *Molecular cell* **1**, 565-574 (1998).
179 Wiertz, E. J. *et al.* The human cytomegalovirus US11 gene product dislocates MHC class I heavy chains from the endoplasmic reticulum to the cytosol. *Cell* **84**, 769-779 (1996).
180 Burr, M. L. *et al.* HRD1 and UBE2J1 target misfolded MHC class I heavy chains for endoplasmic reticulum-associated degradation. *Proceedings of the National Academy of Sciences of the United States of America* **108**, 2034-2039, doi:10.1073/pnas.1016229108 (2011).
181 Stagg, H. R. *et al.* The TRC8 E3 ligase ubiquitinates MHC class I molecules before dislocation from the ER. *The Journal of cell biology* **186**, 685-692, doi:10.1083/jcb.200906110 (2009).
182 Gemmill, R. M. *et al.* The hereditary renal cell carcinoma 3;8 translocation fuses FHIT to a patched-related gene, TRC8. *Proceedings of the National Academy of Sciences of the United States of America* **95**, 9572-9577 (1998).
183 Lilley, B. N. & Ploegh, H. L. A membrane protein required for dislocation of misfolded proteins from the ER. *Nature* **429**, 834-840, doi:10.1038/nature02592 (2004).
184 Ye, Y., Shibata, Y., Yun, C., Ron, D. & Rapoport, T. A. A membrane protein complex mediates retro-translocation from the ER lumen into the cytosol. *Nature* **429**, 841-847, doi:10.1038/nature02656 (2004).
185 Loureiro, J. *et al.* Signal peptide peptidase is required for dislocation from the endoplasmic reticulum. *Nature* **441**, 894-897, doi:10.1038/nature04830 (2006).
186 Plemper, R. K., Bohmler, S., Bordallo, J., Sommer, T. & Wolf, D. H. Mutant analysis links the translocon and BiP to retrograde protein transport for ER degradation. *Nature* **388**, 891-895, doi:10.1038/42276 (1997).
187 Scott, D. C. & Schekman, R. Role of Sec61p in the ER-associated degradation of short-lived transmembrane proteins. *J Cell Biol* **181**, 1095-1105, doi:10.1083/jcb.200804053 (2008).

188 Mehnert, M., Sommer, T. & Jarosch, E. Der1 promotes movement of misfolded proteins through the endoplasmic reticulum membrane. *Nature cell biology* **16**, 77-86, doi:10.1038/ncb2882 (2014).
189 Stein, A., Ruggiano, A., Carvalho, P. & Rapoport, T. A. Key steps in ERAD of luminal ER proteins reconstituted with purified components. *Cell* **158**, 1375-1388, doi:10.1016/j.cell.2014.07.050 (2014).
190 Meyer, H., Bug, M. & Bremer, S. Emerging functions of the VCP/p97 AAA-ATPase in the ubiquitin system. *Nature cell biology* **14**, 117-123, doi:10.1038/ncb2407 (2012).
191 Ye, Y., Meyer, H. H. & Rapoport, T. A. The AAA ATPase Cdc48/p97 and its partners transport proteins from the ER into the cytosol. *Nature* **414**, 652-656, doi:10.1038/414652a (2001).
192 Rabinovich, E., Kerem, A., Frohlich, K. U., Diamant, N. & Bar-Nun, S. AAA-ATPase p97/Cdc48p, a cytosolic chaperone required for endoplasmic reticulum-associated protein degradation. *Molecular and cellular biology* **22**, 626-634 (2002).
193 DeLaBarre, B., Christianson, J. C., Kopito, R. R. & Brunger, A. T. Central pore residues mediate the p97/VCP activity required for ERAD. *Molecular cell* **22**, 451-462, doi:10.1016/j.molcel.2006.03.036 (2006).
194 Wang, Q., Li, L. & Ye, Y. Inhibition of p97-dependent protein degradation by Eeyarestatin I. *The Journal of biological chemistry* **283**, 7445-7454, doi:10.1074/jbc.M708347200 (2008).
195 Ye, Y., Meyer, H. H. & Rapoport, T. A. Function of the p97-Ufd1-Npl4 complex in retrotranslocation from the ER to the cytosol: dual recognition of nonubiquitinated polypeptide segments and polyubiquitin chains. *The Journal of cell biology* **162**, 71-84, doi:10.1083/jcb.200302169 (2003).
196 Nadav, E. *et al.* A novel mammalian endoplasmic reticulum ubiquitin ligase homologous to the yeast Hrd1. *Biochemical and biophysical research communications* **303**, 91-97 (2003).
197 Kikkert, M. *et al.* Human HRD1 is an E3 ubiquitin ligase involved in degradation of proteins from the endoplasmic reticulum. *The Journal of biological chemistry* **279**, 3525-3534, doi:10.1074/jbc.M307453200 (2004).
198 Fang, S. *et al.* The tumor autocrine motility factor receptor, gp78, is a ubiquitin protein ligase implicated in degradation from the endoplasmic reticulum. *Proceedings of the National Academy of Sciences of the United States of America* **98**, 14422-14427, doi:10.1073/pnas.251401598 (2001).
199 Hassink, G. *et al.* TEB4 is a C4HC3 RING finger-containing ubiquitin ligase of the endoplasmic reticulum. *The Biochemical journal* **388**, 647-655, doi:10.1042/BJ20041241 (2005).
200 Younger, J. M. *et al.* Sequential quality-control checkpoints triage misfolded cystic fibrosis transmembrane conductance regulator. *Cell* **126**, 571-582, doi:S0092-8674(06)00908-1 [pii]
10.1016/j.cell.2006.06.041 (2006).
201 Morito, D. *et al.* Gp78 cooperates with RMA1 in endoplasmic reticulum-associated degradation of CFTRDeltaF508. *Molecular biology of the cell* **19**, 1328-1336, doi:10.1091/mbc.E07-06-0601 (2008).

202 Lerner, M. *et al.* The RBCC gene RFP2 (Leu5) encodes a novel transmembrane E3 ubiquitin ligase involved in ERAD. *Molecular biology of the cell* **18**, 1670-1682, doi:10.1091/mbc.E06-03-0248 (2007).
203 Altier, C. *et al.* The Cavbeta subunit prevents RFP2-mediated ubiquitination and proteasomal degradation of L-type channels. *Nature neuroscience* **14**, 173-180, doi:10.1038/nn.2712 (2011).
204 Maruyama, Y., Yamada, M., Takahashi, K. & Yamada, M. Ubiquitin ligase Kf-1 is involved in the endoplasmic reticulum-associated degradation pathway. *Biochemical and biophysical research communications* **374**, 737-741, doi:10.1016/j.bbrc.2008.07.126 (2008).
205 Neutzner, A. *et al.* A systematic search for endoplasmic reticulum (ER) membrane-associated RING finger proteins identifies Nixin/ZNRF4 as a regulator of calnexin stability and ER homeostasis. *The Journal of biological chemistry* **286**, 8633-8643, doi:10.1074/jbc.M110.197459 (2011).
206 Imai, Y. *et al.* CHIP is associated with Parkin, a gene responsible for familial Parkinson's disease, and enhances its ubiquitin ligase activity. *Molecular cell* **10**, 55-67 (2002).
207 Magadan, J. G. *et al.* Multilayered mechanism of CD4 downregulation by HIV-1 Vpu involving distinct ER retention and ERAD targeting steps. *PLoS pathogens* **6**, e1000869, doi:10.1371/journal.ppat.1000869 (2010).
208 Guo, X. *et al.* The E3 ligase Smurf1 regulates Wolfram syndrome protein stability at the endoplasmic reticulum. *The Journal of biological chemistry* **286**, 18037-18047, doi:10.1074/jbc.M111.225615 (2011).
209 Fry, W. H., Simion, C., Sweeney, C. & Carraway, K. L., 3rd. Quantity control of the ErbB3 receptor tyrosine kinase at the endoplasmic reticulum. *Molecular and cellular biology* **31**, 3009-3018, doi:10.1128/MCB.05105-11 (2011).
210 Metzger, M. B. & Weissman, A. M. Working on a chain: E3s ganging up for ubiquitylation. *Nature cell biology* **12**, 1124-1126, doi:10.1038/ncb1210-1124 (2010).
211 Ernst, R., Mueller, B., Ploegh, H. L. & Schlieker, C. The otubain YOD1 is a deubiquitinating enzyme that associates with p97 to facilitate protein dislocation from the ER. *Molecular cell* **36**, 28-38, doi:10.1016/j.molcel.2009.09.016 (2009).
212 Shmueli, A., Tsai, Y. C., Yang, M., Braun, M. A. & Weissman, A. M. Targeting of gp78 for ubiquitin-mediated proteasomal degradation by Hrd1: cross-talk between E3s in the endoplasmic reticulum. *Biochemical and biophysical research communications* **390**, 758-762, doi:10.1016/j.bbrc.2009.10.045 (2009).
213 Ballar, P., Ors, A. U., Yang, H. & Fang, S. Differential regulation of CFTRDeltaF508 degradation by ubiquitin ligases gp78 and Hrd1. *The international journal of biochemistry & cell biology* **42**, 167-173, doi:10.1016/j.biocel.2009.10.005 (2010).
214 Soetandyo, N. & Ye, Y. The p97 ATPase dislocates MHC class I heavy chain in US2-expressing cells via a Ufd1-Npl4-independent mechanism. *The Journal of biological chemistry* **285**, 32352-32359, doi:10.1074/jbc.M110.131649 (2010).
215 Liang, J. *et al.* Characterization of erasin (UBXD2): a new ER protein that promotes ER-associated protein degradation. *Journal of cell science* **119**, 4011-4024, doi:10.1242/jcs.03163 (2006).
216 Suzuki, M. *et al.* Derlin-1 and UBXD8 are engaged in dislocation and degradation of lipidated ApoB-100 at lipid droplets. *Molecular biology of the cell* **23**, 800-810, doi:10.1091/mbc.E11-11-0950 (2012).

217 Ballar, P., Shen, Y., Yang, H. & Fang, S. The role of a novel p97/valosin-containing protein-interacting motif of gp78 in endoplasmic reticulum-associated degradation. *The Journal of biological chemistry* **281**, 35359-35368, doi:10.1074/jbc.M603355200 (2006).
218 Greenblatt, E. J., Olzmann, J. A. & Kopito, R. R. Derlin-1 is a rhomboid pseudoprotease required for the dislocation of mutant alpha-1 antitrypsin from the endoplasmic reticulum. *Nature structural & molecular biology* **18**, 1147-1152, doi:10.1038/nsmb.2111 (2011).
219 Ye, Y. *et al.* Recruitment of the p97 ATPase and ubiquitin ligases to the site of retrotranslocation at the endoplasmic reticulum membrane. *Proceedings of the National Academy of Sciences of the United States of America* **102**, 14132-14138, doi:10.1073/pnas.0505006102 (2005).
220 Li, G., Zhao, G., Zhou, X., Schindelin, H. & Lennarz, W. J. The AAA ATPase p97 links peptide N-glycanase to the endoplasmic reticulum-associated E3 ligase autocrine motility factor receptor. *Proceedings of the National Academy of Sciences of the United States of America* **103**, 8348-8353, doi:10.1073/pnas.0602747103 (2006).
221 Lukacs, G. L. & Verkman, A. S. CFTR: folding, misfolding and correcting the DeltaF508 conformational defect. *Trends in molecular medicine* **18**, 81-91, doi:10.1016/j.molmed.2011.10.003 (2012).
222 Farrell, P. M. *et al.* Guidelines for diagnosis of cystic fibrosis in newborns through older adults: Cystic Fibrosis Foundation consensus report. *The Journal of pediatrics* **153**, S4-S14, doi:10.1016/j.jpeds.2008.05.005 (2008).
223 Riordan, J. R. Assembly of functional CFTR chloride channels. *Annual review of physiology* **67**, 701-718, doi:10.1146/annurev.physiol.67.032003.154107 (2005).
224 Riordan, J. R. CFTR function and prospects for therapy. *Annual review of biochemistry* **77**, 701-726, doi:10.1146/annurev.biochem.75.103004.142532 (2008).
225 Rowntree, R. K. & Harris, A. The phenotypic consequences of CFTR mutations. *Annals of human genetics* **67**, 471-485 (2003).
226 MacDonald, K. D., McKenzie, K. R. & Zeitlin, P. L. Cystic fibrosis transmembrane regulator protein mutations: 'class' opportunity for novel drug innovation. *Paediatric drugs* **9**, 1-10 (2007).
227 Ashlock, M. A. & Olson, E. R. Therapeutics development for cystic fibrosis: a successful model for a multisystem genetic disease. *Annual review of medicine* **62**, 107-125, doi:10.1146/annurev-med-061509-131034 (2011).
228 Cuthbert, A. W. New horizons in the treatment of cystic fibrosis. *British journal of pharmacology* **163**, 173-183, doi:10.1111/j.1476-5381.2010.01137.x (2011).
229 Tarran, R. Regulation of airway surface liquid volume and mucus transport by active ion transport. *Proceedings of the American Thoracic Society* **1**, 42-46, doi:10.1513/pats.2306014 (2004).
230 Winters, S. L. & Yeates, D. B. Roles of hydration, sodium, and chloride in regulation of canine mucociliary transport system. *Journal of applied physiology* **83**, 1360-1369 (1997).
231 Krouse, M. E. Is cystic fibrosis lung disease caused by abnormal ion composition or abnormal volume? *The Journal of general physiology* **118**, 219-222 (2001).
232 Du, K., Sharma, M. & Lukacs, G. L. The DeltaF508 cystic fibrosis mutation impairs domain-domain interactions and arrests post-translational folding of CFTR. *Nature structural & molecular biology* **12**, 17-25, doi:10.1038/nsmb882 (2005).

233 Thibodeau, P. H., Brautigam, C. A., Machius, M. & Thomas, P. J. Side chain and backbone contributions of Phe508 to CFTR folding. *Nature structural & molecular biology* **12**, 10-16, doi:10.1038/nsmb881 (2005).
234 Du, K. & Lukacs, G. L. Cooperative assembly and misfolding of CFTR domains in vivo. *Molecular biology of the cell* **20**, 1903-1915, doi:10.1091/mbc.E08-09-0950 (2009).
235 Amaral, M. D. CFTR and chaperones: processing and degradation. *Journal of molecular neuroscience : MN* **23**, 41-48, doi:10.1385/JMN:23:1-2:041 (2004).
236 Lukacs, G. L. *et al.* Conformational maturation of CFTR but not its mutant counterpart (delta F508) occurs in the endoplasmic reticulum and requires ATP. *The EMBO journal* **13**, 6076-6086 (1994).
237 Jensen, T. J. *et al.* Multiple proteolytic systems, including the proteasome, contribute to CFTR processing. *Cell* **83**, 129-135 (1995).
238 Alberti, S., Bohse, K., Arndt, V., Schmitz, A. & Hohfeld, J. The cochaperone HspBP1 inhibits the CHIP ubiquitin ligase and stimulates the maturation of the cystic fibrosis transmembrane conductance regulator. *Molecular biology of the cell* **15**, 4003-4010, doi:10.1091/mbc.E04-04-0293 (2004).
239 Marozkina, N. V. *et al.* Hsp 70/Hsp 90 organizing protein as a nitrosylation target in cystic fibrosis therapy. *Proceedings of the National Academy of Sciences of the United States of America* **107**, 11393-11398, doi:10.1073/pnas.0909128107 (2010).
240 Wang, X. *et al.* Hsp90 cochaperone Aha1 downregulation rescues misfolding of CFTR in cystic fibrosis. *Cell* **127**, 803-815, doi:10.1016/j.cell.2006.09.043 (2006).
241 Loo, M. A. *et al.* Perturbation of Hsp90 interaction with nascent CFTR prevents its maturation and accelerates its degradation by the proteasome. *The EMBO journal* **17**, 6879-6887, doi:10.1093/emboj/17.23.6879 (1998).
242 Zhang, Y. *et al.* Hsp70 molecular chaperone facilitates endoplasmic reticulum-associated protein degradation of cystic fibrosis transmembrane conductance regulator in yeast. *Molecular biology of the cell* **12**, 1303-1314 (2001).
243 Farinha, C. M., Nogueira, P., Mendes, F., Penque, D. & Amaral, M. D. The human DnaJ homologue (Hdj)-1/heat-shock protein (Hsp) 40 co-chaperone is required for the in vivo stabilization of the cystic fibrosis transmembrane conductance regulator by Hsp70. *The Biochemical journal* **366**, 797-806, doi:10.1042/BJ20011717 (2002).
244 Grove, D. E., Fan, C. Y., Ren, H. Y. & Cyr, D. M. The endoplasmic reticulum-associated Hsp40 DNAJB12 and Hsc70 cooperate to facilitate RMA1 E3-dependent degradation of nascent CFTRDeltaF508. *Molecular biology of the cell* **22**, 301-314, doi:10.1091/mbc.E10-09-0760 (2011).
245 Harada, K. *et al.* Calreticulin negatively regulates the cell surface expression of cystic fibrosis transmembrane conductance regulator. *The Journal of biological chemistry* **281**, 12841-12848, doi:10.1074/jbc.M512975200 (2006).
246 Okiyoneda, T. *et al.* Role of calnexin in the ER quality control and productive folding of CFTR; differential effect of calnexin knockout on wild-type and DeltaF508 CFTR. *Biochimica et biophysica acta* **1783**, 1585-1594, doi:10.1016/j.bbamcr.2008.04.002 (2008).
247 Glozman, R. *et al.* N-glycans are direct determinants of CFTR folding and stability in secretory and endocytic membrane traffic. *The Journal of cell biology* **184**, 847-862, doi:10.1083/jcb.200808124 (2009).

248 Hassink, G. C. *et al.* The ER-resident ubiquitin-specific protease 19 participates in the UPR and rescues ERAD substrates. *EMBO reports* **10**, 755-761, doi:10.1038/embor.2009.69 (2009).
249 Henderson, M. J., Vij, N. & Zeitlin, P. L. Ubiquitin C-terminal hydrolase-L1 protects cystic fibrosis transmembrane conductance regulator from early stages of proteasomal degradation. *The Journal of biological chemistry* **285**, 11314-11325, doi:10.1074/jbc.M109.044057 (2010).
250 Caohuy, H., Jozwik, C. & Pollard, H. B. Rescue of DeltaF508-CFTR by the SGK1/Nedd4-2 signaling pathway. *The Journal of biological chemistry* **284**, 25241-25253, doi:10.1074/jbc.M109.035345 (2009).
251 Ye, S. *et al.* c-Cbl facilitates endocytosis and lysosomal degradation of cystic fibrosis transmembrane conductance regulator in human airway epithelial cells. *The Journal of biological chemistry* **285**, 27008-27018, doi:10.1074/jbc.M110.139881 (2010).
252 Bomberger, J. M., Barnaby, R. L. & Stanton, B. A. The deubiquitinating enzyme USP10 regulates the post-endocytic sorting of cystic fibrosis transmembrane conductance regulator in airway epithelial cells. *The Journal of biological chemistry* **284**, 18778-18789, doi:10.1074/jbc.M109.001685 (2009).
253 Rautaharju, P. M. *et al.* AHA/ACCF/HRS recommendations for the standardization and interpretation of the electrocardiogram: part IV: the ST segment, T and U waves, and the QT interval: a scientific statement from the American Heart Association Electrocardiography and Arrhythmias Committee, Council on Clinical Cardiology; the American College of Cardiology Foundation; and the Heart Rhythm Society. Endorsed by the International Society for Computerized Electrocardiology. *Journal of the American College of Cardiology* **53**, 982-991, doi:10.1016/j.jacc.2008.12.014 (2009).
254 Goldenberg, I., Zareba, W. & Moss, A. J. Long QT Syndrome. *Current problems in cardiology* **33**, 629-694, doi:10.1016/j.cpcardiol.2008.07.002 (2008).
255 Amin, A. S., Pinto, Y. M. & Wilde, A. A. Long QT syndrome: beyond the causal mutation. *The Journal of physiology* **591**, 4125-4139, doi:10.1113/jphysiol.2013.254920 (2013).
256 Vohra, J. The Long QT Syndrome. *Heart, lung & circulation* **16 Suppl 3**, S5-12, doi:10.1016/j.hlc.2007.05.008 (2007).
257 Sanguinetti, M. C. & Tristani-Firouzi, M. hERG potassium channels and cardiac arrhythmia. *Nature* **440**, 463-469, doi:10.1038/nature04710 (2006).
258 Vandenberg, J. I. *et al.* hERG K(+) channels: structure, function, and clinical significance. *Physiological reviews* **92**, 1393-1478 (2012).
259 Eldstrom, J. & Fedida, D. The voltage-gated channel accessory protein KCNE2: multiple ion channel partners, multiple ways to long QT syndrome. *Expert reviews in molecular medicine* **13**, e38, doi:10.1017/S1462399411002092 (2011).
260 Kapplinger, J. D. *et al.* Spectrum and prevalence of mutations from the first 2,500 consecutive unrelated patients referred for the FAMILION long QT syndrome genetic test. *Heart rhythm : the official journal of the Heart Rhythm Society* **6**, 1297-1303, doi:10.1016/j.hrthm.2009.05.021 (2009).
261 Thomas, D., Kiehn, J., Katus, H. A. & Karle, C. A. Defective protein trafficking in hERG-associated hereditary long QT syndrome (LQT2): molecular mechanisms and restoration of intracellular protein processing. *Cardiovascular research* **60**, 235-241 (2003).

262 Anderson, C. L. *et al.* Most LQT2 mutations reduce Kv11.1 (hERG) current by a class 2 (trafficking-deficient) mechanism. *Circulation* **113**, 365-373, doi:10.1161/CIRCULATIONAHA.105.570200 (2006).
263 Gong, Q., Anderson, C. L., January, C. T. & Zhou, Z. Role of glycosylation in cell surface expression and stability of HERG potassium channels. *American journal of physiology. Heart and circulatory physiology* **283**, H77-84, doi:10.1152/ajpheart.00008.2002 (2002).
264 Zhou, Z. *et al.* Properties of HERG channels stably expressed in HEK 293 cells studied at physiological temperature. *Biophysical journal* **74**, 230-241, doi:10.1016/S0006-3495(98)77782-3 (1998).
265 Ellgaard, L., Molinari, M. & Helenius, A. Setting the standards: quality control in the secretory pathway. *Science* **286**, 1882-1888 (1999).
266 Ficker, E., Dennis, A. T., Wang, L. & Brown, A. M. Role of the cytosolic chaperones Hsp70 and Hsp90 in maturation of the cardiac potassium channel HERG. *Circ Res* **92**, e87-100 (2003).
267 Walker, V. E., Atanasiu, R., Lam, H. & Shrier, A. Co-chaperone FKBP38 promotes HERG trafficking. *The Journal of biological chemistry* **282**, 23509-23516, doi:10.1074/jbc.M701006200 (2007).
268 Li, P. *et al.* Reciprocal control of hERG stability by Hsp70 and Hsc70 with implication for restoration of LQT2 mutant stability. *Circulation research* **108**, 458-468, doi:10.1161/CIRCRESAHA.110.227835 (2011).
269 Hageman, J., van Waarde, M. A., Zylicz, A., Walerych, D. & Kampinga, H. H. The diverse members of the mammalian HSP70 machine show distinct chaperone-like activities. *The Biochemical journal* **435**, 127-142, doi:10.1042/BJ20101247 (2011).
270 Sharma, K. *et al.* Quantitative proteomics reveals that Hsp90 inhibition preferentially targets kinases and the DNA damage response. *Molecular & cellular proteomics : MCP* **11**, M111 014654, doi:10.1074/mcp.M111.014654 (2012).
271 Gong, Q., Keeney, D. R., Molinari, M. & Zhou, Z. Degradation of trafficking-defective long QT syndrome type II mutant channels by the ubiquitin-proteasome pathway. *The Journal of biological chemistry* **280**, 19419-19425, doi:10.1074/jbc.M502327200 (2005).
272 Wang, Y. *et al.* Trafficking-deficient G572R-hERG and E637K-hERG activate stress and clearance pathways in endoplasmic reticulum. *PloS one* **7**, e29885, doi:10.1371/journal.pone.0029885 (2012).
273 Kelly, J. W. & Balch, W. E. The integration of cell and chemical biology in protein folding. *Nature chemical biology* **2**, 224-227, doi:10.1038/nchembio0506-224 (2006).
274 Araki, K. & Nagata, K. Protein folding and quality control in the ER. *Cold Spring Harbor perspectives in biology* **3**, a007526, doi:10.1101/cshperspect.a007526 (2011).
275 Gurkan, C., Stagg, S. M., Lapointe, P. & Balch, W. E. The COPII cage: unifying principles of vesicle coat assembly. *Nature reviews. Molecular cell biology* **7**, 727-738, doi:10.1038/nrm2025 (2006).
276 Hirsch, C., Gauss, R., Horn, S. C., Neuber, O. & Sommer, T. The ubiquitylation machinery of the endoplasmic reticulum. *Nature* **458**, 453-460, doi:10.1038/nature07962 (2009).
277 Smith, M. H., Ploegh, H. L. & Weissman, J. S. Road to ruin: targeting proteins for degradation in the endoplasmic reticulum. *Science* **334**, 1086-1090, doi:10.1126/science.1209235 (2011).

278 Gong, Q., Jones, M. A. & Zhou, Z. Mechanisms of pharmacological rescue of trafficking-defective hERG mutant channels in human long QT syndrome. *The Journal of biological chemistry* **281**, 4069-4074, doi:10.1074/jbc.M511765200 (2006).
279 Fan, C. Y., Ren, H. Y., Lee, P., Caplan, A. J. & Cyr, D. M. The type I Hsp40 zinc finger-like region is required for Hsp70 to capture non-native polypeptides from Ydj1. *The Journal of biological chemistry* **280**, 695-702, doi:10.1074/jbc.M410645200 (2005).
280 Banecki, B. *et al.* Structure-function analysis of the zinc finger region of the DnaJ molecular chaperone. *The Journal of biological chemistry* **271**, 14840-14848 (1996).
281 Linke, K., Wolfram, T., Bussemer, J. & Jakob, U. The roles of the two zinc binding sites in DnaJ. *The Journal of biological chemistry* **278**, 44457-44466, doi:10.1074/jbc.M307491200 (2003).
282 Wu, Y., Li, J., Jin, Z., Fu, Z. & Sha, B. The crystal structure of the C-terminal fragment of yeast Hsp40 Ydj1 reveals novel dimerization motif for Hsp40. *Journal of molecular biology* **346**, 1005-1011, doi:10.1016/j.jmb.2004.12.040 (2005).
283 Rosales-Hernandez, A., Beck, K. E., Zhao, X., Braun, A. P. & Braun, J. E. RDJ2 (DNAJA2) chaperones neural G protein signaling pathways. *Cell stress & chaperones* **14**, 71-82, doi:10.1007/s12192-008-0056-y (2009).
284 Goldfarb, S. B. *et al.* Differential effects of Hsc70 and Hsp70 on the intracellular trafficking and functional expression of epithelial sodium channels. *Proceedings of the National Academy of Sciences of the United States of America* **103**, 5817-5822, doi:10.1073/pnas.0507903103 (2006).
285 Sanguinetti, M. C. HERG1 channelopathies. *Pflugers Archiv : European journal of physiology* **460**, 265-276, doi:10.1007/s00424-009-0758-8 (2010).
286 Akhavan, A. *et al.* Identification of the cyclic-nucleotide-binding domain as a conserved determinant of ion-channel cell-surface localization. *Journal of cell science* **118**, 2803-2812, doi:10.1242/jcs.02423 (2005).
287 Walker, V. E. *et al.* Hsp40 chaperones promote degradation of the HERG potassium channel. *The Journal of biological chemistry* **285**, 3319-3329, doi:10.1074/jbc.M109.024000 (2010).
288 Takayama, S. & Reed, J. C. Molecular chaperone targeting and regulation by BAG family proteins. *Nature cell biology* **3**, E237-241 (2001).
289 Kanelakis, K. C. *et al.* Differential effects of the hsp70-binding protein BAG-1 on glucocorticoid receptor folding by the hsp90-based chaperone machinery. *J Biol Chem* **274**, 34134-34140 (1999).
290 Demand, J., Alberti, S., Patterson, C. & Hohfeld, J. Cooperation of a ubiquitin domain protein and an E3 ubiquitin ligase during chaperone/proteasome coupling. *Curr Biol* **11**, 1569-1577, doi:S0960-9822(01)00487-0 [pii] (2001).
291 Sroka, K. *et al.* BAG1 modulates huntingtin toxicity, aggregation, degradation, and subcellular distribution. *Journal of neurochemistry* **111**, 801-807, doi:10.1111/j.1471-4159.2009.06363.x (2009).
292 Hampton, R. Y. & Sommer, T. Finding the will and the way of ERAD substrate retrotranslocation. *Current opinion in cell biology* **24**, 460-466, doi:10.1016/j.ceb.2012.05.010 (2012).
293 Lin, P. H., Lan, W. M. & Chau, L. Y. TRC8 suppresses tumorigenesis through targeting heme oxygenase-1 for ubiquitination and degradation. *Oncogene* **32**, 2325-2334, doi:10.1038/onc.2012.244 (2013).

294 Sondermann, H. *et al.* Prediction of novel Bag-1 homologs based on structure/function analysis identifies Snl1p as an Hsp70 co-chaperone in Saccharomyces cerevisiae. *The Journal of biological chemistry* **277**, 33220-33227, doi:10.1074/jbc.M204624200 (2002).
295 Apaja, P. M. *et al.* Ubiquitination-dependent quality control of hERG K+ channel with acquired and inherited conformational defect at the plasma membrane. *Molecular biology of the cell* **24**, 3787-3804, doi:10.1091/mbc.E13-07-0417 (2013).
296 Weissman, A. M. Themes and variations on ubiquitylation. *Nat Rev Mol Cell Biol* **2**, 169-178, doi:10.1038/35056563 (2001).
297 Deshaies, R. J. & Joazeiro, C. A. RING domain E3 ubiquitin ligases. *Annual review of biochemistry* **78**, 399-434, doi:10.1146/annurev.biochem.78.101807.093809 (2009).
298 Chen, B. *et al.* The activity of a human endoplasmic reticulum-associated degradation E3, gp78, requires its Cue domain, RING finger, and an E2-binding site. *Proceedings of the National Academy of Sciences of the United States of America* **103**, 341-346, doi:10.1073/pnas.0506618103 (2006).
299 Jo, Y., Hartman, I. Z. & DeBose-Boyd, R. A. Ancient ubiquitous protein-1 mediates sterol-induced ubiquitination of 3-hydroxy-3-methylglutaryl CoA reductase in lipid droplet-associated endoplasmic reticulum membranes. *Molecular biology of the cell* **24**, 169-183, doi:10.1091/mbc.E12-07-0564 (2013).
300 Soss, S. E., Yue, Y., Dhe-Paganon, S. & Chazin, W. J. E2 conjugating enzyme selectivity and requirements for function of the E3 ubiquitin ligase CHIP. *J Biol Chem* **286**, 21277-21286, doi:10.1074/jbc.M111.224006 (2011).
301 Liu, T. F. *et al.* Ablation of gp78 in liver improves hyperlipidemia and insulin resistance by inhibiting SREBP to decrease lipid biosynthesis. *Cell metabolism* **16**, 213-225, doi:10.1016/j.cmet.2012.06.014 (2012).
302 Tsai, Y. C. *et al.* Differential regulation of HMG-CoA reductase and Insig-1 by enzymes of the ubiquitin-proteasome system. *Molecular biology of the cell* **23**, 4484-4494, doi:10.1091/mbc.E12-08-0631 (2012).
303 Mata-Greenwood, E., Stewart, J. M., Steinhorn, R. H. & Pearce, W. J. Role of BCL2-associated athanogene 1 in differential sensitivity of human endothelial cells to glucocorticoids. *Arteriosclerosis, thrombosis, and vascular biology* **33**, 1046-1055, doi:10.1161/ATVBAHA.113.301247 (2013).
304 Matsumura, Y., David, L. L. & Skach, W. R. Role of Hsc70 binding cycle in CFTR folding and endoplasmic reticulum-associated degradation. *Molecular biology of the cell* **22**, 2797-2809, doi:mbc.E11-02-0137 [pii]
10.1091/mbc.E11-02-0137 (2011).
305 Morishima, Y. *et al.* CHIP deletion reveals functional redundancy of E3 ligases in promoting degradation of both signaling proteins and expanded glutamine proteins. *Human molecular genetics* **17**, 3942-3952, doi:10.1093/hmg/ddn296 (2008).
306 Sultana, R., Theodoraki, M. A. & Caplan, A. J. UBR1 promotes protein kinase quality control and sensitizes cells to Hsp90 inhibition. *Experimental cell research* **318**, 53-60, doi:10.1016/j.yexcr.2011.09.010 (2012).
307 Sultana, R., Theodoraki, M. A. & Caplan, A. J. Specificity in the actions of the UBR1 ubiquitin ligase in the degradation of nuclear receptors. *FEBS open bio* **3**, 394-397, doi:10.1016/j.fob.2013.09.003 (2013).

308 Jehle, J., Schweizer, P. A., Katus, H. A. & Thomas, D. Novel roles for hERG K(+) channels in cell proliferation and apoptosis. *Cell death & disease* **2**, e193, doi:10.1038/cddis.2011.77 (2011).
309 Neckers, L. & Workman, P. Hsp90 molecular chaperone inhibitors: are we there yet? *Clinical cancer research : an official journal of the American Association for Cancer Research* **18**, 64-76, doi:10.1158/1078-0432.CCR-11-1000 (2012).
310 Rodina, A. *et al.* Identification of an allosteric pocket on human hsp70 reveals a mode of inhibition of this therapeutically important protein. *Chemistry & biology* **20**, 1469-1480, doi:10.1016/j.chembiol.2013.10.008 (2013).
311 Taldone, T., Ochiana, S. O., Patel, P. D. & Chiosis, G. Selective targeting of the stress chaperome as a therapeutic strategy. *Trends in pharmacological sciences* **35**, 592-603, doi:10.1016/j.tips.2014.09.001 (2014).
312 Sheppard, D. N. & Welsh, M. J. Structure and function of the CFTR chloride channel. *Physiological reviews* **79**, S23-45 (1999).
313 Rowe, S. M., Miller, S. & Sorscher, E. J. Cystic fibrosis. *The New England journal of medicine* **352**, 1992-2001, doi:10.1056/NEJMra043184 (2005).
314 Riordan, J. R. *et al.* Identification of the cystic fibrosis gene: cloning and characterization of complementary DNA. *Science* **245**, 1066-1073 (1989).
315 Cyr, D. M. Arrest of CFTRDeltaF508 folding. *Nature structural & molecular biology* **12**, 2-3, doi:10.1038/nsmb0105-2 (2005).
316 Rosser, M. F., Grove, D. E., Chen, L. & Cyr, D. M. Assembly and misassembly of cystic fibrosis transmembrane conductance regulator: folding defects caused by deletion of F508 occur before and after the calnexin-dependent association of membrane spanning domain (MSD) 1 and MSD2. *Molecular biology of the cell* **19**, 4570-4579, doi:10.1091/mbc.E08-04-0357 (2008).
317 Pind, S., Riordan, J. R. & Williams, D. B. Participation of the endoplasmic reticulum chaperone calnexin (p88, IP90) in the biogenesis of the cystic fibrosis transmembrane conductance regulator. *The Journal of biological chemistry* **269**, 12784-12788 (1994).
318 Wang, B. *et al.* BAP31 interacts with Sec61 translocons and promotes retrotranslocation of CFTRDeltaF508 via the derlin-1 complex. *Cell* **133**, 1080-1092, doi:10.1016/j.cell.2008.04.042 (2008).
319 Dalal, S., Rosser, M. F., Cyr, D. M. & Hanson, P. I. Distinct roles for the AAA ATPases NSF and p97 in the secretory pathway. *Molecular biology of the cell* **15**, 637-648, doi:10.1091/mbc.E03-02-0097 (2004).
320 Muller, P. *et al.* C-terminal phosphorylation of Hsp70 and Hsp90 regulates alternate binding to co-chaperones CHIP and HOP to determine cellular protein folding/degradation balances. *Oncogene* **32**, 3101-3110, doi:10.1038/onc.2012.314 (2013).
321 Polier, S., Dragovic, Z., Hartl, F. U. & Bracher, A. Structural basis for the cooperation of Hsp70 and Hsp110 chaperones in protein folding. *Cell* **133**, 1068-1079, doi:S0092-8674(08)00678-8 [pii]
10.1016/j.cell.2008.05.022 (2008).
322 Schuermann, J. P. *et al.* Structure of the Hsp110:Hsc70 nucleotide exchange machine. *Mol Cell* **31**, 232-243, doi:S1097-2765(08)00339-0 [pii]
10.1016/j.molcel.2008.05.006 (2008).

323 Morais Cabral, J. H. *et al.* Crystal structure and functional analysis of the HERG potassium channel N terminus: a eukaryotic PAS domain. *Cell* **95**, 649-655 (1998).
324 Haitin, Y., Carlson, A. E. & Zagotta, W. N. The structural mechanism of KCNH-channel regulation by the eag domain. *Nature* **501**, 444-448, doi:10.1038/nature12487 (2013).
325 Marques-Carvalho, M. J. *et al.* Structural, biochemical, and functional characterization of the cyclic nucleotide binding homology domain from the mouse EAG1 potassium channel. *Journal of molecular biology* **423**, 34-46, doi:10.1016/j.jmb.2012.06.025 (2012).
326 Ridsdale, A. *et al.* Cholesterol is required for efficient endoplasmic reticulum-to-Golgi transport of secretory membrane proteins. *Molecular biology of the cell* **17**, 1593-1605, doi:10.1091/mbc.E05-02-0100 (2006).
327 Wu, Z. Y., Yu, D. J., Soong, T. W., Dawe, G. S. & Bian, J. S. Progesterone impairs human ether-a-go-go-related gene (HERG) trafficking by disruption of intracellular cholesterol homeostasis. *The Journal of biological chemistry* **286**, 22186-22194, doi:10.1074/jbc.M110.198853 (2011).
328 Coppinger, J. A. *et al.* A chaperone trap contributes to the onset of cystic fibrosis. *PloS one* **7**, e37682, doi:10.1371/journal.pone.0037682 (2012).
329 Massey, A. J. *et al.* A novel, small molecule inhibitor of Hsc70/Hsp70 potentiates Hsp90 inhibitor induced apoptosis in HCT116 colon carcinoma cells. *Cancer chemotherapy and pharmacology* **66**, 535-545, doi:10.1007/s00280-009-1194-3 (2010).
330 Rousaki, A. *et al.* Allosteric drugs: the interaction of antitumor compound MKT-077 with human Hsp70 chaperones. *Journal of molecular biology* **411**, 614-632, doi:10.1016/j.jmb.2011.06.003 (2011).
331 Chang, L. *et al.* Chemical screens against a reconstituted multiprotein complex: myricetin blocks DnaJ regulation of DnaK through an allosteric mechanism. *Chemistry & biology* **18**, 210-221, doi:10.1016/j.chembiol.2010.12.010 (2011).
332 Leu, J. I., Pimkina, J., Frank, A., Murphy, M. E. & George, D. L. A small molecule inhibitor of inducible heat shock protein 70. *Molecular cell* **36**, 15-27, doi:10.1016/j.molcel.2009.09.023 (2009).
333 Cho, H. J. *et al.* A small molecule that binds to an ATPase domain of Hsc70 promotes membrane trafficking of mutant cystic fibrosis transmembrane conductance regulator. *Journal of the American Chemical Society* **133**, 20267-20276, doi:10.1021/ja206762p (2011).
334 Mendoza, J. L. *et al.* Requirements for efficient correction of DeltaF508 CFTR revealed by analyses of evolved sequences. *Cell* **148**, 164-174, doi:S0092-8674(11)01367-5 [pii] 10.1016/j.cell.2011.11.023 (2012).
335 Rabeh, W. M. *et al.* Correction of both NBD1 energetics and domain interface is required to restore DeltaF508 CFTR folding and function. *Cell* **148**, 150-163, doi:10.1016/j.cell.2011.11.024 (2012).
336 Okiyoneda, T. *et al.* Mechanism-based corrector combination restores DeltaF508-CFTR folding and function. *Nature chemical biology* **9**, 444-454, doi:10.1038/nchembio.1253 (2013).
337 Loo, T. W., Bartlett, M. C. & Clarke, D. M. Rescue of DeltaF508 and other misprocessed CFTR mutants by a novel quinazoline compound. *Molecular pharmaceutics* **2**, 407-413, doi:10.1021/mp0500521 (2005).
338 Wang, Y., Loo, T. W., Bartlett, M. C. & Clarke, D. M. Correctors promote maturation of cystic fibrosis transmembrane conductance regulator (CFTR)-processing mutants by

binding to the protein. *The Journal of biological chemistry* **282**, 33247-33251, doi:10.1074/jbc.C700175200 (2007).
339 Yoo, C. L. *et al.* 4'-Methyl-4,5'-bithiazole-based correctors of defective delta F508-CFTR cellular processing. *Bioorganic & medicinal chemistry letters* **18**, 2610-2614, doi:10.1016/j.bmcl.2008.03.037 (2008).
340 Loo, T. W., Bartlett, M. C. & Clarke, D. M. Correctors enhance maturation of DeltaF508 CFTR by promoting interactions between the two halves of the molecule. *Biochemistry* **48**, 9882-9890, doi:10.1021/bi9004842 (2009).
341 Kim Chiaw, P., Wellhauser, L., Huan, L. J., Ramjeesingh, M. & Bear, C. E. A chemical corrector modifies the channel function of F508del-CFTR. *Molecular pharmacology* **78**, 411-418, doi:10.1124/mol.110.065862 (2010).
342 Van Goor, F. *et al.* Correction of the F508del-CFTR protein processing defect in vitro by the investigational drug VX-809. *Proceedings of the National Academy of Sciences of the United States of America* **108**, 18843-18848, doi:10.1073/pnas.1105787108 (2011).
343 He, L. *et al.* Correctors of DeltaF508 CFTR restore global conformational maturation without thermally stabilizing the mutant protein. *FASEB journal : official publication of the Federation of American Societies for Experimental Biology* **27**, 536-545, doi:10.1096/fj.12-216119 (2013).
344 Loo, T. W., Bartlett, M. C. & Clarke, D. M. Corrector VX-809 stabilizes the first transmembrane domain of CFTR. *Biochemical pharmacology* **86**, 612-619, doi:10.1016/j.bcp.2013.06.028 (2013).
345 Ren, H. Y. *et al.* VX-809 corrects folding defects in cystic fibrosis transmembrane conductance regulator protein through action on membrane-spanning domain 1. *Molecular biology of the cell* **24**, 3016-3024, doi:10.1091/mbc.E13-05-0240 (2013).
346 Chanoux, R. A. *et al.* Hsp70 promotes epithelial sodium channel functional expression by increasing its association with coat complex II and its exit from endoplasmic reticulum. *The Journal of biological chemistry* **287**, 19255-19265, doi:10.1074/jbc.M112.357756 (2012).
347 Vila-Carriles, W. H., Zhou, Z. H., Bubien, J. K., Fuller, C. M. & Benos, D. J. Participation of the chaperone Hsc70 in the trafficking and functional expression of ASIC2 in glioma cells. *The Journal of biological chemistry* **282**, 34381-34391, doi:10.1074/jbc.M705354200 (2007).
348 Grifoni, S. C., McKey, S. E. & Drummond, H. A. Hsc70 regulates cell surface ASIC2 expression and vascular smooth muscle cell migration. *American journal of physiology. Heart and circulatory physiology* **294**, H2022-2030, doi:10.1152/ajpheart.01271.2007 (2008).
349 Gao, Y., Yechikov, S., Vazquez, A. E., Chen, D. & Nie, L. Distinct roles of molecular chaperones HSP90alpha and HSP90beta in the biogenesis of KCNQ4 channels. *PloS one* **8**, e57282, doi:10.1371/journal.pone.0057282 (2013).
350 Wisen, S. *et al.* Binding of a small molecule at a protein-protein interface regulates the chaperone activity of hsp70-hsp40. *ACS chemical biology* **5**, 611-622, doi:10.1021/cb1000422 (2010).
351 Milarski, K. L. & Morimoto, R. I. Mutational analysis of the human HSP70 protein: distinct domains for nucleolar localization and adenosine triphosphate binding. *J Cell Biol* **109**, 1947-1962 (1989).